NASA Contractor Report 198191

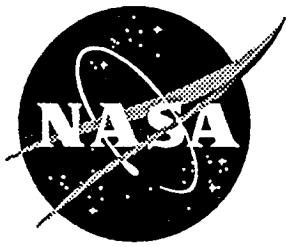

Calculated Values of Atomic Oxygen Fluences and Solar Exposure on Selected Surfaces of LDEF

J. R. Gillis, H. G. Pippin, R. J. Bourassa, and P. E. Gruenbaum
Boeing Defense & Space Group, Seattle, Washington

Contracts NAS1-18224 and NAS1-19247

August 1995

National Aeronautics and
Space Administration
Langley Research Center
Hampton, Virginia 23681-0001

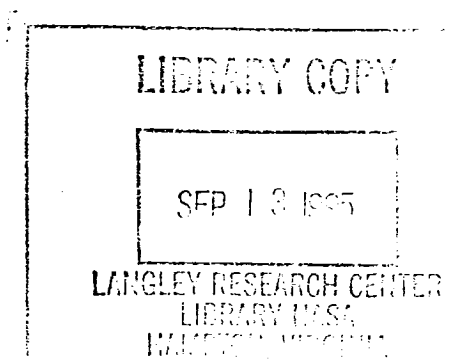

CALCULATED VALUES OF ATOMIC OXYGEN FLUENCES AND SOLAR EXPOSURE ON SELECTED SURFACES OF LDEF

J. R. Gillis
H. G. Pippin
R. J. Bourassa
P. E. Gruenbaum

BOEING DEFENSE & SPACE GROUP

CALCULATED VALUES OF ATOMIC OXYGEN FLUENCES AND SOLAR EXPOSURE ON SELECTED SURFACES OF LDEF

FOREWORD

This report describes the results of calculating atomic oxygen fluences and solar exposure to selected LDEF surfaces. Boeing Defense & Space Group's activities were supported by the following NASA Langley Research Center Contracts (LaRC); "LDEF Special Investigation Group Support" contracts NAS1-18224, Tasks 12 and 15 (October 1989 through January 1991), NAS1-19247 Tasks 1 & 2 (May 1991 through October 1992), and NAS1-19247 Task 8 (initiated October 1992). Sponsorship for these programs was provided by National Aeronautics and Space Administration, Langley Research Center, Hampton, VA, and The Strategic Defense Initiative Organization, Key Technologies Office, Washington, D.C.

Mr. Lou Teichman, NASA LaRC, was the initial NASA Task Technical Monitor. Following Mr. Teichman's retirement, Ms. Joan Funk, NASA LaRC, became the Task Technical Monitor. The Materials & Processes Technology organization of the Boeing Defense & Space Group performed the five contract tasks with the following Boeing personnel providing critical support throughout the program.

Sylvester Hill	Task Manager
Roger Bourassa	Modeling
Dr. James R. Gillis	Scientific Computing
Dr. Peter Gruenbaum	User Interface Programming
Dr. Gary Pippin	Project Coordination

CONTENTS

FIGURES

1.0 INTRODUCTION

Atomic oxygen (AO) fluences in atoms/cm^2 and solar exposure in cumulative equivalent sun hours (CESH) have been modeled for selected LDEF hardware. Figure 1-1 lists the hardware modeled. This document describes the modeling done for these surfaces. All photographs of LDEF hardware are printed as black and white in the section of text near the figure reference and in color in the Appendix A.

Hardware	AO Exposure	Solar Exposure
S0069 Row 9A thermal control surfaces experiment	√	√
LDEF FEP blanket fold row 6 toward row 7	√	√
LDEF FEP blanket fold row 7 toward row 6	√	√
M0001 space end NRL cosmic ray experiment	√	√
Tray D-11 copper ground strap	√	
Tray F-9 angle bracket	√	
Tray D-11 FEP blanket fold at tray edge toward row 10	√	
Tray B-7 FEP blanket fold at longeron toward row 8	√	
Tray C-5 FEP blanket fold near tray edge		√
Tray D-1 FEP blanket fold near row 2 edge		√
C-9 scuff plate	√	√
Space end tray clamp H-12 with three bolts	√	
B-9 Environment Exposure Control Canister (EECC) Experiment Tray	√	√
C-2 Environment Exposure Control Canister (EECC) Experiment Tray	√	√
E-3 Environment Exposure Control Canister (EECC) Experiment Tray	√	√
D-4 Environment Exposure Control Canister (EECC) Experiment Tray	√	√
D-8 Environment Exposure Control Canister (EECC) Experiment Tray	√	√

Figure 1-1. LDEF AO and Solar Exposures Modeled.

1.1 Atomic Oxygen Exposure Modeling

Atomic oxygen exposure reported in this appendix was modeled using the microenvironment modeling code SHADOWV2 (ref. 1). This code is an extensive upgrade of SHADOW Version 1.1 (ref. 2) and calculates scattered fluence more accurately than Version 1.1. The current results should be used in preference to previously calculated AO exposures (refs. 3 and 4). The LDEF mission average atmospheric temperature, atomic oxygen density, and satellite speed relative to the atmosphere for the current calculations were calculated by AVESHAD (ref. 2) using the FLUXAVG (ref. 5) generated mission file. This resulted in the mission average values given in figure 1.1-1. SHADOWV2 normally calculates AO fluxes. However, SHADOWV2 was used to calculate fluences by inputting LDEF mission average AO density times mission duration rather than the LDEF mission average AO density. This was done for all microenvironment atomic oxygen fluence calculations. All plots report AO exposure as $\log_{10}$ (fluence in atoms/cm^2).

Parameter	Value
AO Density	6.4136E7 atoms/cm^3
Temperature	1182.9 K
Satellite Speed Relative to Atmosphere	7.21E5 cm/s
Mission Duration	2105.9085 days = 1.81950E8 s
AO Density Times Mission Duration	1.17E16 (atoms/cm^3) s

Figure 1.1-1. LDEF Mission Average Values for AO Microenvironment Calculations.

The accuracy of the atomic oxygen modeling may be estimated as follows. The FLUXAVG ram and side direction mission fluxes (from which the LDEF mission average values of figure 1.1-1 are calculated) are about 8% greater than those estimated using detailed orbit position calculations (ref. 6). Both calculations use the MSIS-86 atmospheric model (ref. 7) to estimate atomic oxygen densities on orbit during the LDEF mission. The MSIS-86 model is estimated to have an uncertainty of about 25% (ref. 7). The uncertainty in the MSIS-86 model is the greatest uncertainty in the modeled fluences. SHADOWV2 reproduces the primary exposure ram and side direction fluences to unshielded surfaces in the mission file to three significant digits. The accuracy of the very low fluences to trailing surfaces is less. The uncertainty in scattered AO exposure to surfaces is somewhat more difficult to estimate because it is a function of the gridding of the surfaces and the number of rays scattered. Tests of specular reflection between two surfaces have shown that all flux incident on the reflecting surface is reflected to the receiving surface. By implication this suggests that high intensity scattered fluences to satellite surfaces are modeled with accuracy similar to that of direct fluence. Low intensity scattered fluences may be expected to have somewhat greater uncertainty.

Surface properties of materials used for calculating AO exposures are given in figure 1.1-2. The materials properties are defined as the fraction of AO striking a surface which undergoes specular reflection, diffuse reflection, recombination, or surface reaction. Materials surface properties for atomic oxygen scattering are not well known. These surface properties are the authors' best estimates. It will be noted that the surface properties of FEP have been changed from our previously recommended values (ref. 2). Reanalysis of the FEP thickness vs. AO fluence for the tray F-9 angle bracket, tray D-11 FEP blanket fold, and tray B-7 blanket fold indicates that the current values for FEP surface properties yield better agreement between observed and predicted FEP thicknesses than the previous values.

Material	Specular Reflection	Diffuse Reflection	Recombination Efficiency	Surface Reactivity
Aluminum	0.50	0.46	0.04	0.00
Kapton	0.40	0.45	0.15	0.00
FEP (Aluminized Teflon)	0.98	0.00	0.00	0.02
Copper	0.50	0.40	0.08	0.02
Polyethylene	0.40	0.40	0.00	0.20
Gold	0.65	0.20	0.00	0.15
Silica Glass	0.67	0.33	0.00	0.0002
Silver Oxide	0.25	0.25	0.50	0.00
Yellow Paint Chem Glaze-II	0.00	0.90	0.00	0.10

Figure 1.1-2. Surface Properties of Some Materials for Atomic Oxygen Scattering.

1.2 Solar Exposure Modeling

Solar exposure reported in this appendix was modeled using the microenvironment modeling code SOLSHAD Version 1.0 (ref. 8). SOLSHAD Version 1.0 allows more accurate calculation of scattered CESH than did previous versions. The current results should be used in preference to previously calculated solar microenvironment exposures (ref. 4). All plots report solar exposure as CESH.

The uncertainty in primary and Earth-reflected solar exposure to LDEF surfaces is proportional to one over the square root of the number of Sun and satellite positions used to model exposure. For the 3000 Sun and satellite positions typically used to model solar exposure to LDEF surfaces, this implies about a 2% standard deviation for the 50542 hour LDEF mission.This translates to about 7% standard deviation for the 14500 CESH space-end primary and Earth-reflected solar exposure and proportionately larger standard deviations for surfaces with smaller CESH. As with atomic oxygen exposure, the accuracy of scattered CESH is a function of the surface gridding and the number of solar rays scattered per unit surface area. High intensity scattered CESH should have uncertainties comparable to the direct CESH on the surfaces which produced the scattering and low intensity scattered CESH will have greater uncertainties.

Surface optical properties of materials used for calculating solar exposures are given in figure 1.2-1. The surface properties are defined as the fraction of sunlight striking a surface which undergoes specular reflection, diffuse reflection, or absorption. These surface optical properties are typical values from measurements on these materials.

Material	Specular Reflection	Diffuse Reflection	Absorption
Aluminum	0.06	0.60	0.34
FEP (Aluminized Teflon)	0.83	0.10	0.07
Yellow Paint Chem Glaze-II	0.05	0.50	0.45

Figure 1.2-1. Surface Properties of Some Materials for Solar Scattering.

2.0 S0069 THERMAL CONTROL SURFACES EXPERIMENT

2.1 Experiment Location and Description

The S0069 thermal control surfaces experiment is located in LDEF experiment tray 9A. Figure 2.1-1 (and color photo A2.1-1, p. A2) shows the location of this experiment. Row 9 is the LDEF row most nearly facing ram direction. All surfaces on the experiment are FEP except for the experiment disk, which is modeled as an aluminum surface.

2.2 Atomic Oxygen Exposure

Figure 2.2-1 shows LDEF mission atomic oxygen exposure to the S0069 thermal control surfaces experiment. Several AO fluences in log atoms/cm^2 are marked. Because the experiment is facing nearly directly into the ram direction, it receives a nearly uniform AO exposure of approximately 7.5 x 10^{21} to 9.1 x 10^{21} atoms/cm^2. The slightly increased exposure on the flat surfaces on either side of the central rib in the upper half of the figure is due mostly to specular reflections from the sides of the central rib.

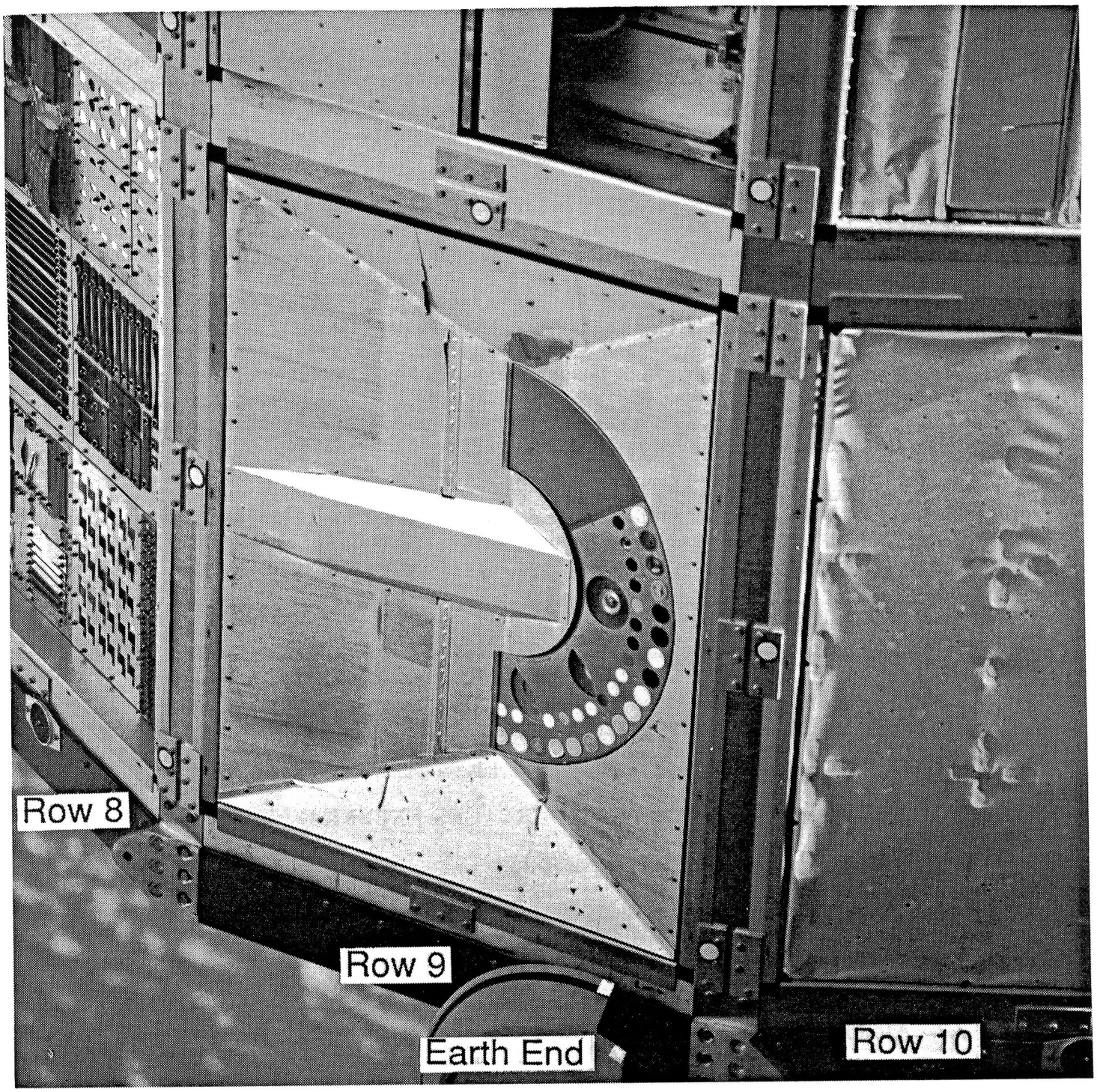

Figure 2.1-1. S0069 Thermal Control Surfaces Experiment On-Orbit Photo.

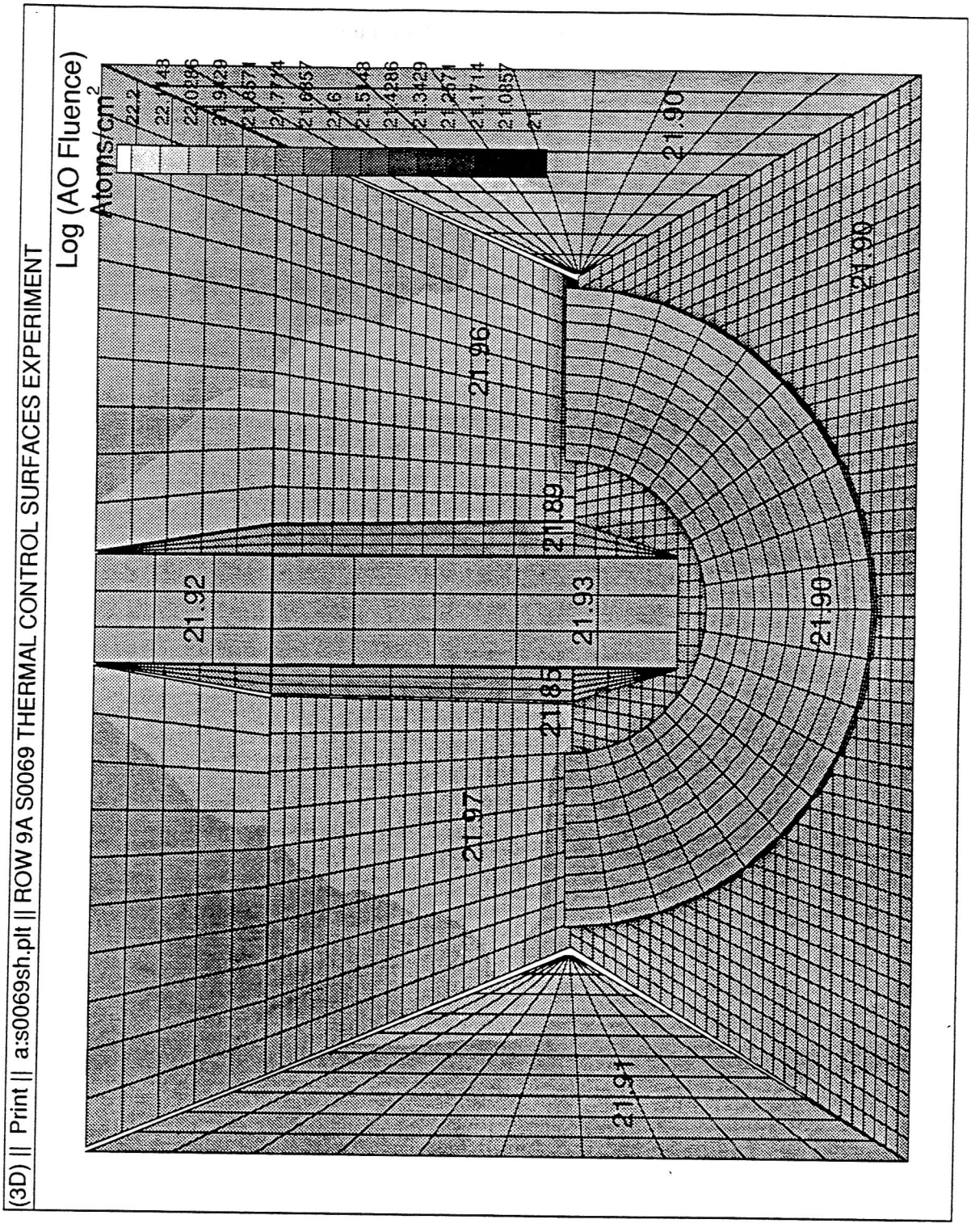

Figure 2.2-1. S0069 Thermal Control Surfaces Experiment Atomic Oxygen Exposure Given as Log_{10} AO Fluence (Atoms/cm^2).

2.3 Solar Exposure

Figure 2.3-1 shows LDEF mission solar exposure in CESH to the S0069 thermal control surfaces experiment. The disk shaped experiment wheel on the bottom of the figure is toward row 10 and the right side of the figure corresponds to the space-end side of the experiment. As oriented on the spacecraft, the right side of the central rib receives the highest solar exposure because it is the surface most nearly perpendicular to the average Sun direction. The left side of the rib is in the shade most often and receives the lowest solar exposure. The left side triangular surface receives somewhat less exposure than the right side of the central rib because the triangular surface is less nearly perpendicular to the average Sun position than the right side of the central rib. The partially shaded right side triangular surface receives about two thirds the exposure of the right side of the central rib. This triangular surface receives about a 5% CESH enhancement near its apex due to reflections from other surfaces. The area of the bottom large trapezoidal surface around the experiment disk shows increased CESH due to reflections from the sunny side of the disk edge due to reflections and shows decreased CESH due to shadowing on the shady side.

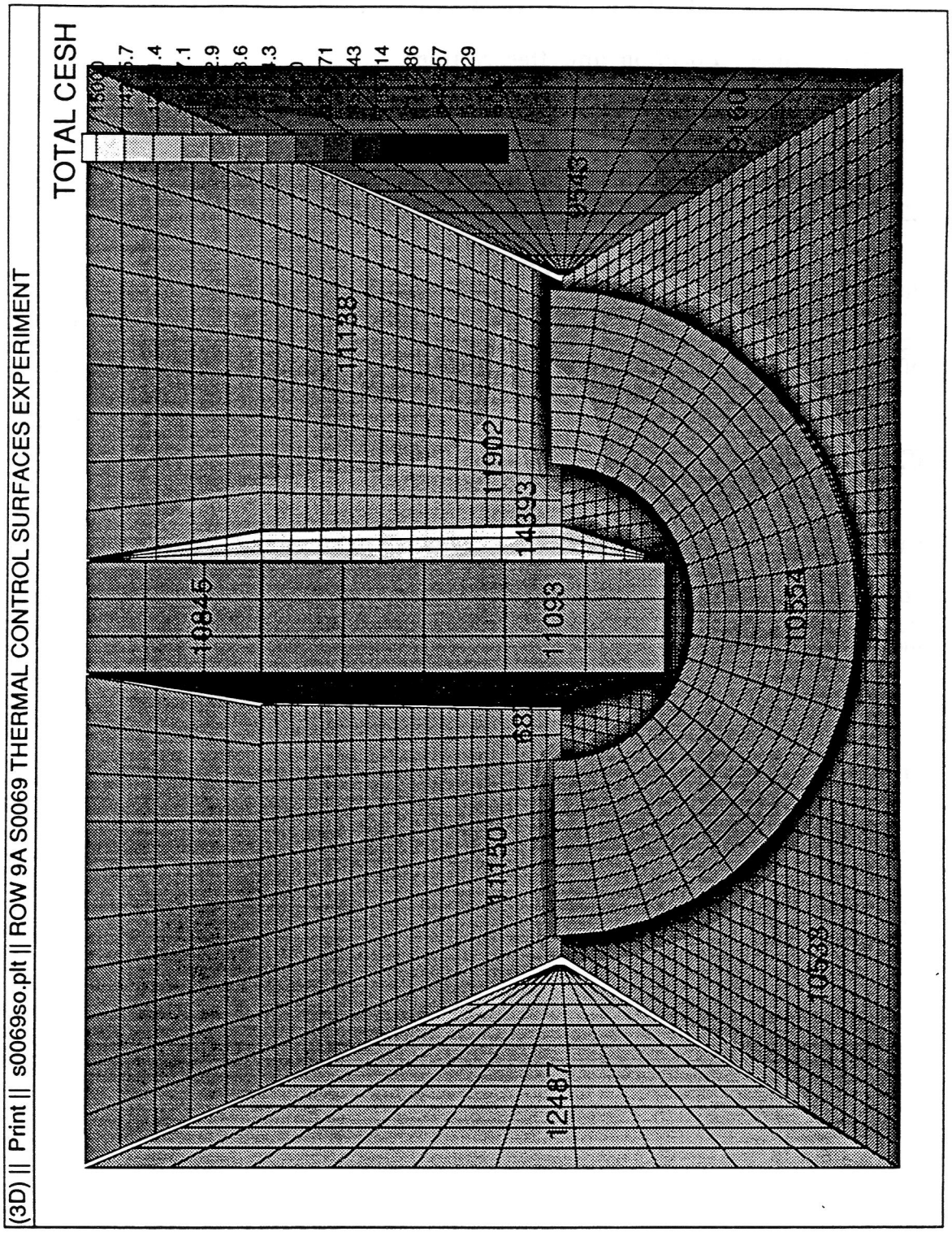

Figure 2.3-1. S0069 Thermal Control Surfaces Experiment Solar Exposure in CESH.

3.0 ROW 6 FEP BLANKET EDGE ADJACENT TO ROW 7

3.1 Experiment Location and Description

The row 6 FEP blanket edge is on the side of row 6 next to row 7. The FEP blanket is folded into the LDEF to meet the aluminum row 6 tray edge. Row 6 is oriented with its outward surface normal 98.1 degrees from the ram direction.

3.2 Atomic Oxygen Exposure

Figure 3.2-1 shows the LDEF mission AO fluence to the FEP blanket and the aluminum tray edge in the region of the row 6 FEP blanket fold at the tray edge parallel to row 7. In the figure, the FEP blanket is on the left and the aluminum tray edge is on the right. Figure 3.2-2 shows a cross section of the AO exposure. Total, primary, specular reflected and diffuse reflected AO fluences are reported. The cross section is taken along a line on the surfaces about midway from top to bottom in figure 3.2-1. Distance (the horizontal axis) in the cross section is measured from the left side of the FEP blanket in figure 3.2-1 along the surface of the blanket and the aluminum tray side to the right side of the aluminum tray .

Figure 3.2-2 shows that, depending on position, either primary AO or reflected AO may be responsible for most of the fluence. Reflected AO fluence contributes essentially all of the dose in the "V" of the blanket fold and tray side while primary AO impacts contribute most of the fluence to the parallel flat surfaces of the FEP blanket and tray edge. Atomic oxygen fluence on the flat surfaces parallel to row 6 is approximately 0.3 percent of the fluence on a ram facing surface.

Due to the orientation of row 6, it is shadowed from direct exposure to AO from any direction within 8.1 degrees of the ram direction. The AO fluence as a function of angle from ram decreases very rapidly as the angle from ram increases. The fluence on a surface is the fluence from all allowed directions times the projected area of the surface to each direction (that is, the area of the surface times the cosine of the angle between the outward surface normal vector and the fluence direction). We may assume, with little loss of accuracy, that the vast majority of the direct fluence comes from angles as near to ram as possible. Consideration of these two factors explains the shape of the primary AO fluence cross section. As expected, the primary AO fluence on the FEP surface parallel to row 6 is constant at about 0.3 percent of the ram fluence because of the small projected area of the plane surface.

The shape of the primary fluence curve on the curved portion of the FEP blanket (from left to right, a small increase in fluence followed by a decrease followed by an increase to a maximum followed by a rapid decrease to near zero fluence as the cross section drops in the "V") occurs because of the interaction of directional fluence and surface normal angle. Because the aluminum tray edge is assumed to be 2 mm above the FEP blanket, the angle to ram from which primary AO fluence can come increases as one traverses the surface from left to right. At the same time, the cosine of the angle between the surface normal and the direction of maximum allowed fluence increases. The interaction of these two factors, which both vary nonlinearly with distance, accounts for the shape of the primary fluence on the curved surface of the FEP blanket.

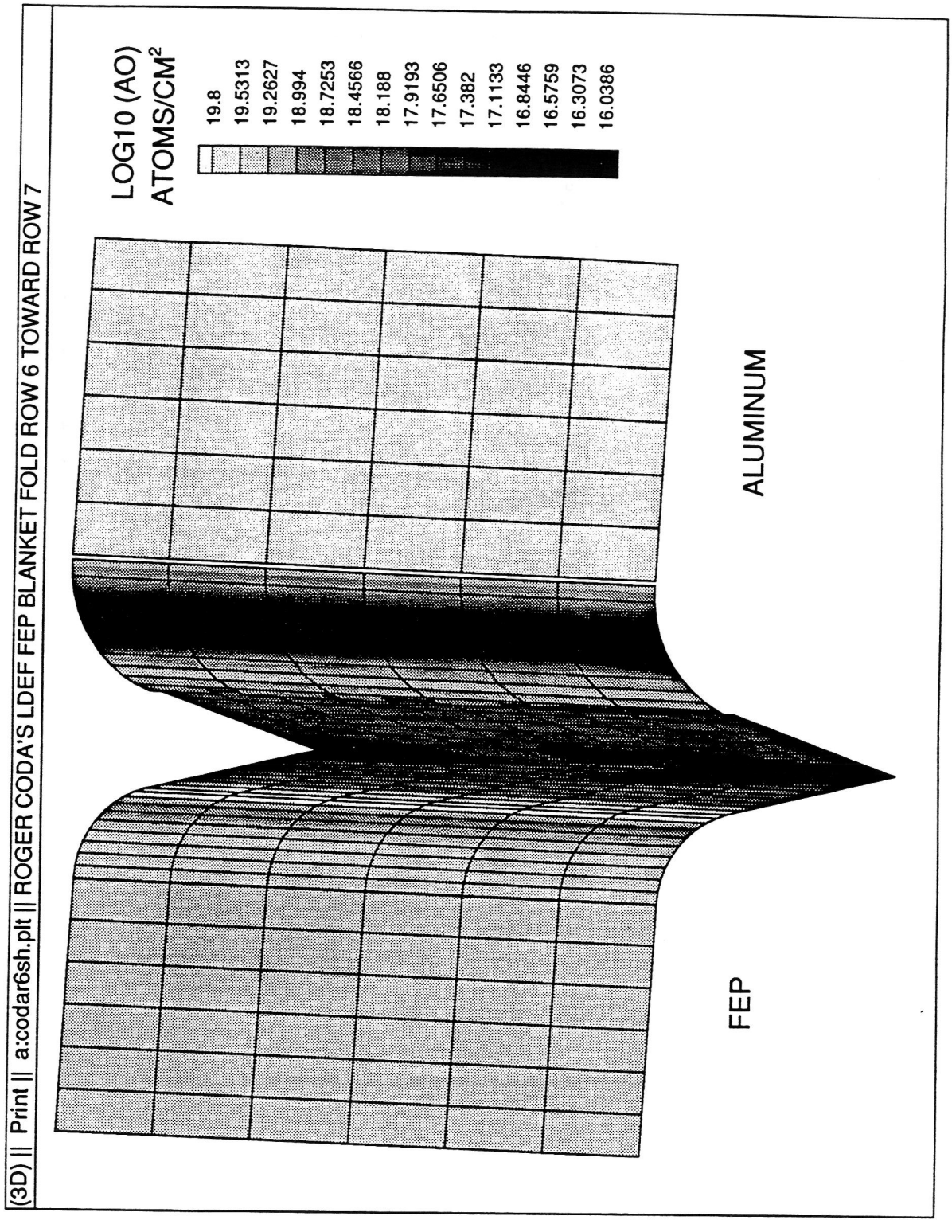

3.2-1. Row 6 Toward Row 7 FEP Blanket Fold Atomic Oxygen Exposure Given as Log_{10} AO Fluence (Atoms/cm^2).

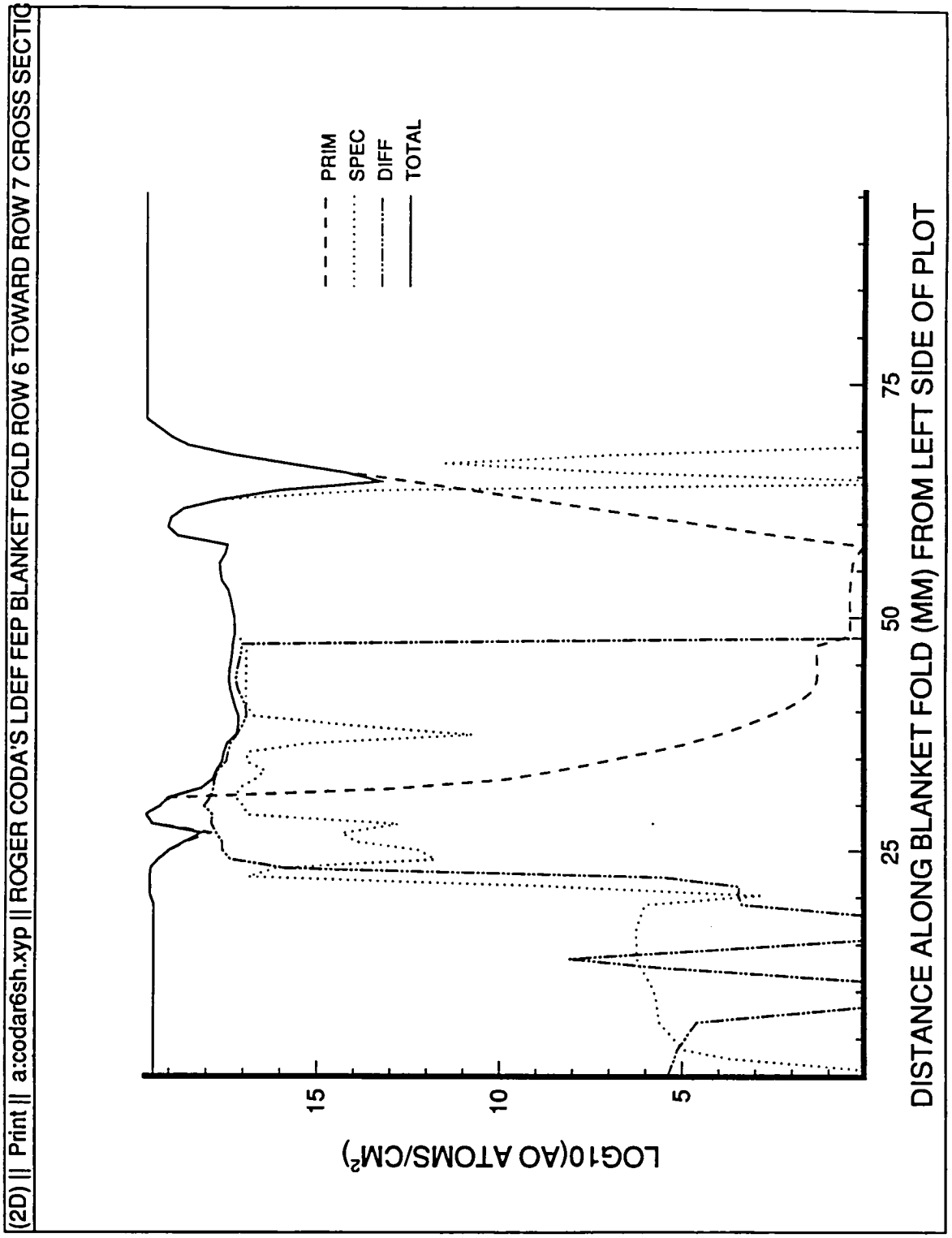

Figure 3.2-2. Atomic Oxygen Exposure Cross Section of Figure 3.2-1.

The relatively constant total AO fluence in the "V" between the FEP blanket and the tray edge is due to specular reflection from the FEP to the aluminum and to both specular and diffuse reflection from the aluminum to the FEP. If both materials were specular reflectors, the "V" would act as a trap concentrating AO at the bottom on the "V," leaving recombination and surface reactivity as the primary removal mechanisms. This would yield a high concentration of AO at the point of the "V." The 0.46 diffuse reflectivity of aluminum allows enough AO to escape to space to balance the concentrating effects of specular reflection.

The fluence peak at approximately 60 mm in figure 3.2-2 is due almost entirely to specular reflection from the FEP peak fluence at about 28 mm.

3.3 Solar Exposure

Figure 3.3-1 shows the LDEF mission solar exposure to the FEP blanket and the aluminum tray edge in the region of the row 6 FEP blanket fold at the tray edge parallel to row 7. Figure 3.3-2 shows a cross section of the solar exposure. Solar exposure is given for total direct and Earth-reflected solar exposure (GRTOT), direct primary solar exposure (PRIM), direct specular reflected solar exposure (SPEC), direct diffuse reflected solar exposure (DIFF), and total direct solar exposure (TOTAL). The cross section is taken along a line on the surfaces about midway from top to bottom in figure 3.3-1. Distance (the horizontal axis) in the cross section is measured from the left side of the FEP blanket in figure 3.3-1 along the surface of the blanket and the aluminum tray side to the right side of the aluminum tray .

Examination of figure 3.3-2 shows that approximately one fourth of the total solar exposure is due to Earth-reflected solar radiation (the difference between the total direct and Earth reflected solar exposure and total direct solar exposure). As with the AO exposure, the solar exposure to the flat FEP and aluminum surfaces parallel to row 6 is constant. The average Sun position is most nearly perpendicular to the curved part of the aluminum tray and results in the highest exposure to this surface because of the combined effects of direct and reflected solar radiation. Nearly all of the exposure in the "V" is due to reflections. That on the FEP is due mainly to diffuse reflection from the aluminum side of the "V"; that on the aluminum is due mainly to specular reflection from the FEP side of the "V."

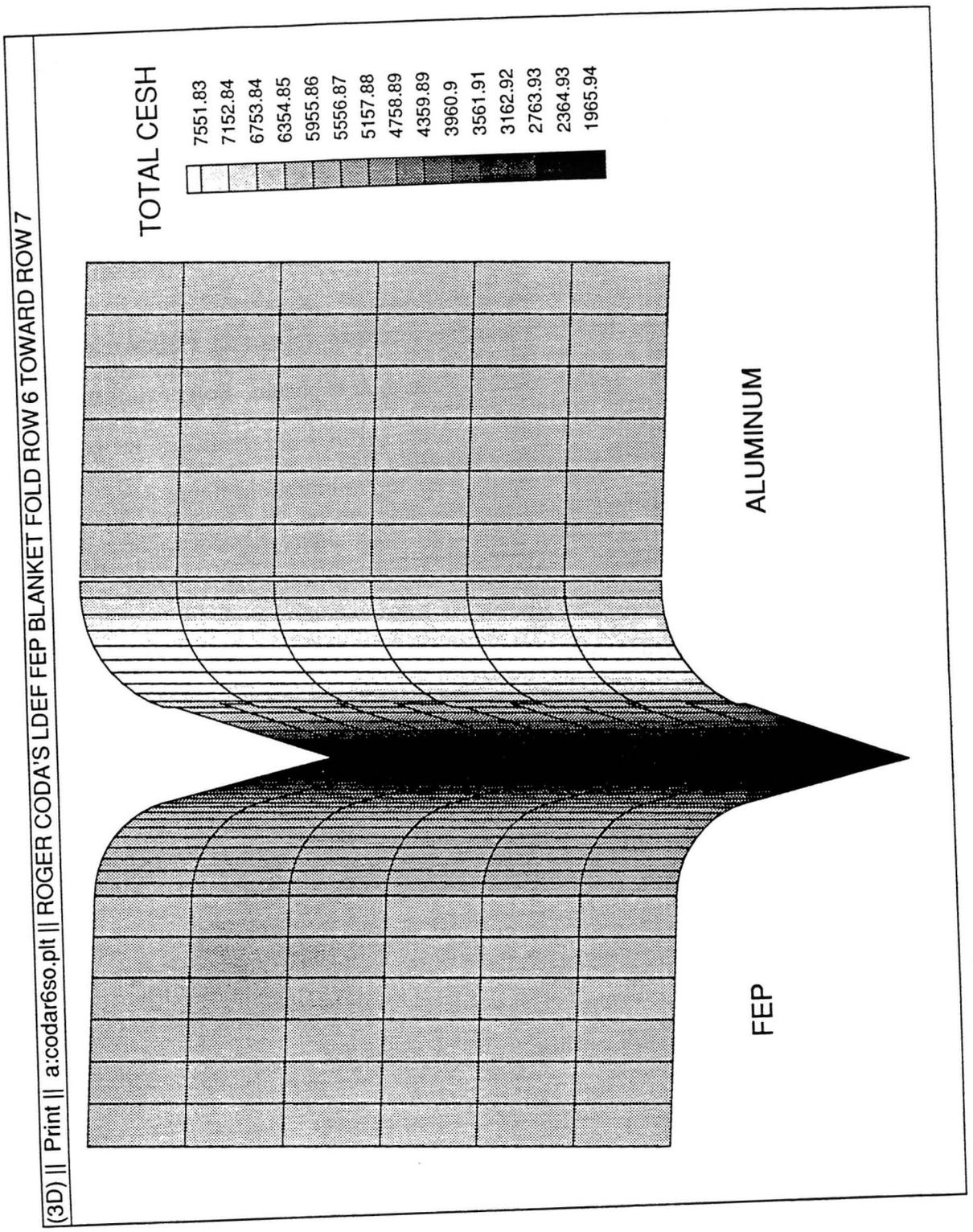

Figure 3.3-1. Row 6 Toward Row 7 FEP Blanket Fold Solar Exposure in CESH.

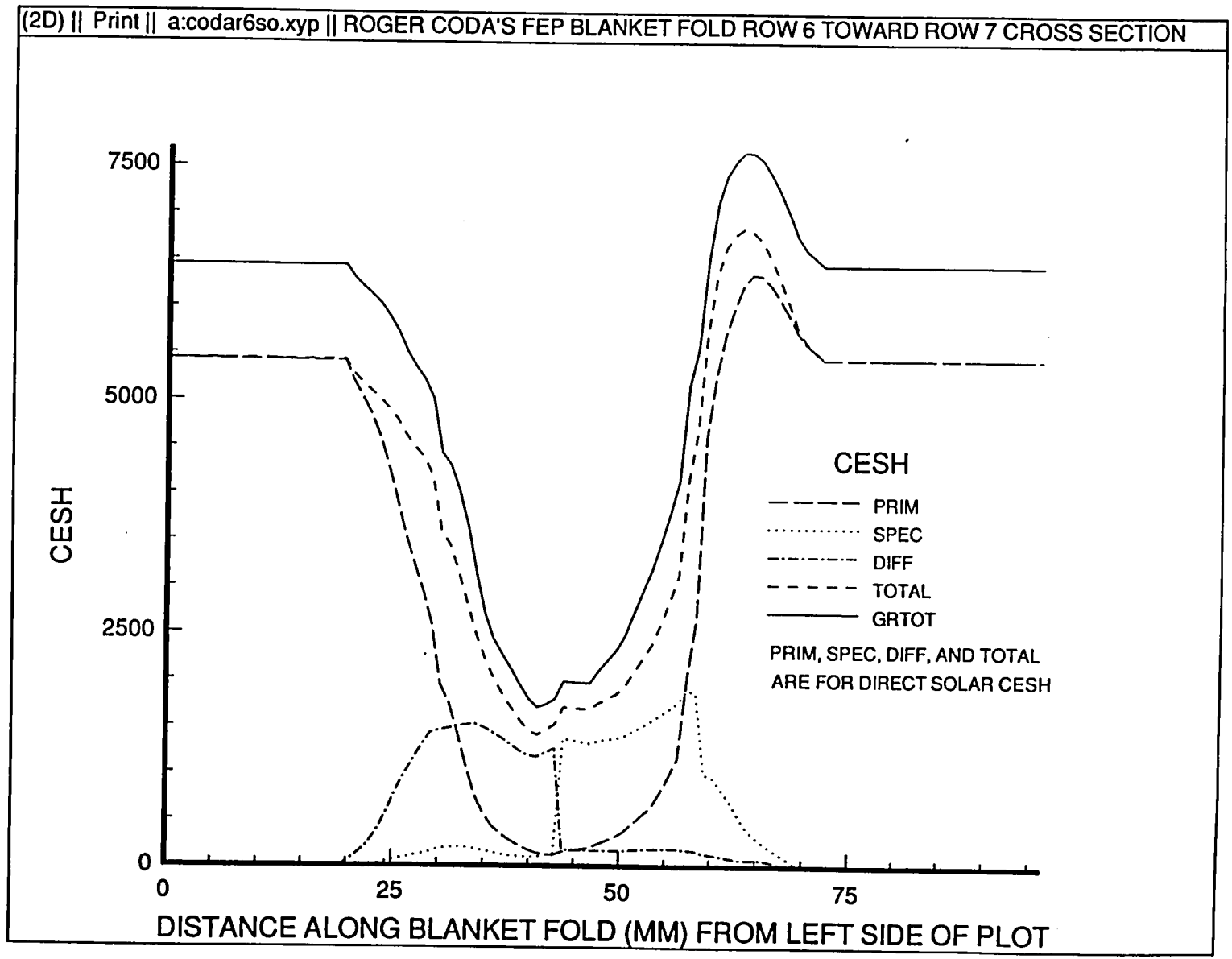

Figure 3.3-2. Solar Exposure Cross Section of Figure 3.3-1.

4.0 ROW 7 FEP BLANKET FOLD TOWARD ROW 6

4.1 Experiment Location and Description

The row 7 FEP blanket fold on the edge of row 7 next to row 6 is shown in figure 4.1-1 (and color photo A4.1-1, p. A3). The FEP blanket is folded into the LDEF to meet the aluminum row 7 tray edge. Row 7 is oriented with its outward surface normal 68.1 degrees from the ram direction. The row 7 FEP blanket fold is on the opposite side of the longeron between rows 6 and 7 from the row 6 FEP blanket fold. The primary difference between the two blanket folds is that row 7 receives much higher AO exposure than does row 6. Both rows receive similar solar exposure.

4.2 Atomic Oxygen Exposure

Figure 4.2-1 shows the LDEF mission AO fluence to the FEP blanket and the aluminum tray edge in the region of the row 7 FEP blanket fold at the tray edge parallel to row 6. Figure 4.2-2 shows a cross section of the AO exposure. Total, primary, specular reflected and diffuse reflected AO fluences are reported. The cross section is taken along a line on the surfaces about midway from top to bottom in figure 4.2-1. Distance (the horizontal axis) in the cross section is measured from the left side of the aluminum tray in Figure 4.2-1 along the surface of the tray and the FEP blanket to the right side of the FEP blanket .

As with the row 6 FEP blanket fold described in the preceding section, figure 4.2-2 shows that, depending on position, either primary AO or reflected AO may be responsible for most of the exposure to the row 7 FEP blanket fold. Again, reflected AO fluence contributes essentially all of the exposure in the "V" of the blanket fold and tray side while primary AO fluence contributes most of the exposure to the parallel flat surfaces of the FEP blanket and tray edge. The net effect of primary and reflected AO is to give a nearly constant fluence across the blanket fold. Atomic oxygen fluence on the flat surfaces parallel to row 7 is approximately one third of the fluence on a ram facing surface or approximately 100 times the fluence on surfaces parallel to row 6.

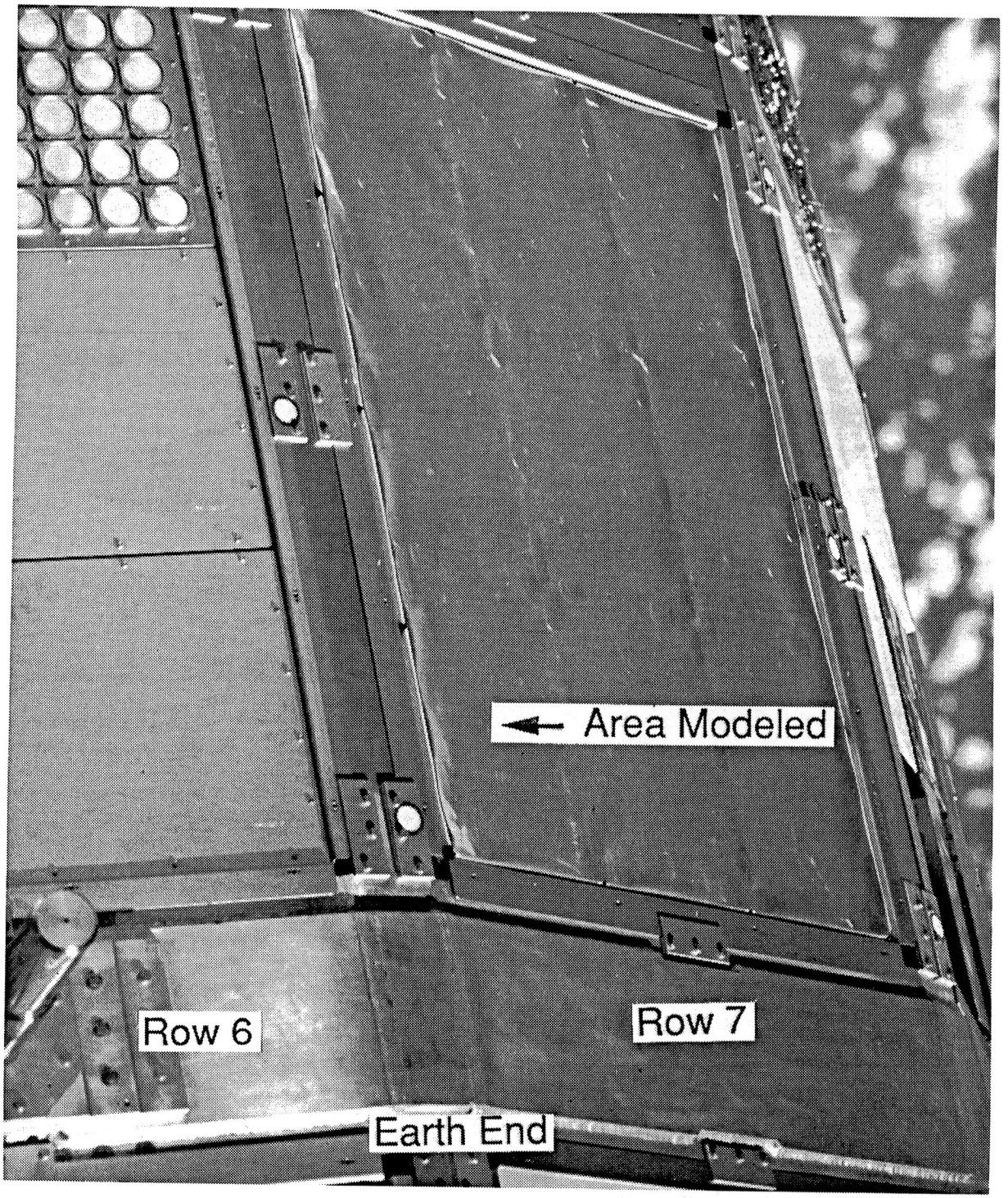

Figure 4.1-1. Row 7 Toward Row 6 FEP Blanket Fold On-Orbit Photo.

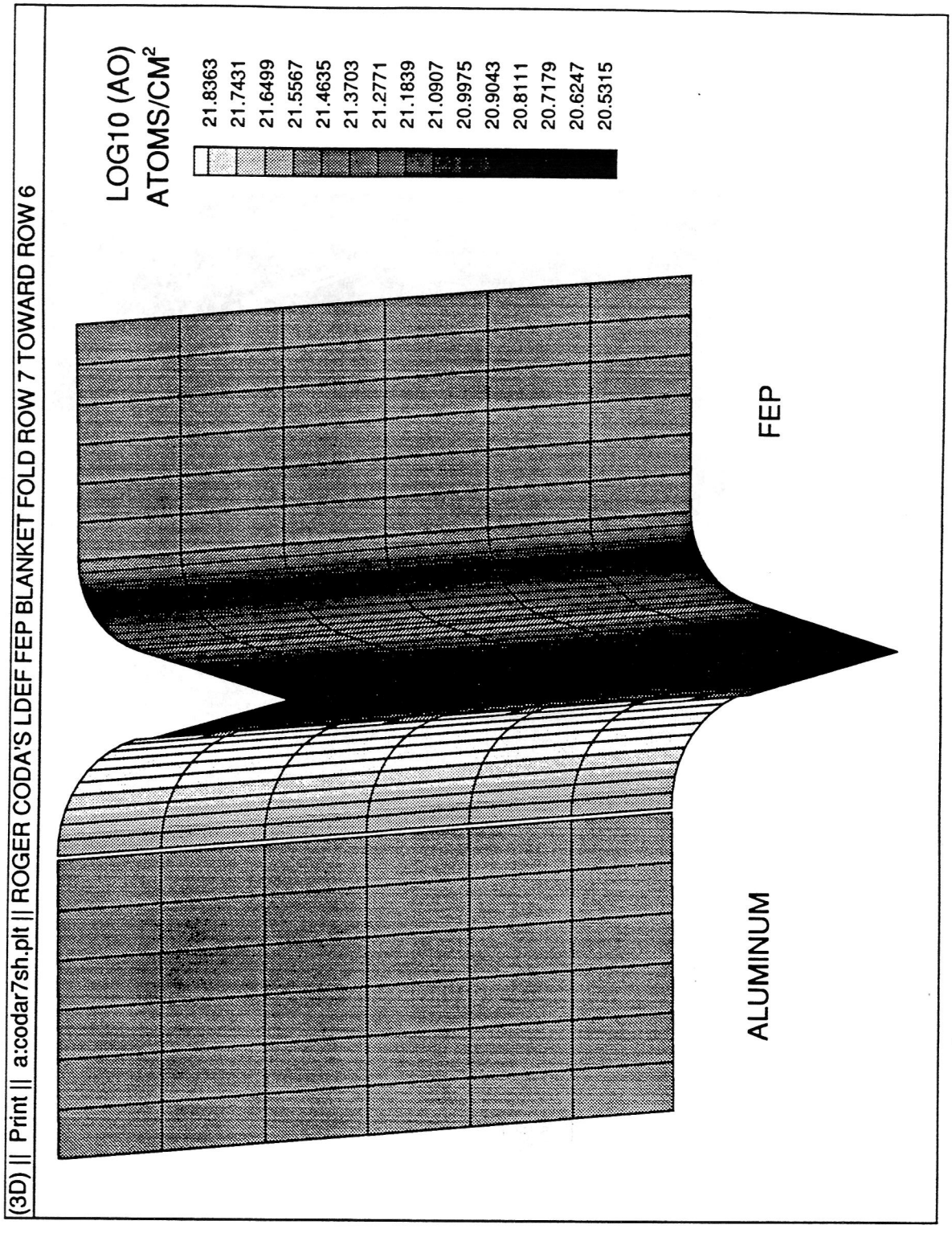

Figure 4.2-1. Row 7 Toward Row 6 FEP Blanket Fold Atomic Oxygen Exposure Given as Log_{10} AO Fluence (Atoms/cm^2).

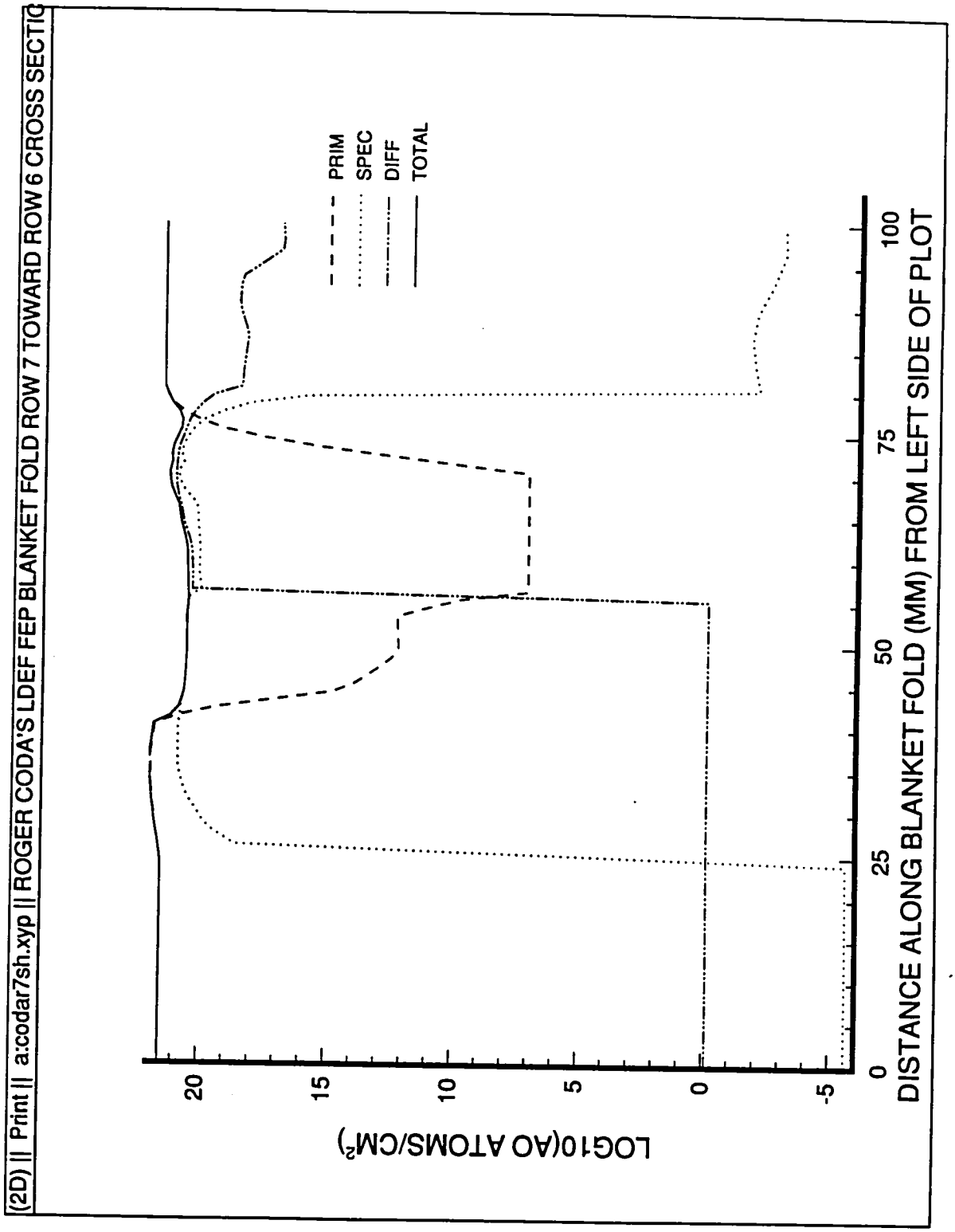

Figure 4.2-2. Atomic Oxygen Exposure Cross Section of Figure 4.2-1.

4.3 Solar Exposure

Figure 4.3-1 shows the LDEF mission solar exposure to the FEP blanket and the aluminum tray edge in the region of the row 7 FEP blanket fold at the tray edge parallel to row 6. Figure 4.3-2 shows a cross section of the solar exposure. Solar exposure is given for total direct and Earth-reflected solar exposure (GRTOT), direct primary solar exposure (PRIM), direct specular reflected solar exposure (SPEC), direct diffuse reflected solar exposure (DIFF), and total direct solar exposure (TOTAL). The cross section is taken along a line on the surfaces about midway from top to bottom in figure 4.3-1. Distance (the horizontal axis) in the cross section is measured from the left side of the aluminum tray side in figure 4.3-1 along the surface of the tray side and the FEP blanket to the right side of the FEP blanket.

Examination of figure 4.3-2 shows that it is approximately a mirror image of figure 3.3.2. As in figure 3.3.2, approximately one fourth of the total solar exposure is due to Earth-reflected solar radiation (the difference between the total direct and Earth reflected solar exposure and total direct solar exposure). The solar exposure to the flat FEP and aluminum surfaces parallel to row 7 is constant. The average Sun position is most nearly perpendicular to the curved part of the aluminum tray and results in the highest exposure to this surface because of the combined effects of direct and reflected solar radiation. Nearly all of the exposure in the "V" is due to reflections. That on the FEP is due mainly to diffuse reflection from the aluminum side of the "V"; that on the aluminum is due mainly to specular reflection from the FEP side of the "V."

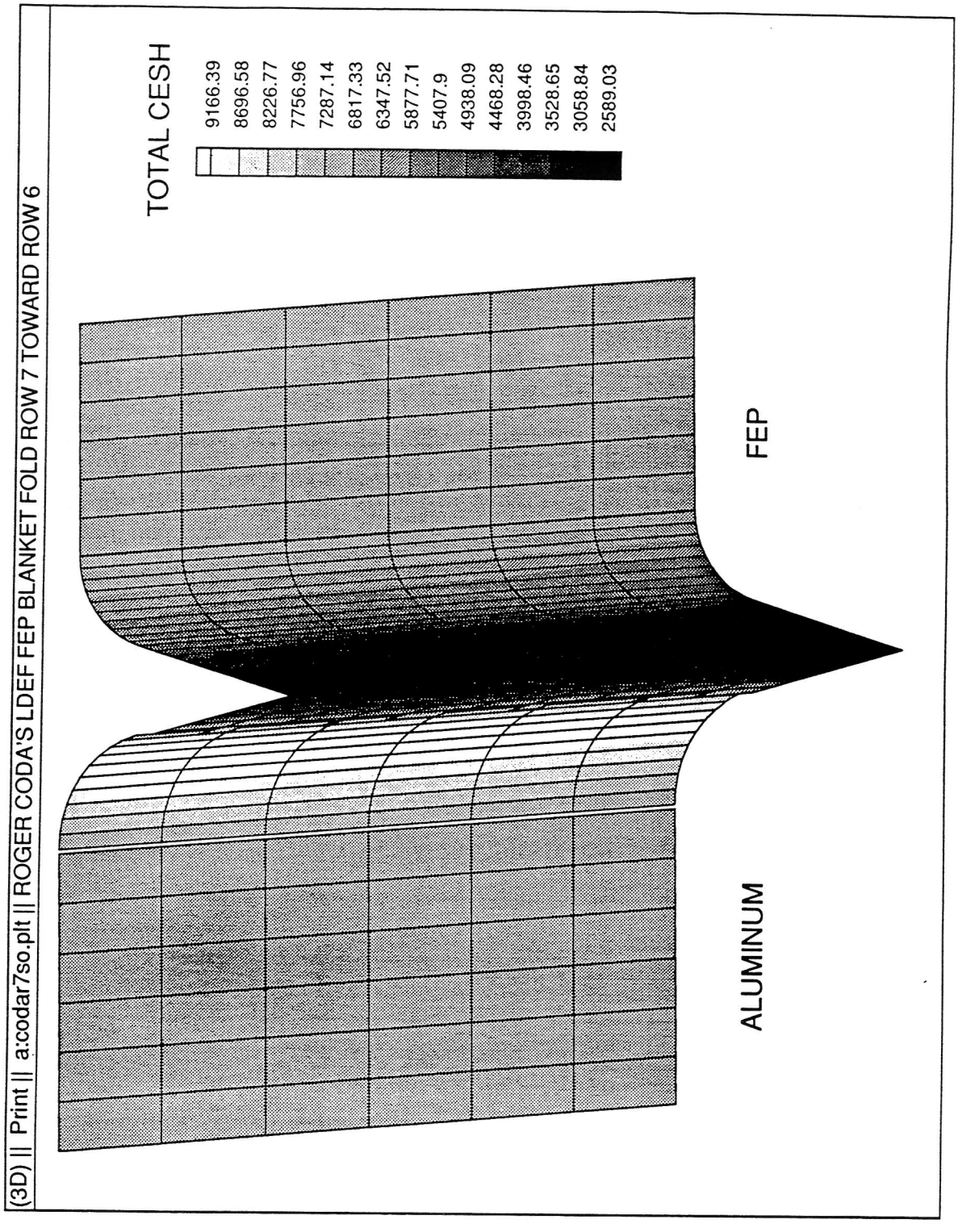

Figure 4.3-1. Row 7 Toward Row 6 FEP Blanket Fold Solar Exposure in CESH.

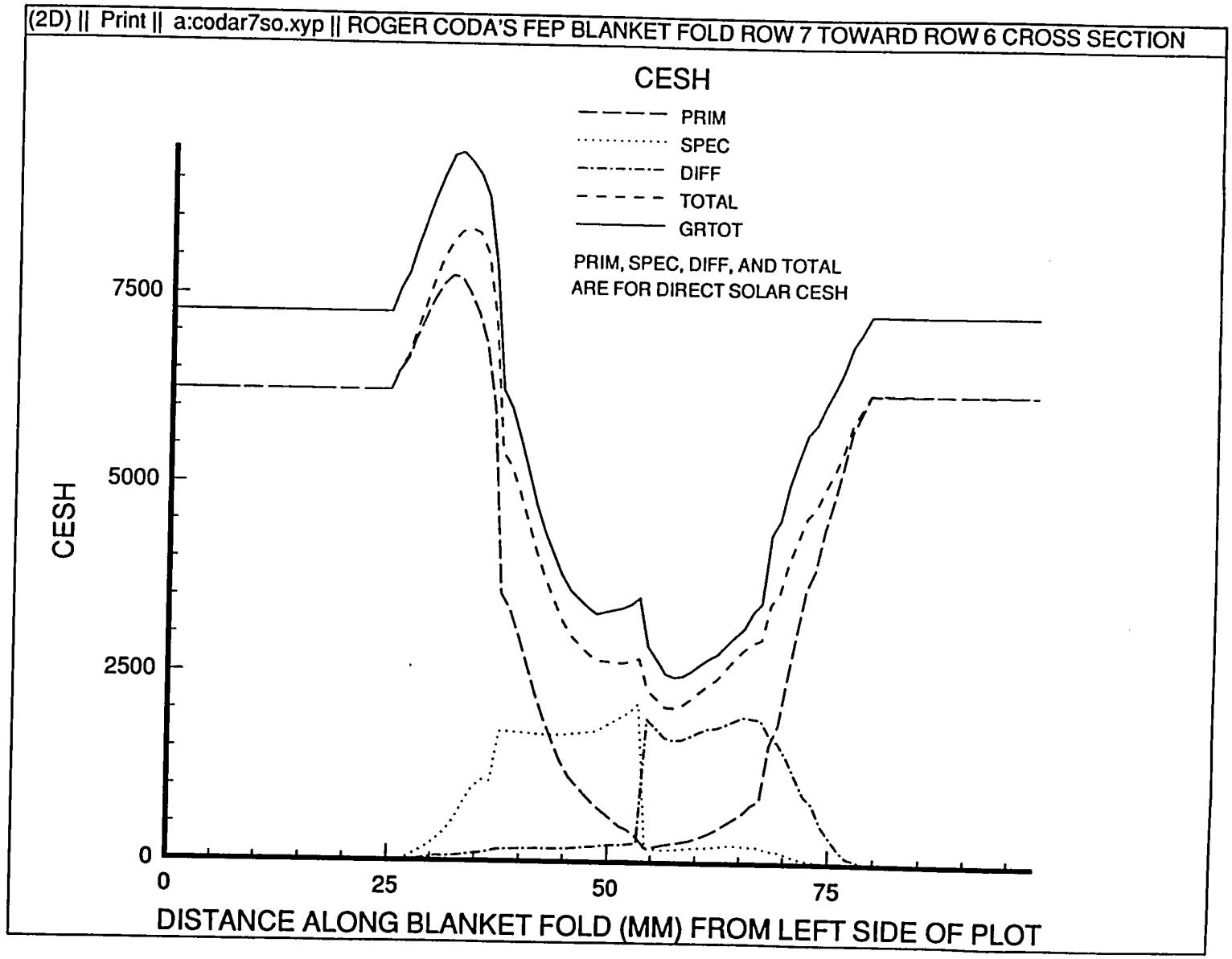

Figure 4.3-2. Solar Exposure Cross Section of Figure 4.3-1.

5.0 M0001 NRL COSMIC RAY EXPERIMENT

5.1 Experiment Location and Description

The M0001 NRL cosmic ray experiment is located on the space end of LDEF as shown in figure 5.1-1 (and color photo A5.1-1, p. A4). The experiment is modeled as a square FEP plate surrounded by a square sided trough. The inner and bottom walls of the trough are FEP and the outer walls are aluminum.

5.2 Atomic Oxygen Exposure

Figure 5.2-1 shows LDEF mission atomic oxygen fluence to the M0001 NRL cosmic ray experiment. In the figure, the active side of the surfaces making up the edges of the trough face the inside of the trough. The left side of the figure faces ram, with the ram direction oriented to the left and 8.1 degrees below horizontal in the figure. The large space-facing top plate receives uniform primary AO and no reflected AO. The trough receives the highest AO fluence in the upper and lower right outer corners due to the upper and lower sections of the trough being nearly aligned with the ram direction.

Figures 5.2-2 and 5.2-3 show the total, primary, specularly reflected and diffusely reflected AO fluence cross section down the middle of the top and bottom troughs, respectively, from left to right. In the figures, the distance is measured from the top of the left outside edge of the trough, down the edge, across the bottom to the bottom of the right outside edge, and up to the top of the edge. Because of an artifact of TECPLOT, the portion of the bottom of the trough shaded by the left vertical side of the trough is not included in the cross sections. The cross sections for the top and bottom troughs are quite similar. The left edge of the trough receives most of its exposure from specular reflection from the inside walls of the the trough. As one moves from left to right along the bottom of the trough, specular reflection generally dominates over primary and diffuse fluences. On the right vertical end of the trough primary AO fluence dominates, although diffuse and specular AO fluences are also significant.

Figures 5.2-4 and 5.2-5 show the the total, primary, specularly reflected and diffusely reflected AO fluence cross section of the left and right troughs, respectively, approximately down the middle from top to bottom. The cross sections are taken from top to bottom in the same manner as the cross sections in figures 5.2-2 and 5.2-3. The left trough shows relatively constant total fluence due mostly to diffusely reflected fluence. The right trough shows decreased fluence away from the ends. In both cases diffuse reflections contribute the majority of the fluence.

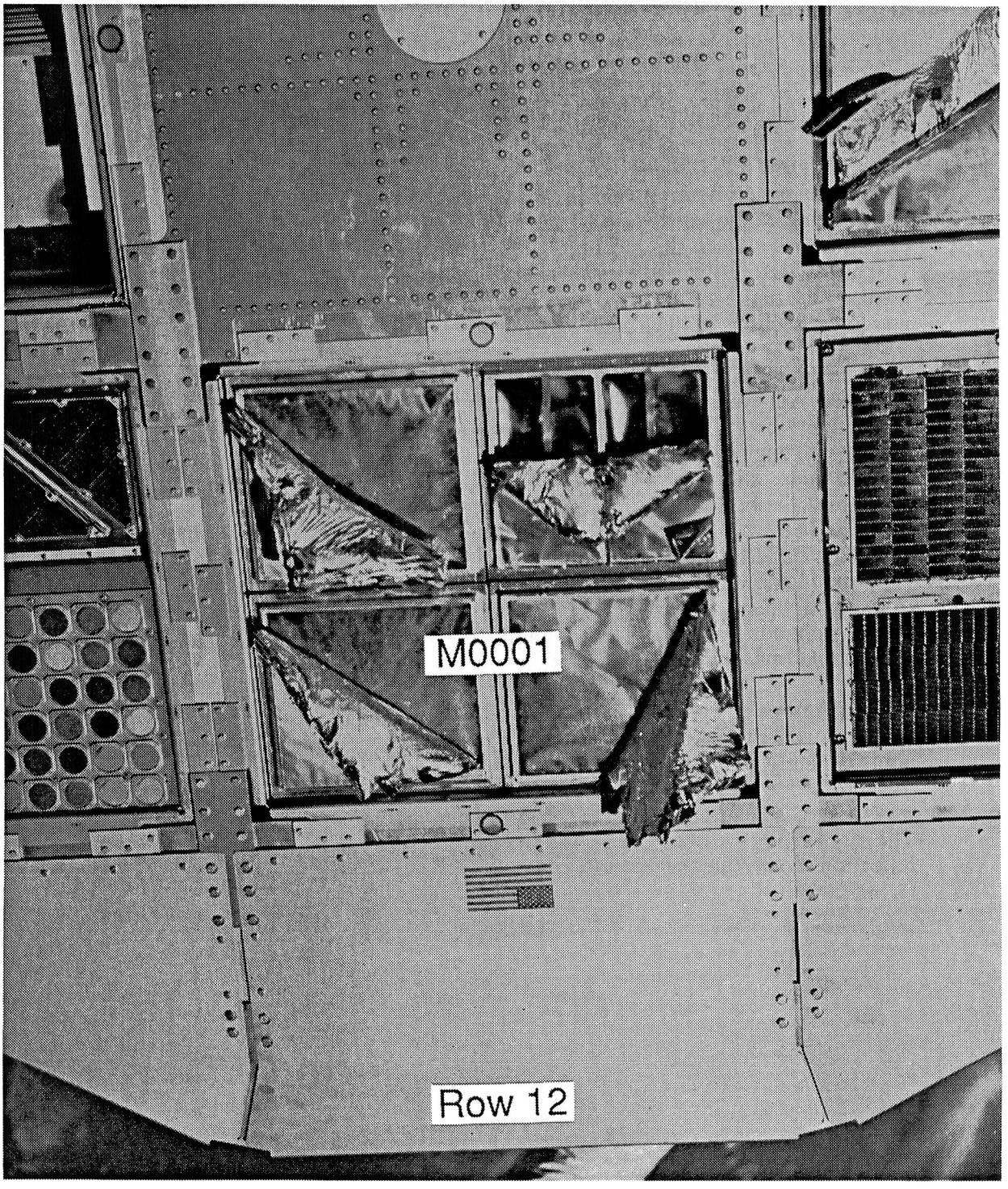

Figure 5.1-1. M0001 NRL Cosmic Ray Experiment On-Orbit Photo.

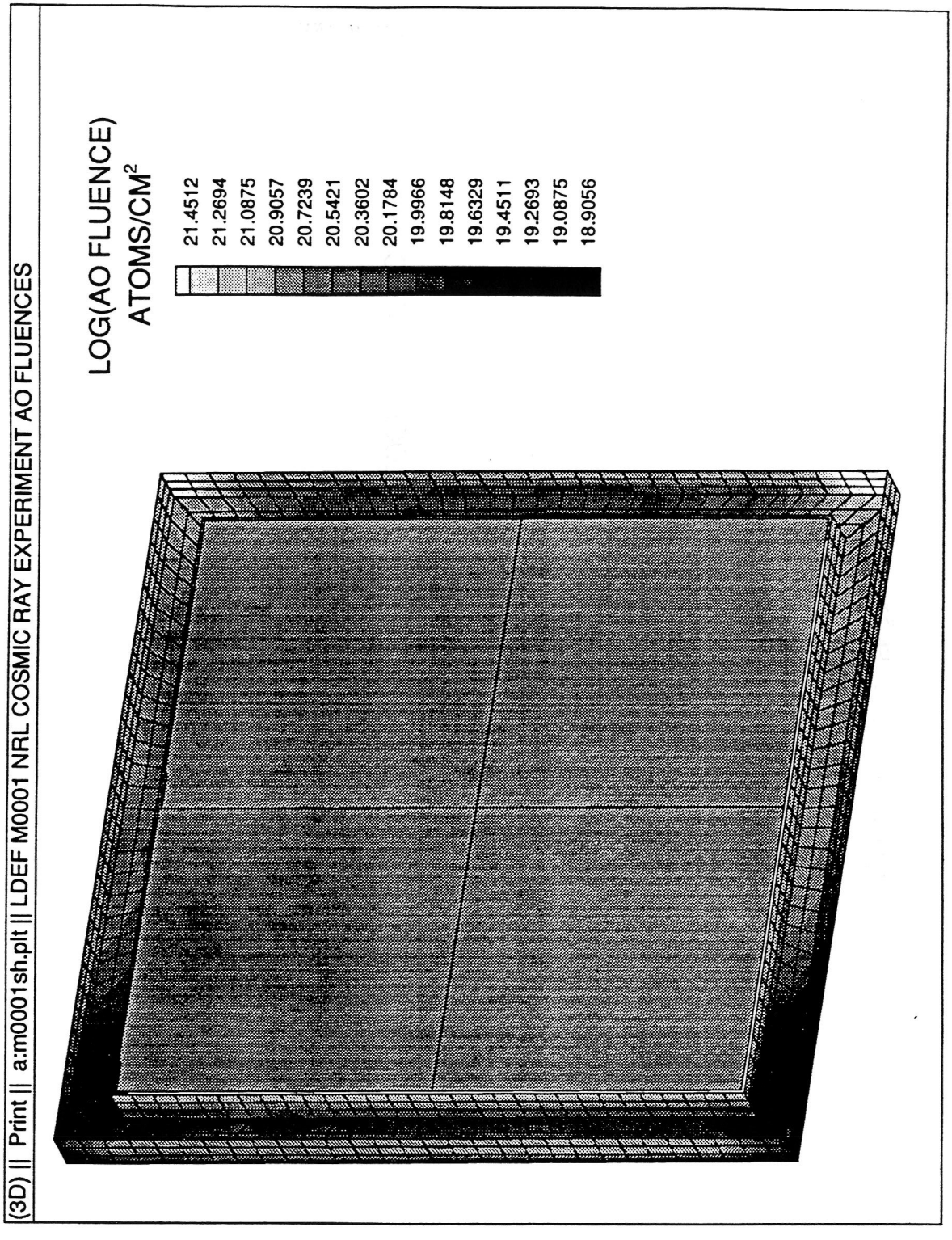

Figure 5.2-1. M0001 NRL Cosmic Ray Experiment Atomic Oxygen Exposure Given as Log_{10} AO Fluence (Atoms/cm^2).

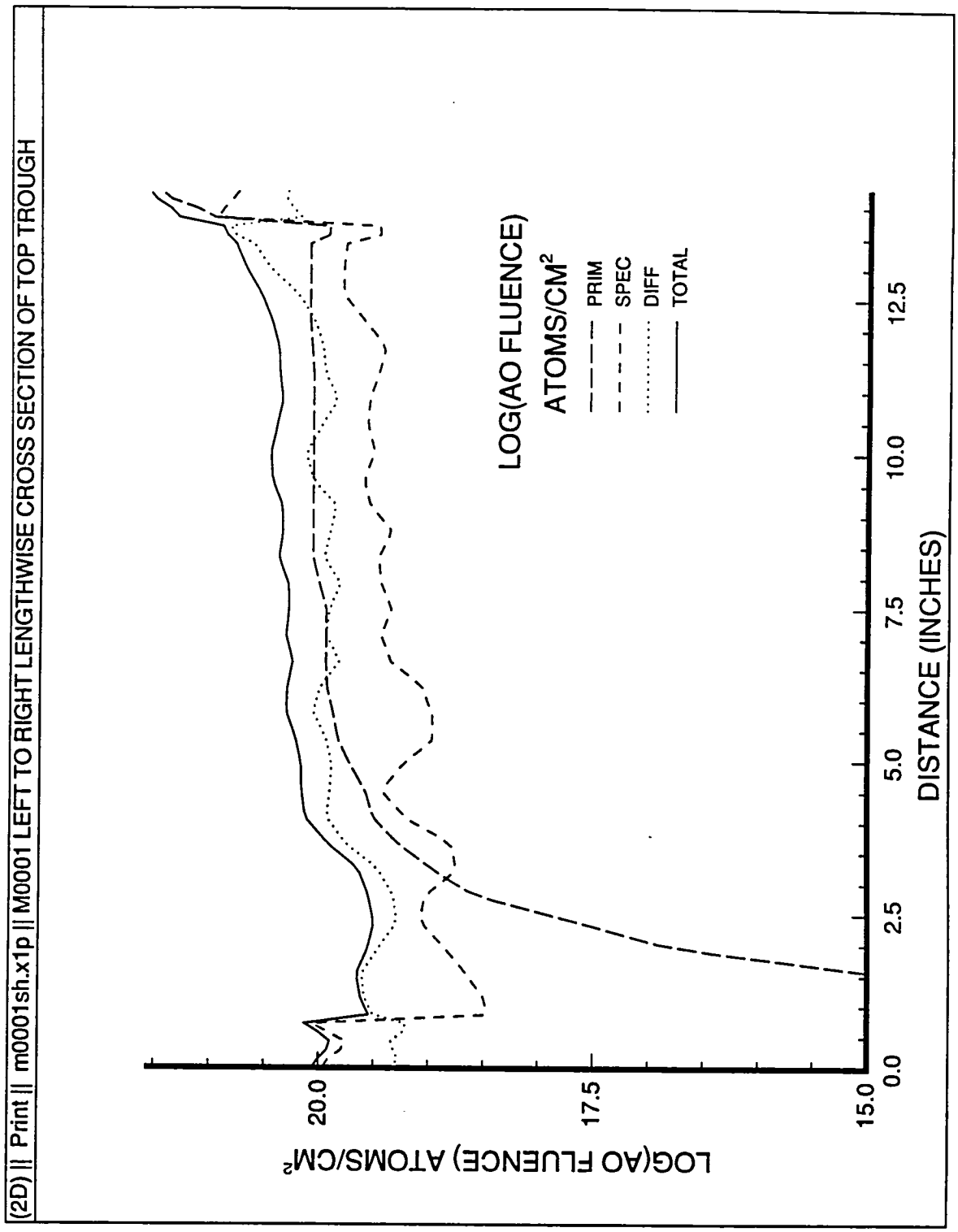

Figure 5.2-2. M0001 NRL Cosmic Ray Experiment Atomic Oxygen Fluence Cross Section From Left to Right Along the Upper Trough in Figure 5.2-1.

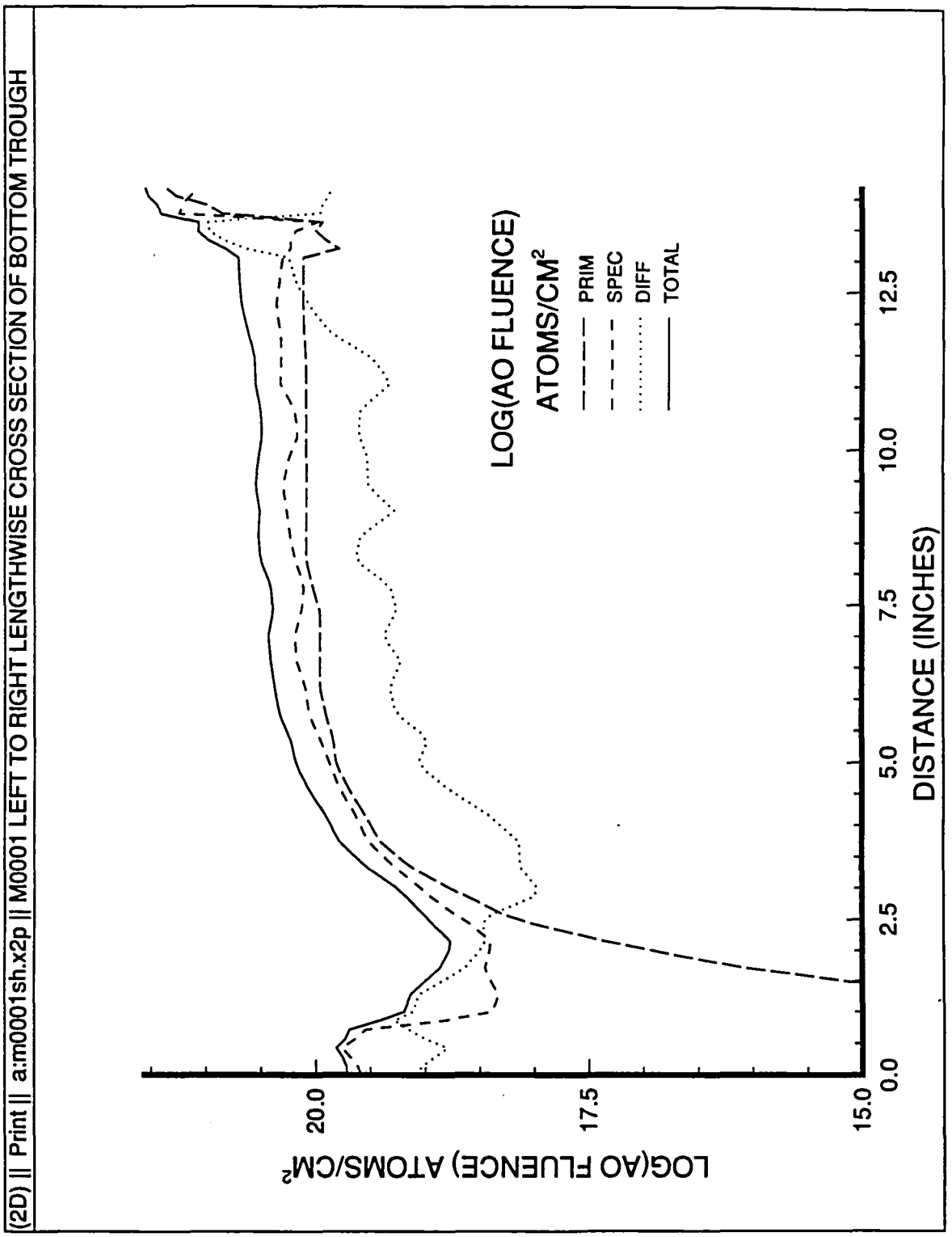

Figure 5.2-3. M0001 NRL Cosmic Ray Experiment Atomic Oxygen Fluence Cross Section From Left to Right Along the Lower Trough in Figure 5.2-1.

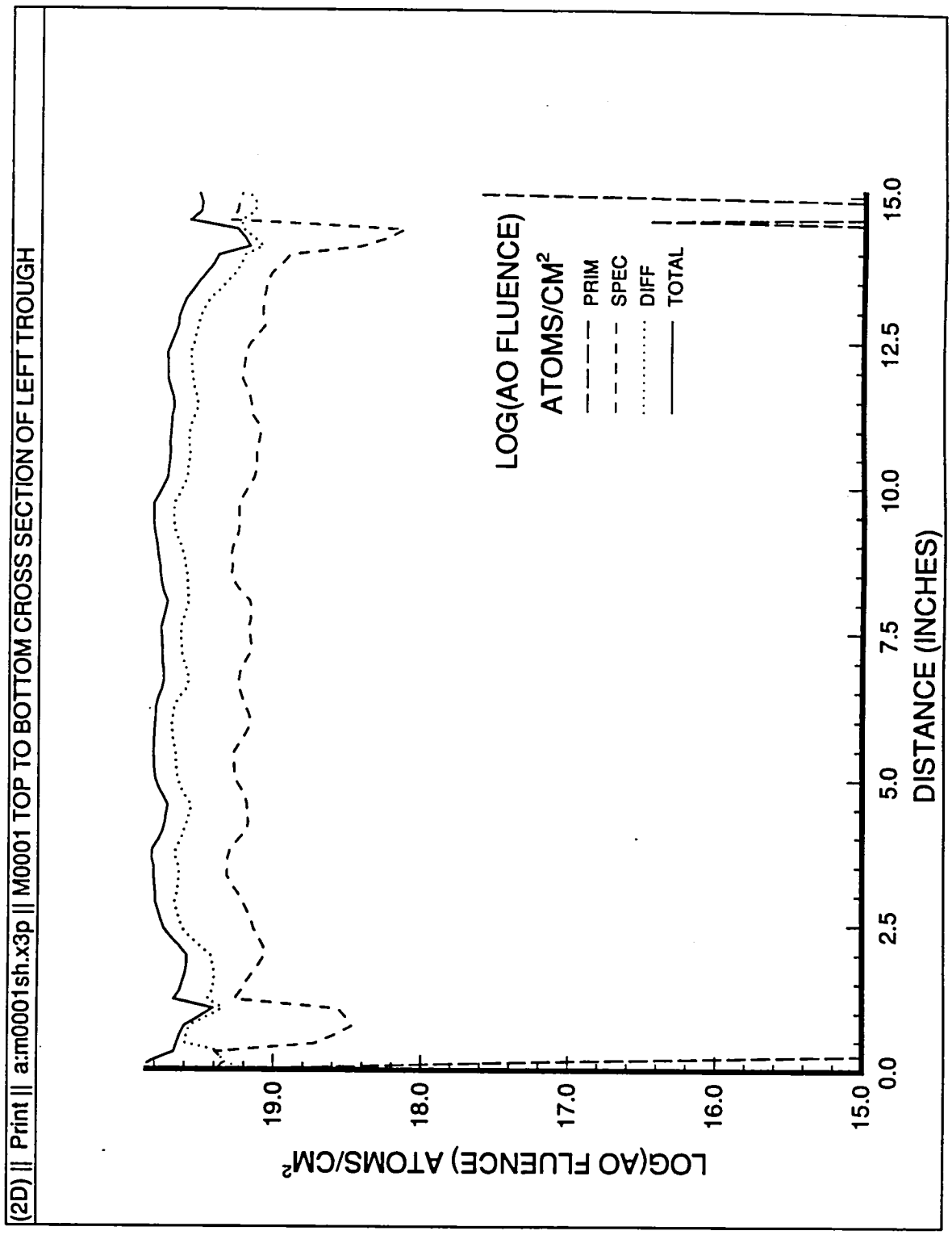

Figure 5.2-4. M0001 NRL Cosmic Ray Experiment Atomic Oxygen Fluence Cross Section From Top to Bottom Along the Left Trough in Figure 5.2-1.

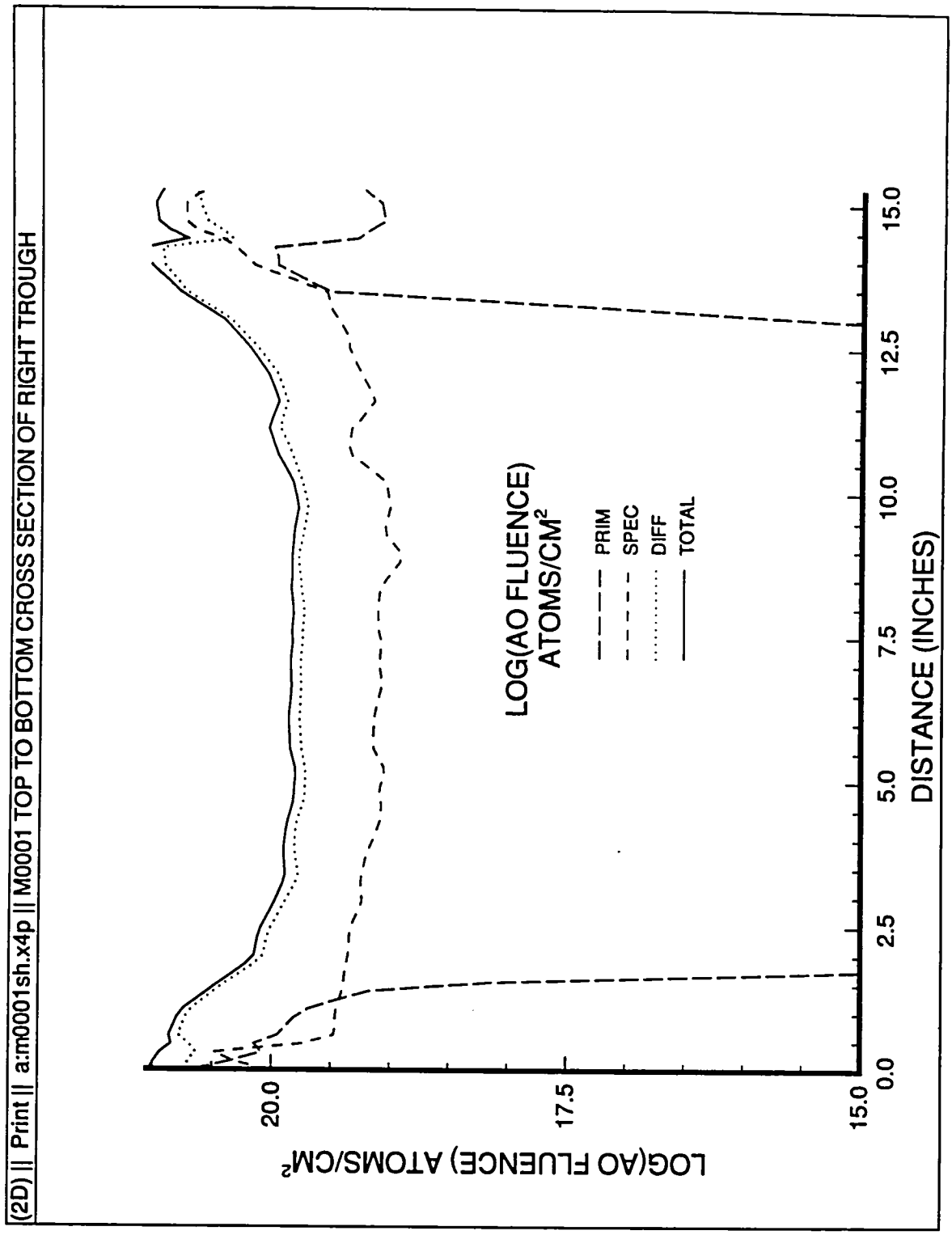

Figure 5.2-5. M0001 NRL Cosmic Ray Experiment Atomic Oxygen Fluence Cross Section From Top to Bottom Along the Right Trough in Figure 5.2-1.

5.3 Solar Exposure

Figure 5.3-1 shows LDEF mission solar exposure to the M0001 NRL cosmic ray experiment. In the figure, the active side of the surfaces making up the edges of the trough face the inside of the trough. The left side of the figure faces ram, with the ram direction oriented to the left and 8.1 degrees below horizontal in the figure. The large space-facing top plate receives the maximum CESH of any of the surfaces making up the experiment, with uniform primary direct CESH and no reflected CESH. The trough bottom surfaces receive relatively uniform solar exposure at somewhat lower values than the top square surface because the trough sides shield the bottom from some direct solar exposure. The sides of the trough, being more nearly perpendicular to the average Sun position, receive less CESH than the trough bottom.

Figures 5.3-2 through 5.3-5 show the total, primary, specularly reflected and diffusely reflected CESH cross sections for the same portions of the trough as figures 5.2-2 through 5.2-5 show for AO. As these figures show, primary CESH account for half to two thirds as much exposure to the tray bottoms as it does to the square top plate. The remainder of the exposure is due to specularly and diffusely reflected CESH. As expected, the cross sections show a decrease in CESH on the vertical ends of the cross section.

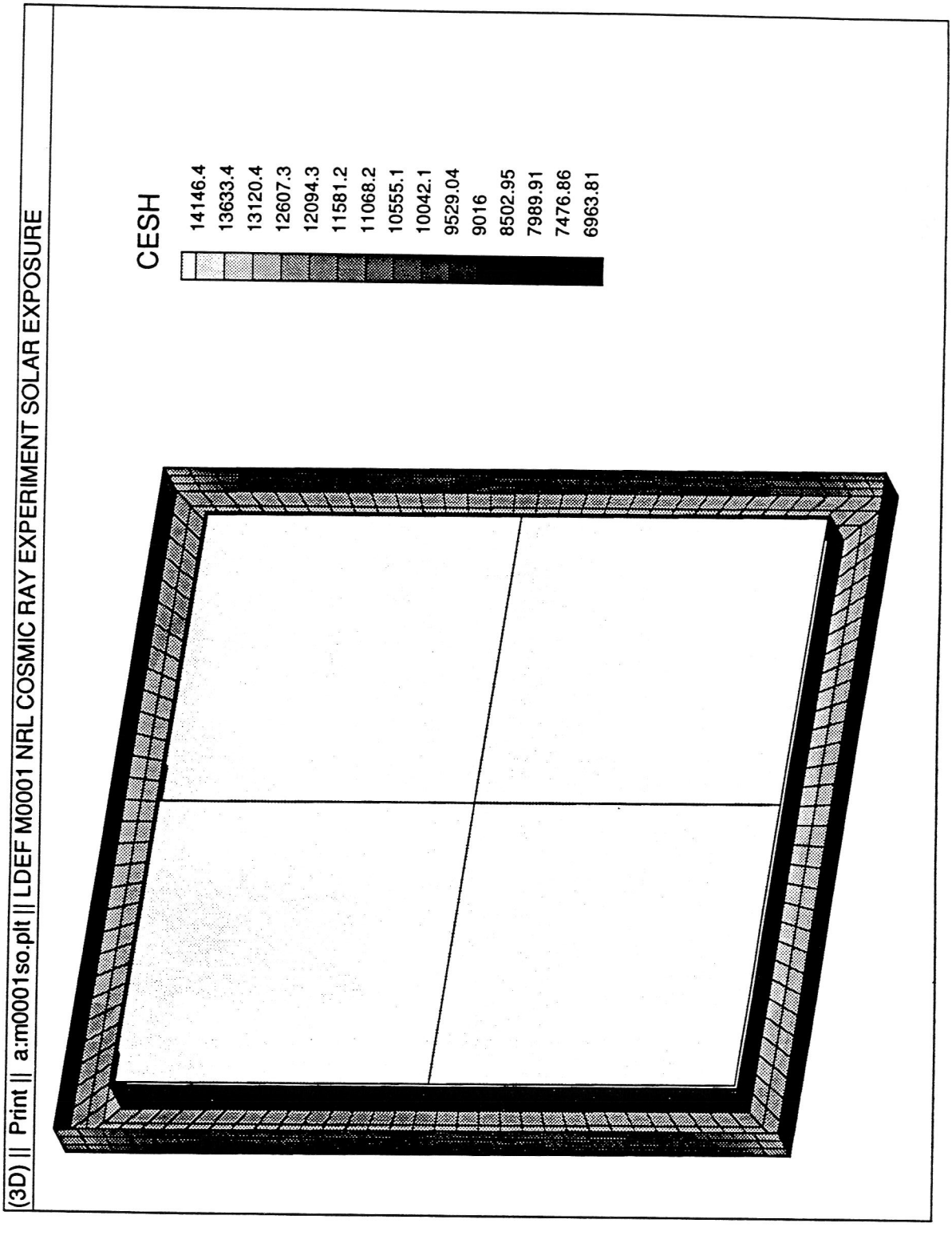

Figure 5.3-1. M0001 NRL Cosmic Ray Experiment Total Solar Exposure.

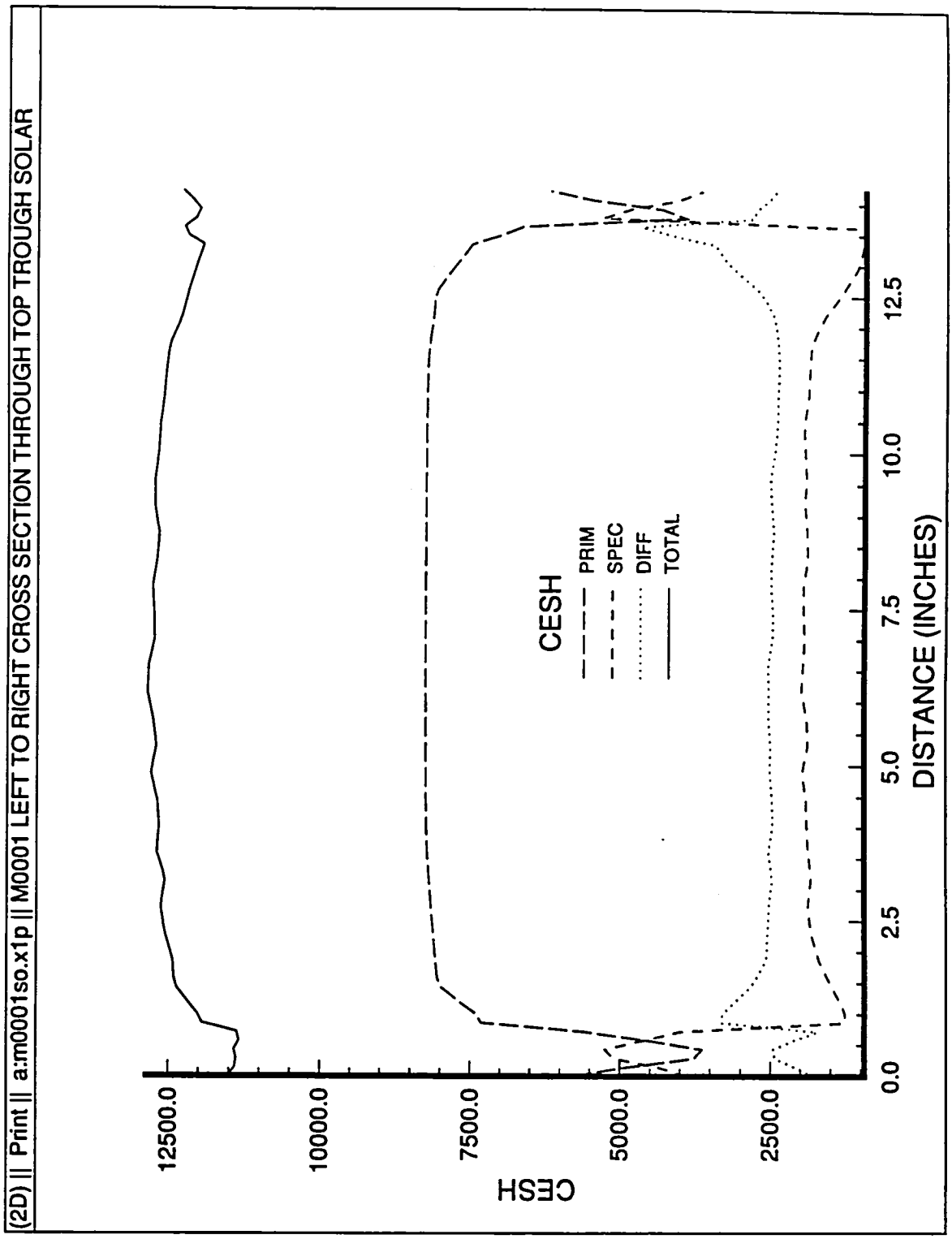

Figure 5.3-2. M0001 NRL Cosmic Ray Experiment Solar Exposure Cross Section From Left to Right Along the Upper Trough in Figure 5.3-1.

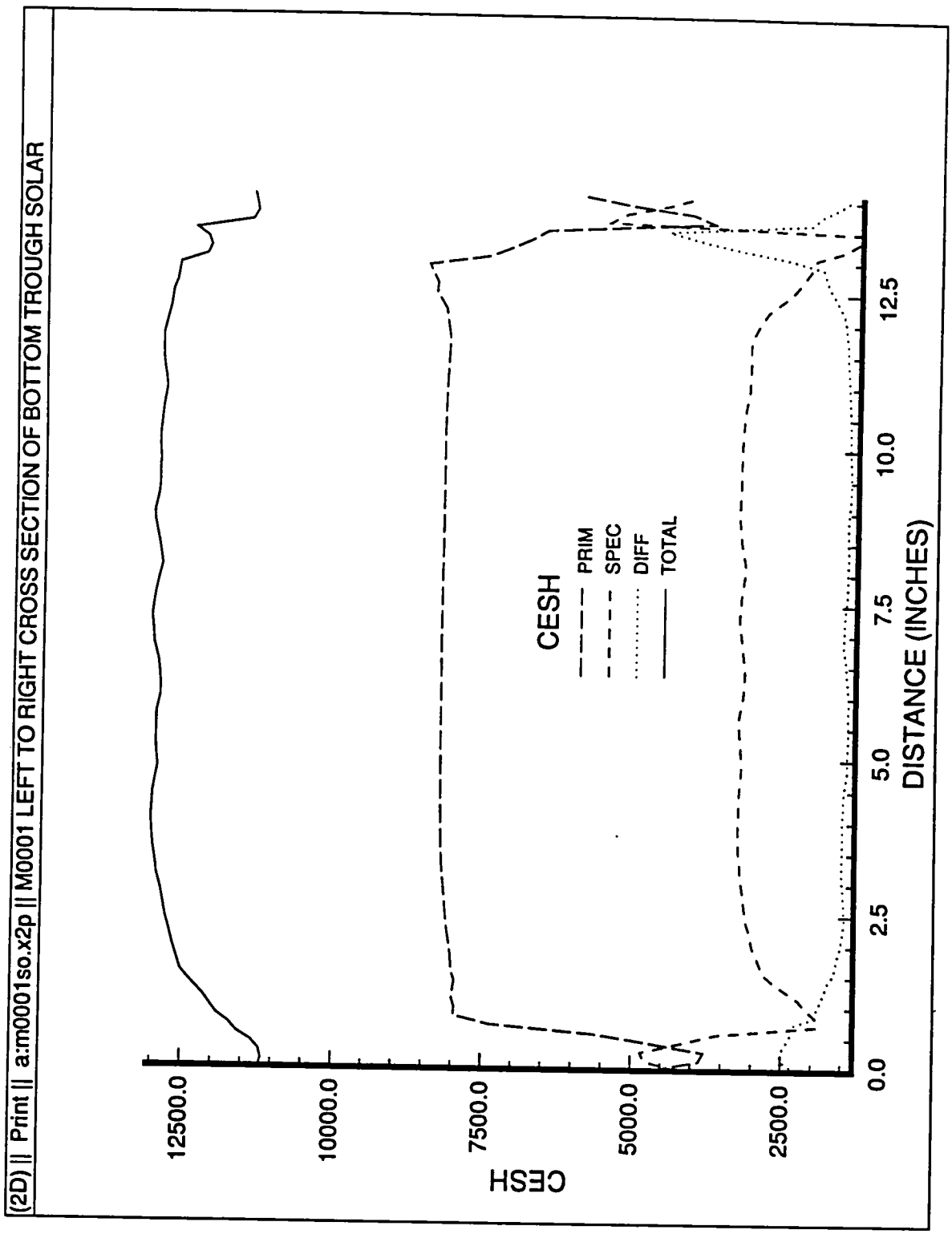

Figure 5.3-3. M0001 NRL Cosmic Ray Experiment Solar Exposure Cross Section From Left to Right Along the Lower Trough in Figure 5.3-1.

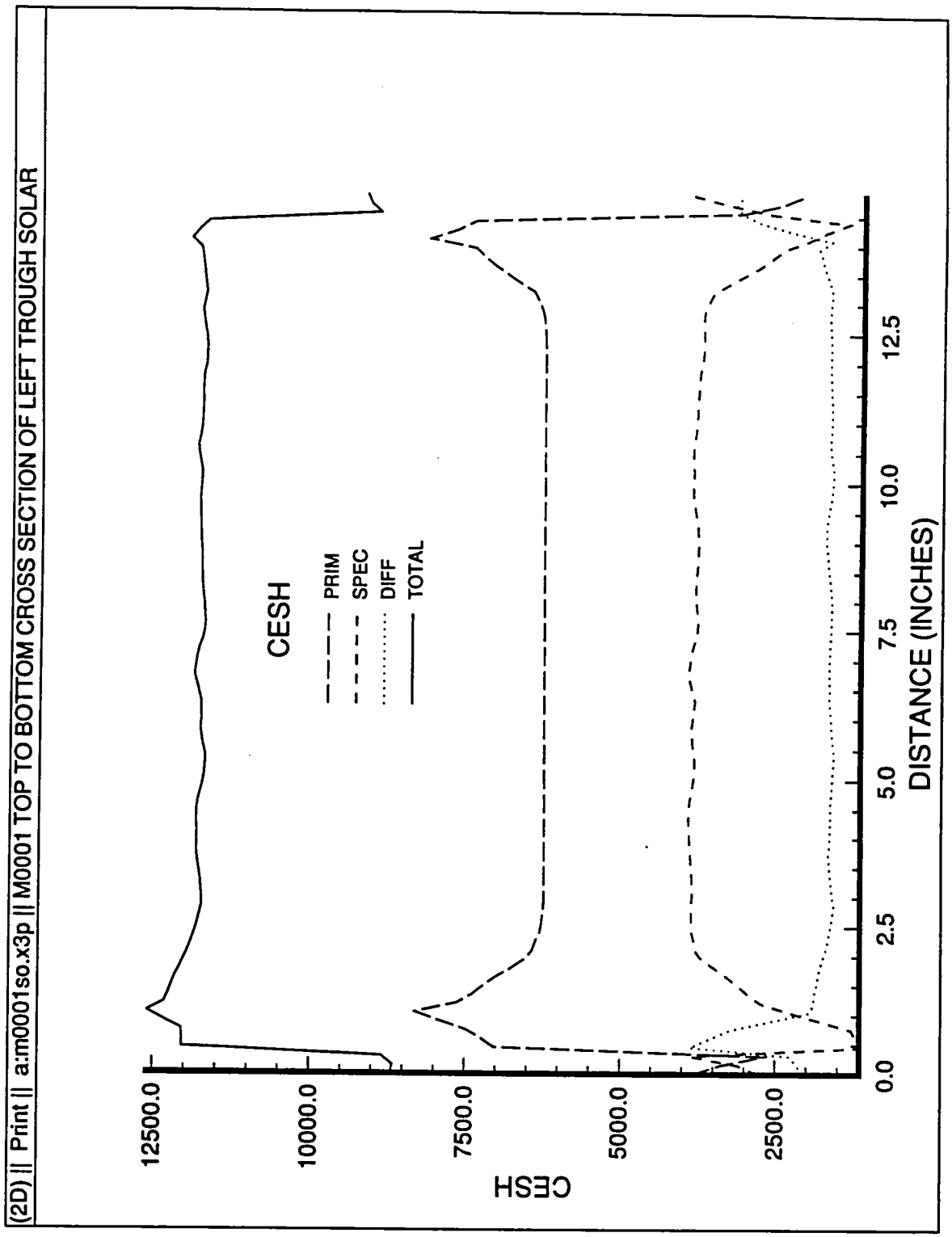

Figure 5.3-4. M0001 NRL Cosmic Ray Experiment Solar Exposure Cross Section From Top to Bottom Along the Left Trough in Figure 5.3-1.

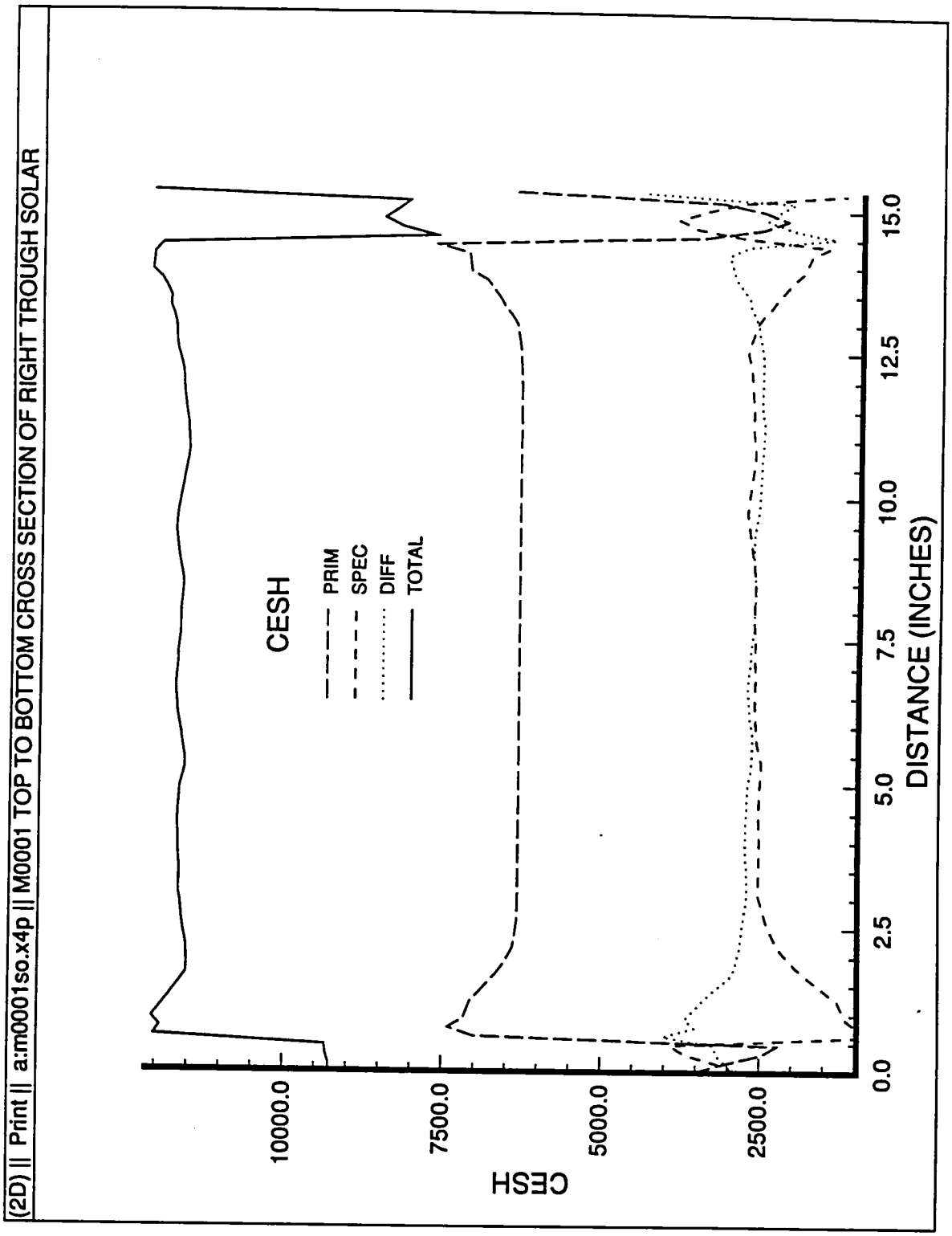

Figure 5.3-5. M0001 NRL Cosmic Ray Experiment Solar Exposure Cross Section From Top to Bottom Along the Right Trough in Figure 5.3-1.

6.0 TRAY D-11 COPPER GROUND STRAP

6.1 Experiment Location and Description

The tray D-11 copper ground strap is located on LDEF as shown in figure 6.1-1 (and color photo A6.1-1, p. A5). The area modeled includes the copper ground strap, the aluminum tray edge, a clamp plate, bolts, and the FEP blanket near the copper ground strap. Row 11 is oriented 51.9 degrees from the ram direction. The longeron between rows 11 and 12 on which the clamp plate is mounted is oriented 66.9 degrees from the ram direction. The copper ground strap extends from under the clamp plate to the bend of the tray edge, where it is covered by the edge of the FEP blanket.

6.2 Atomic Oxygen Exposure

Figure 6.2-1 shows AO exposure fluence in the area of the tray D-11 copper ground strap. The values of log (fluence) have been labeled for several representative locations on the figure. The top of the figure corresponds to the space end direction. The ram direction is toward the left. The missing and distorted areas of the bolt heads and the clamp plate are artifacts of the plotting program.

The effects of reflected and shadowed AO fluence are clearly shown in figure 6.2-1. The fluence is most intense on surfaces facing nearest the ram direction, namely the curved part of the aluminum tray edge and the near vertical left-facing aluminum plate edges on the longeron. Specular reflection from the curved part of the aluminum tray edge accounts for increased exposure to the FEP blanket in the fold "V." The otherwise near uniform fluence on both sides of the "V" is due to a combination of specular and diffuse reflections in the "V." The near vertical left-facing clamp plate edges on the longeron reflect fluence on the copper ground strap and aluminum tray edge nearby. Portions of the tray edge not near the clamp plate edge do not show this increased fluence.

Shadowing is clearly evident in the reduced AO fluences to the right of the bolt heads. The appearance of the structure near the middle bolt head is an artifact of the TECPLOT plotting program. The different apparent AO fluences downwind of the bolts is an artifact of the grid sizes and of the portions of the grid areas hidden by the bolt heads. The grid sizes used were chosen to give a reasonable representation of the AO fluence while maintaining computational efficiency. These artifacts do not affect the AO fluence predicted for the copper surface being modeled.

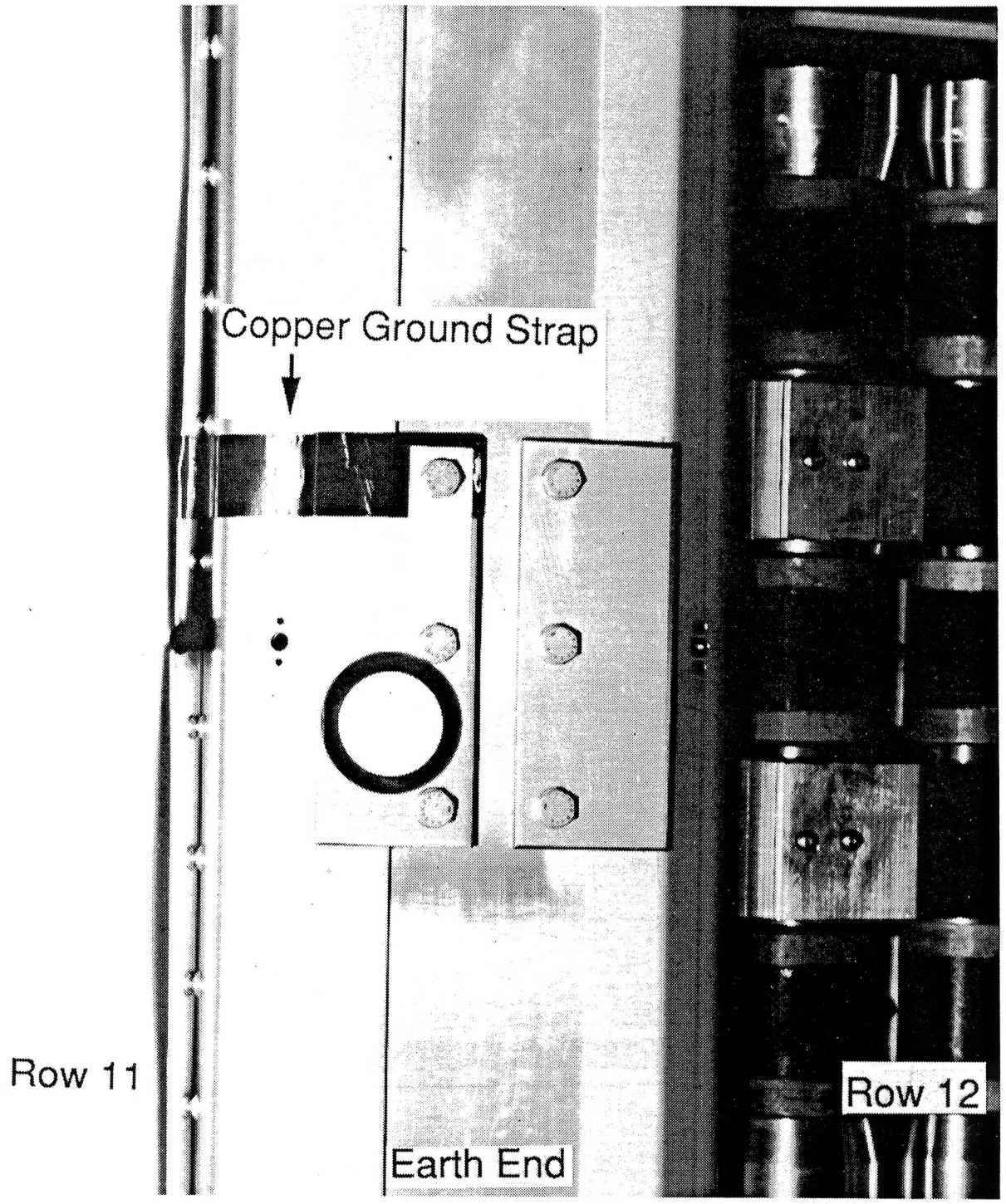

Figure 6.1-1. Tray D-11 Copper Ground Strap Photo.

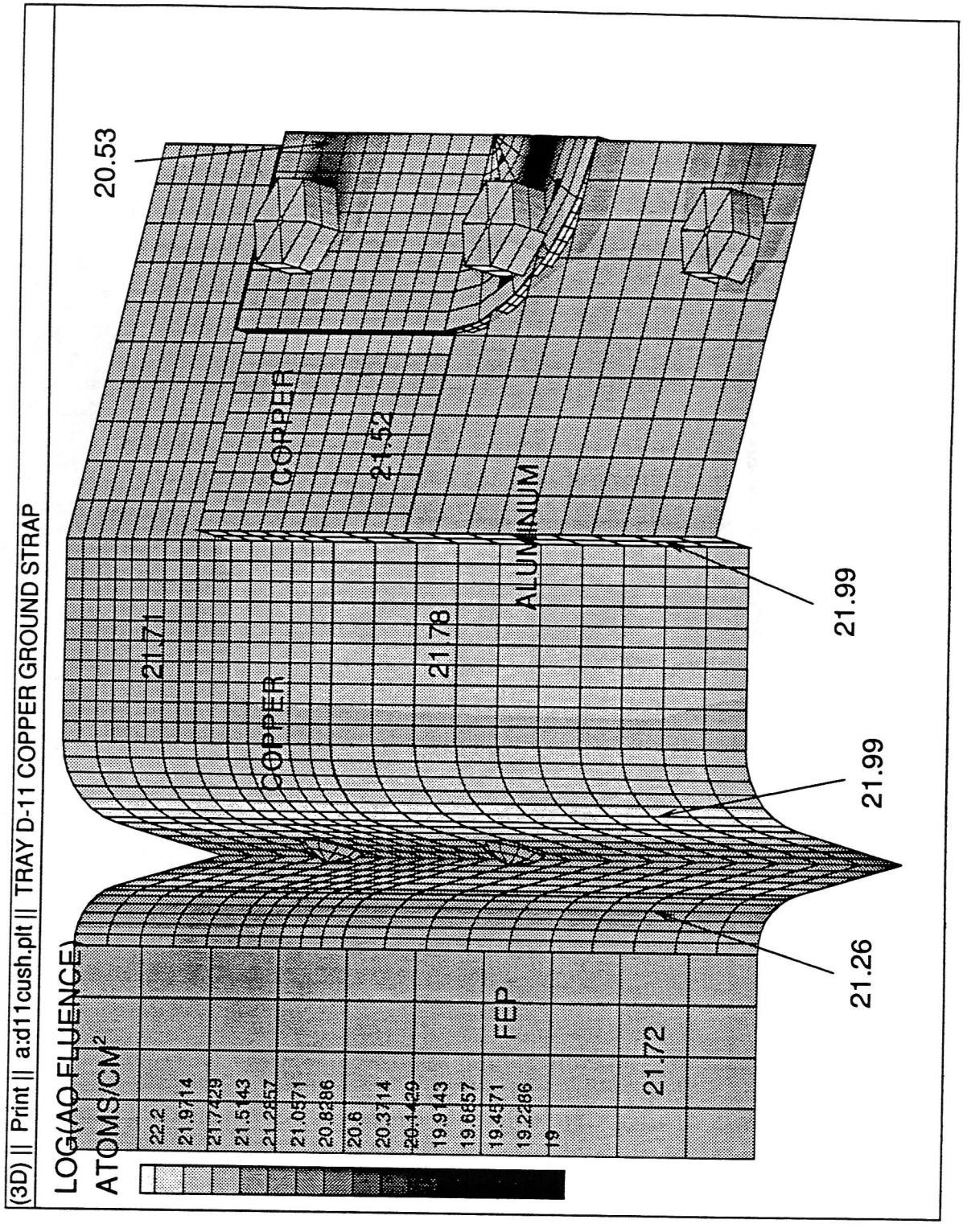

6.2-1. Tray D-11 Copper Ground Strap Atomic Oxygen Exposure Given as Log_{10} AO Fluence (Atoms/cm^2).

7.0 F-9 ANGLE BRACKET

7.1 Experiment Location and Description

The tray F-9 angle bracket is located on LDEF as shown in figure 7.1-1 (and color photo A7.1-1, p. A6). Figure 7.1-2 shows the orientation of the F-9 angle bracket on LDEF. The ram direction is oriented 8.1 degrees toward row 10 and 0.8 degrees toward the space end from the row F-9 surface normal. The top of figure 7.1-1 is oriented toward the space end of LDEF. The F-9 angle bracket is coated with a thin layer of FEP.

7.2 Atomic Oxygen Exposure

Figure 7.2-1 shows LDEF mission atomic oxygen exposure to the F-9 angle bracket. In the figure, ram fluence strikes the bracket at an angle of 8.1 degrees to the vertical face of the bracket. Figure 7.2-2 is a cross section of the fluence to the angle bracket from left to right across the middle of the bracket. The figure shows primary, specular, and total AO fluence. The figures show that the vertical surface of the angle bracket receive about 10% of the fluence of the horizontal surfaces and that reflected fluence contributes significantly to the fluence on the lower horizontal surface.

The FEP thickness along a cross section of the F-9 angle bracket was measured. The measured cross section started at the left side of the upper curved surface in figure 7.2-1 (or at about 1.0 cm in figure 7.2-2) and extends on to the flat surface at the lower right of figure 7.2-1 (or to about 3.6 cm in figure 7.2-2). Figure 7.2-3 shows these experimentally measured FEP thicknesses superimposed on a plot of calculated FEP thickness due to erosion from primary and total AO exposure. The calculated FEP thickness is based on

$$\text{Thickness (mm)} = 0.125 \text{ mm} - [3.4 \times 10^{-26} \text{ mm}/(\text{AO}/\text{cm}^2)] * [\text{AO fluence } (\text{AO}/\text{cm}^2)] .$$

In this equation 0.125 mm is the initial FEP thickness before exposure to atomic oxygen fluence. This value was determined by adjusting the initial FEP thickness to give the best fit between the experimentally measured and calculated FEP thicknesses. The recession rate of 3.4×10^{-26} mm/(AO/cm^2) is based on the value given by Stein and Pippin (ref. 9).

Figure 7.2-3 shows that primary AO fluence alone is not sufficient to model the erosion of the FEP on the F-9 angle bracket. Reflected AO contributes significant erosion to the FEP on the lower flat surface of the angle bracket. The measured FEP thickness is less than the calculated thickness from about 30 to 35 mm. This difference in thicknesses is unexplained, but may indicate a greater contribution due to scattered AO than predicted by the model. In all other regions, the agreement between measured and calculated FEP thickness is quite good.

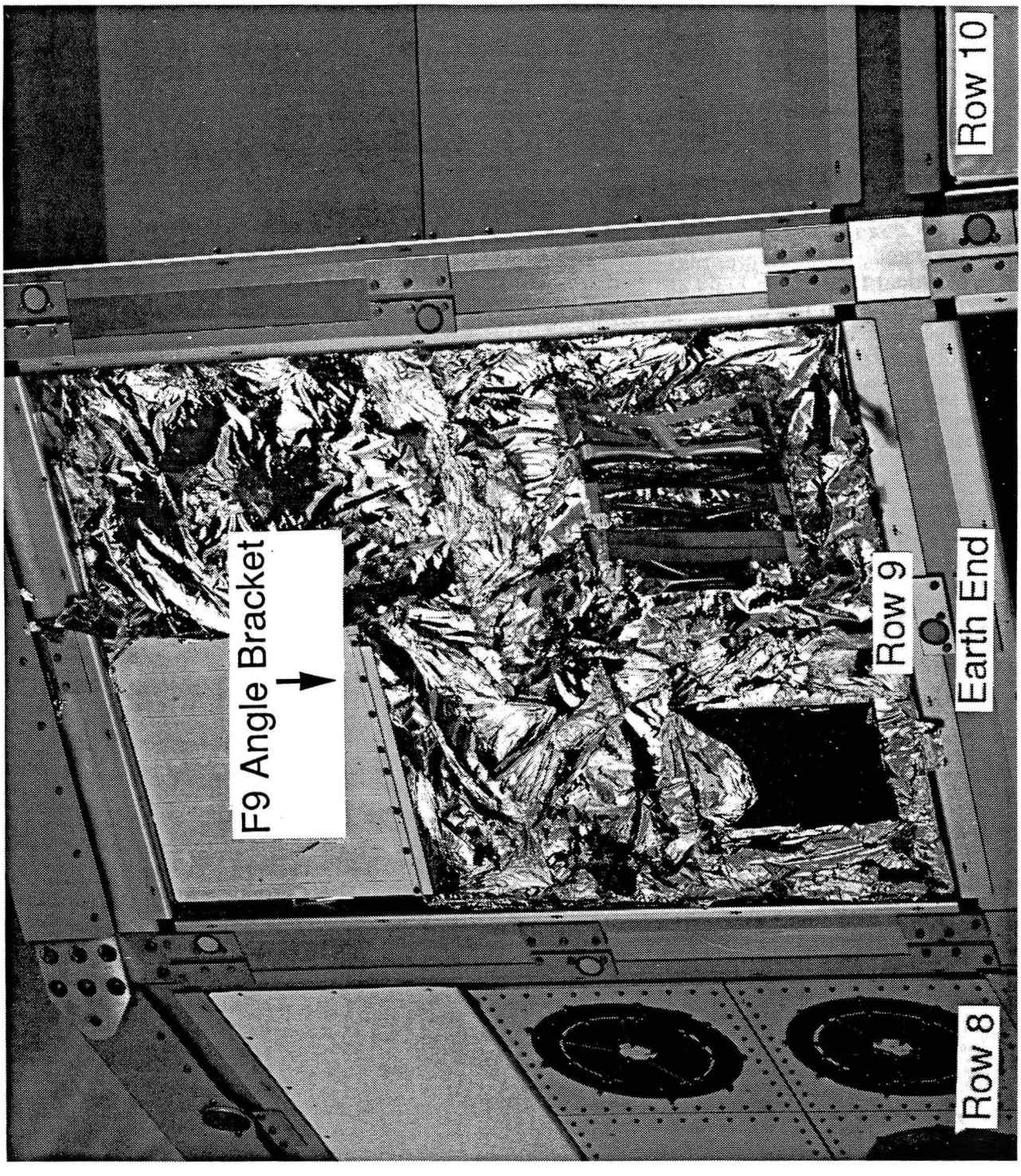

Figure 7.1-1. F-9 Angle Bracket On-Orbit Photo.

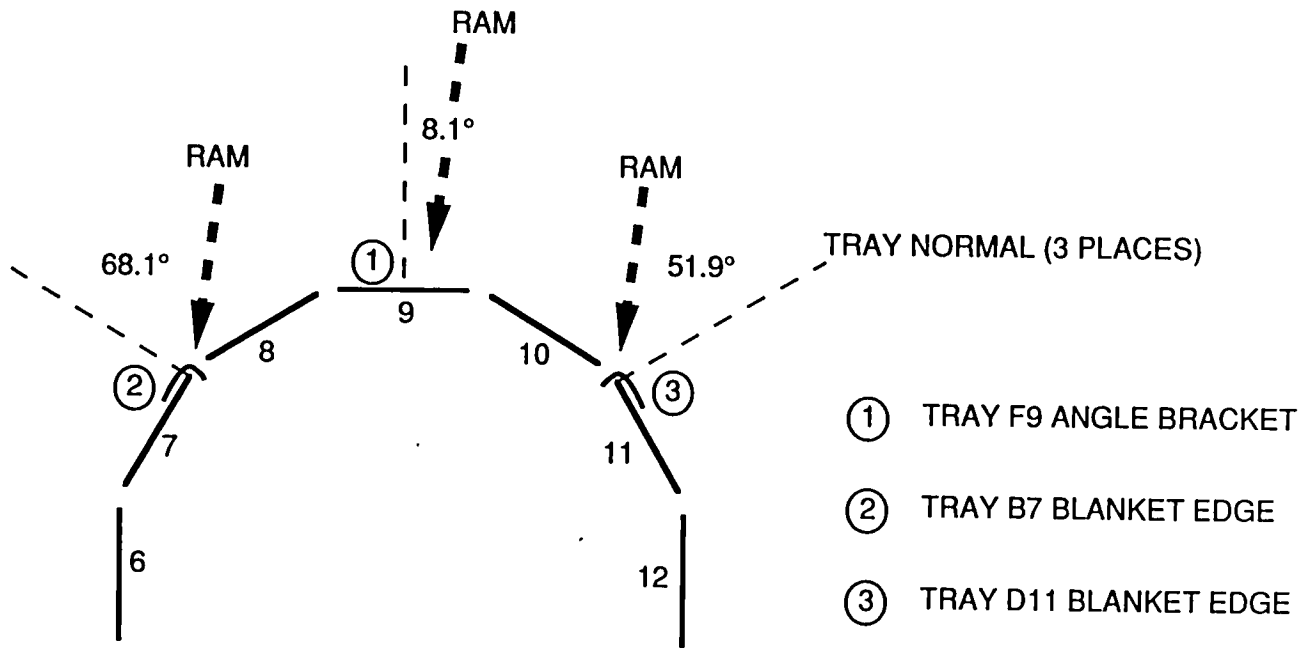

Figure 7.1-2. Orientation Of FEP Specimens.

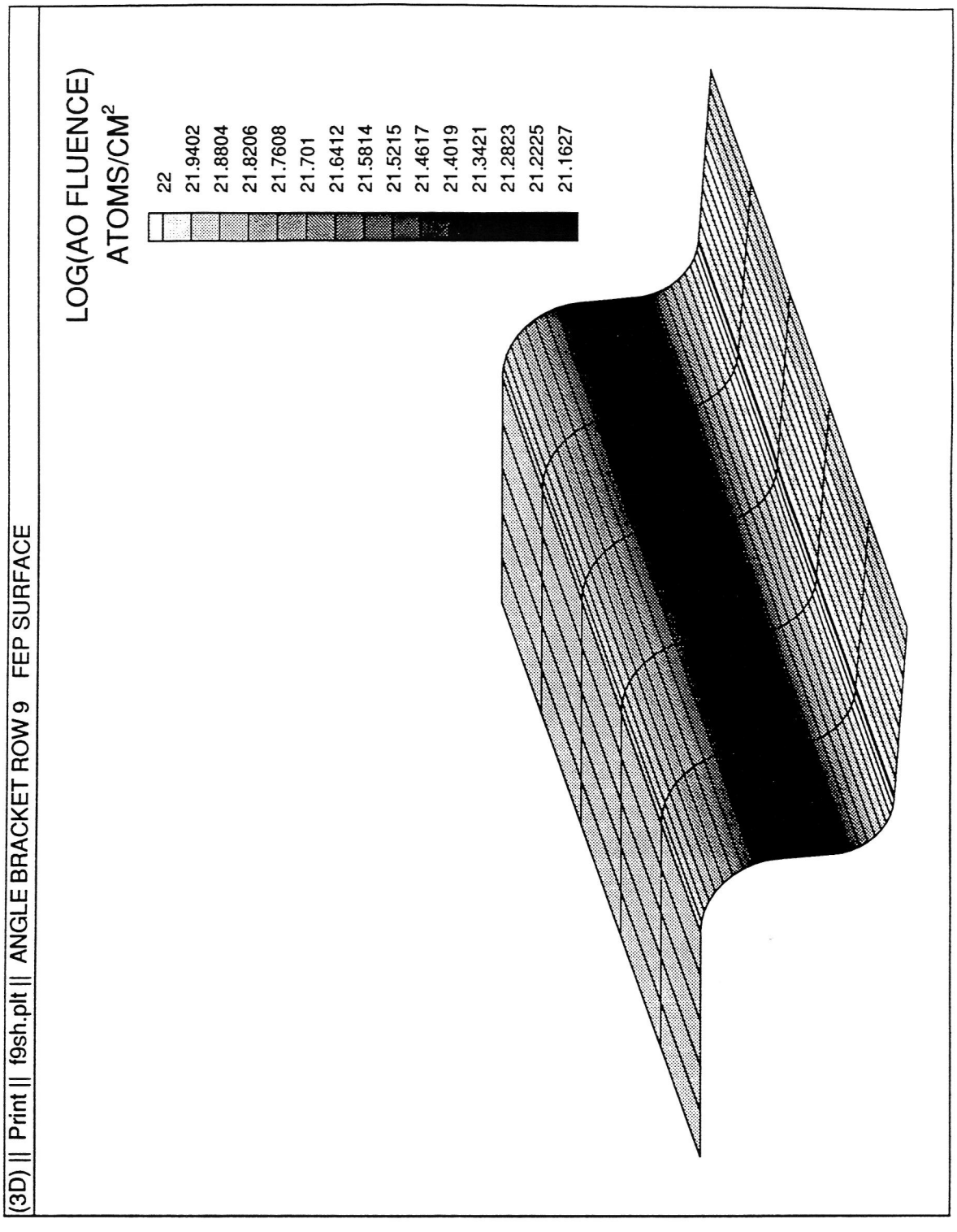

Figure 7.2-1. F-9 Angle Bracket Atomic Oxygen Exposure Given as Log_{10} AO Fluence (Atoms/cm^2).

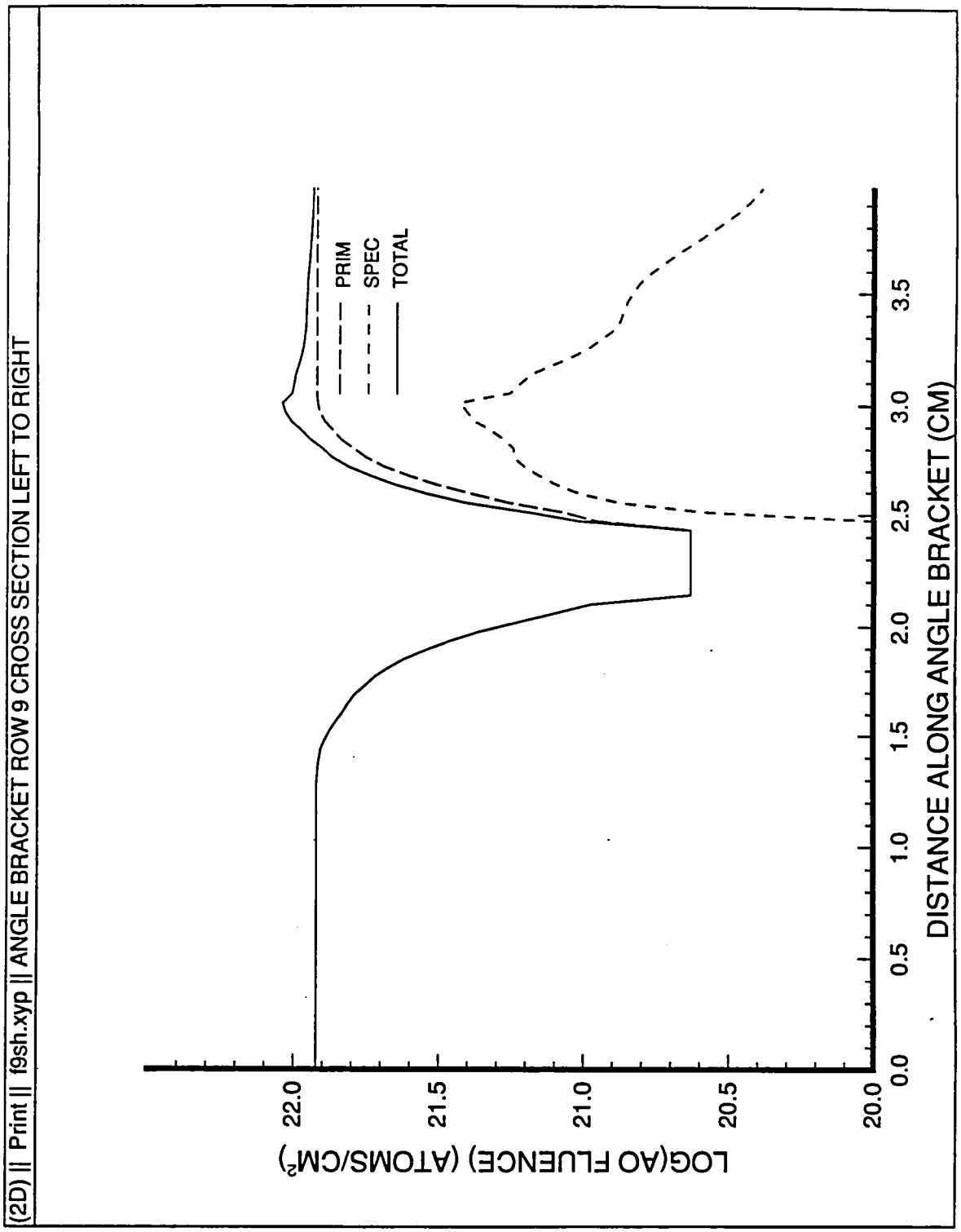

Figure 7.2-2. Atomic Oxygen Exposure Cross Section of Figure 7.2-1.

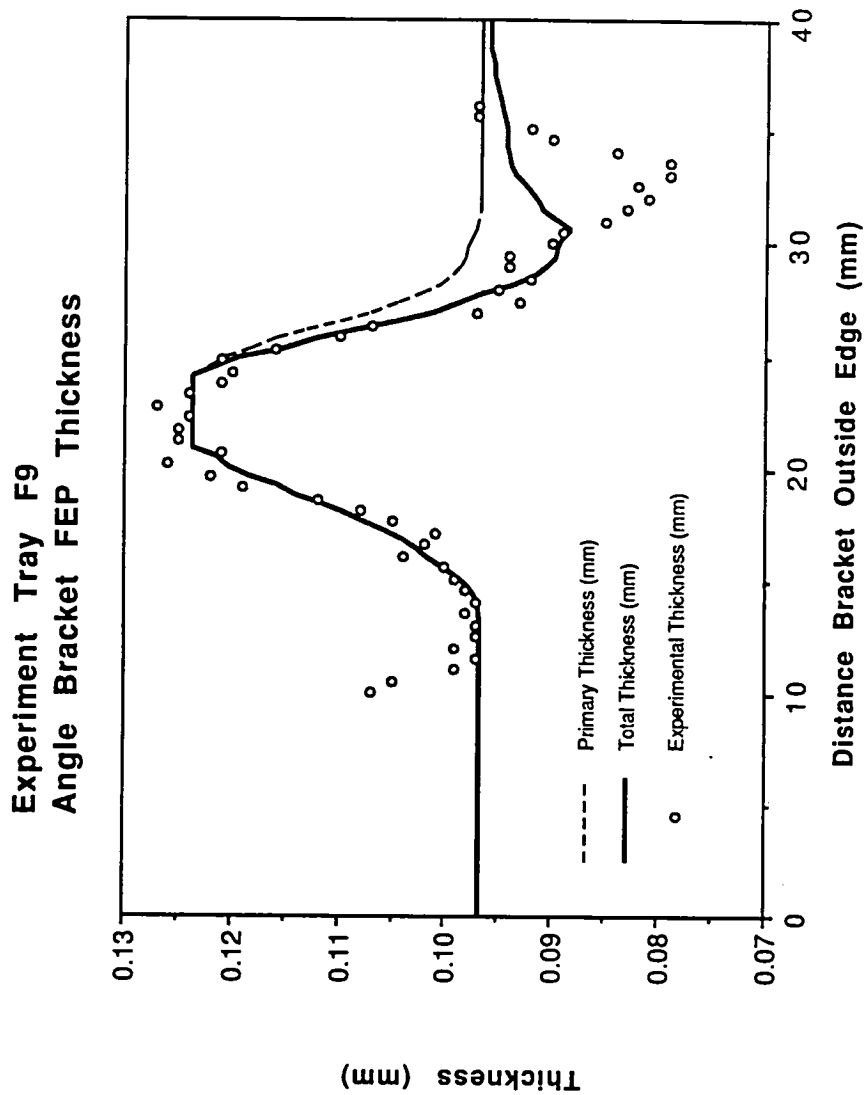

Figure 7.2-3. F-9 Angle Bracket Calculated vs Experimental FEP Thickness.

8.0 D-11 FEP BLANKET FOLD AT TRAY EDGE TOWARD ROW 10

8.1 Experiment Location and Description

The tray D-11 blanket fold is located on LDEF on the row 10 side of tray 11 as shown in figure 8.1-1 (and color photo A8.1-1, p. A7). Figures 7.1-2 and 8.1-2 show the orientation of the D-11 blanket fold on LDEF. The row 11 surface normal is oriented 51.9 degrees from ram direction. The top of figure 8.1-1 is oriented toward the space end of LDEF. The thermal control blanket is FEP and the tray edge is aluminum.

8.2 Atomic Oxygen Exposure

Figure 8.2-1 shows LDEF mission atomic oxygen exposure to the D-11 blanket fold. In the figure, ram fluence strikes the parallel flat surfaces of the FEP blanket and aluminum tray edge at an angle of 51.9 degrees from the vertical to these surfaces. In figure 8.2-1 the ram fluence comes from the right of the figure toward the left of the figure. Figure 8.2-2 is a cross section of the fluence to the blanket fold from left to right across the middle of the blanket fold. The figure shows primary, specular, and total AO fluence. Examination of the figures shows that primary fluence is uniform on the parallel surfaces of the FEP and aluminum and is most intense on the curved surface of the FEP because this surface is most nearly normal to the ram fluence. The curved surface of the aluminum tray edge is shielded from primary AO fluence. The curved surface of the FEP reflects fluence on to the aluminum surface of the "V" formed by the FEP blanket and aluminum tray edge. Almost all of the fluence in the "V" is due to reflected fluence. The lower part of the "V" receives about 10% as much fluence as the parallel flat surfaces of the FEP blanket and tray edge.

The FEP thickness along a cross section of the FEP blanket was measured. The measured cross section started to the left of the curved FEP surface in figure 8.2-1 (or at about 16 mm in figure 8.2-2) and extends beyond the bottom of the "V" (the FEP blanket is in contact with the aluminum tray side below the bottom of the "V" and is shielded from AO fluence; this the region from 42 to 52 mm in figure 8.2-2). Figure 8.2-3 shows these experimentally measured FEP thicknesses superimposed on a plot of calculated FEP thickness due to erosion from primary and total AO exposure. The calculated FEP thickness is based on

$$\text{Thickness (mm)} = 0.135 \text{ mm} - [3.4 \times 10^{-26} \text{ mm}/(\text{AO}/\text{cm}^2)] * [\text{AO fluence } (\text{AO}/\text{cm}^2)] .$$

In this equation 0.135 mm is the initial FEP thickness before exposure to atomic oxygen fluence. This value was determined by measuring the FEP thickness in the area shielded from AO fluence. The recession rate of 3.4×10^{-26} mm/(AO/cm^2) is based on the value given by Stein and Pippin (ref. 9).

Figure 8.2-3 shows that primary AO fluence alone is not sufficient to model the erosion of the FEP on the D-11 FEP blanket. However, when reflected AO fluence is accounted for, the fit between calculated erosion and measured erosion is much better.

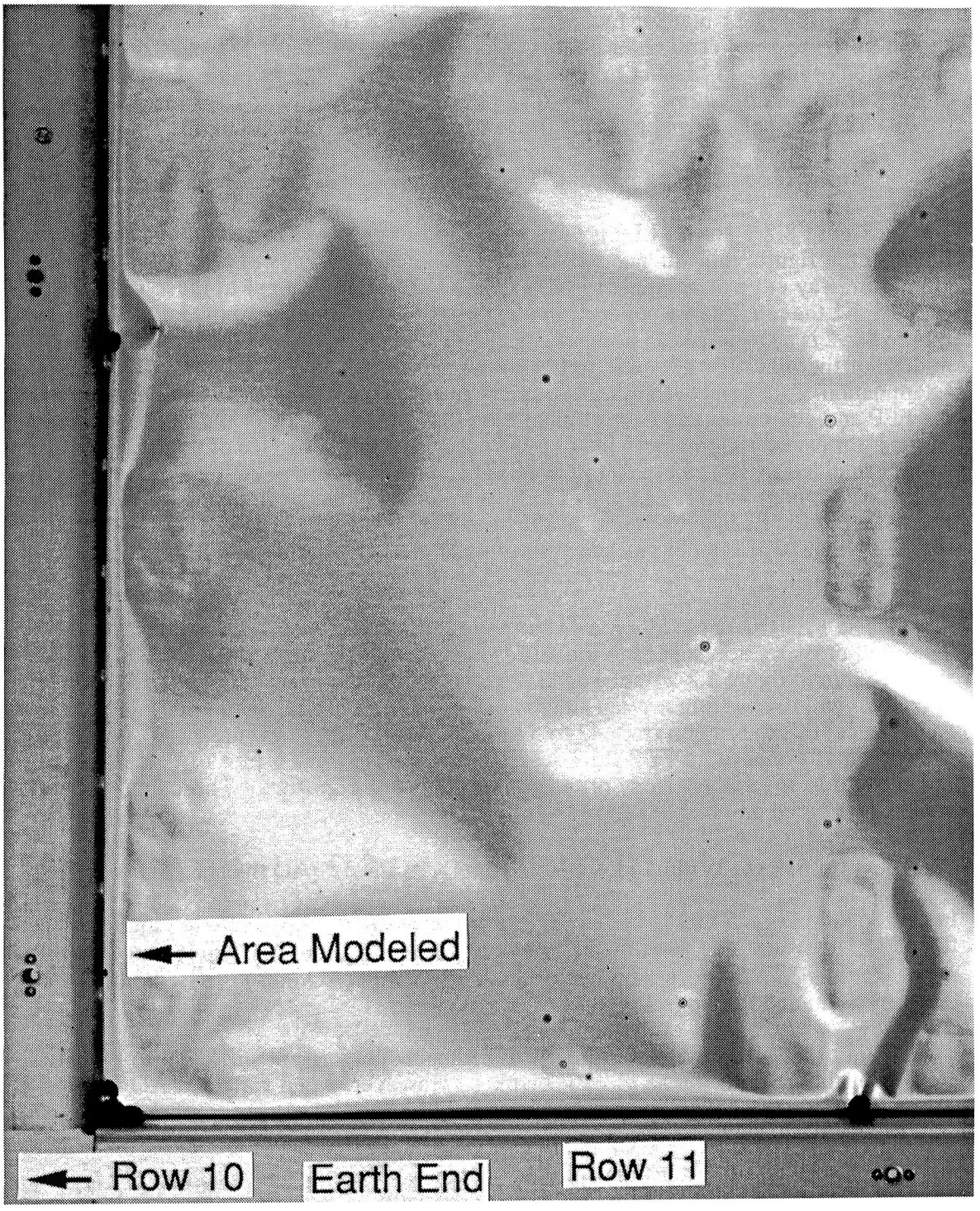

Figure 8.1-1. D-11 FEP Blanket Fold at Tray Edge Photo.

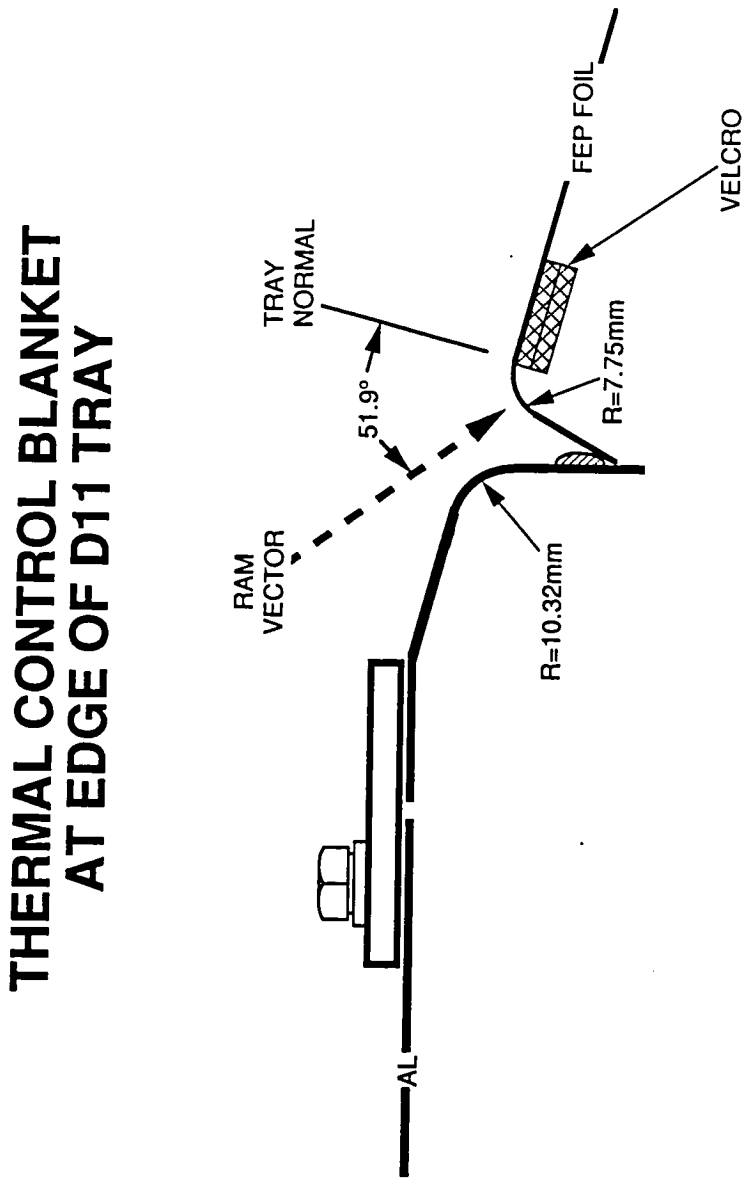

Figure 8.1-2. D-11 FEP Blanket Fold Cross Section View.

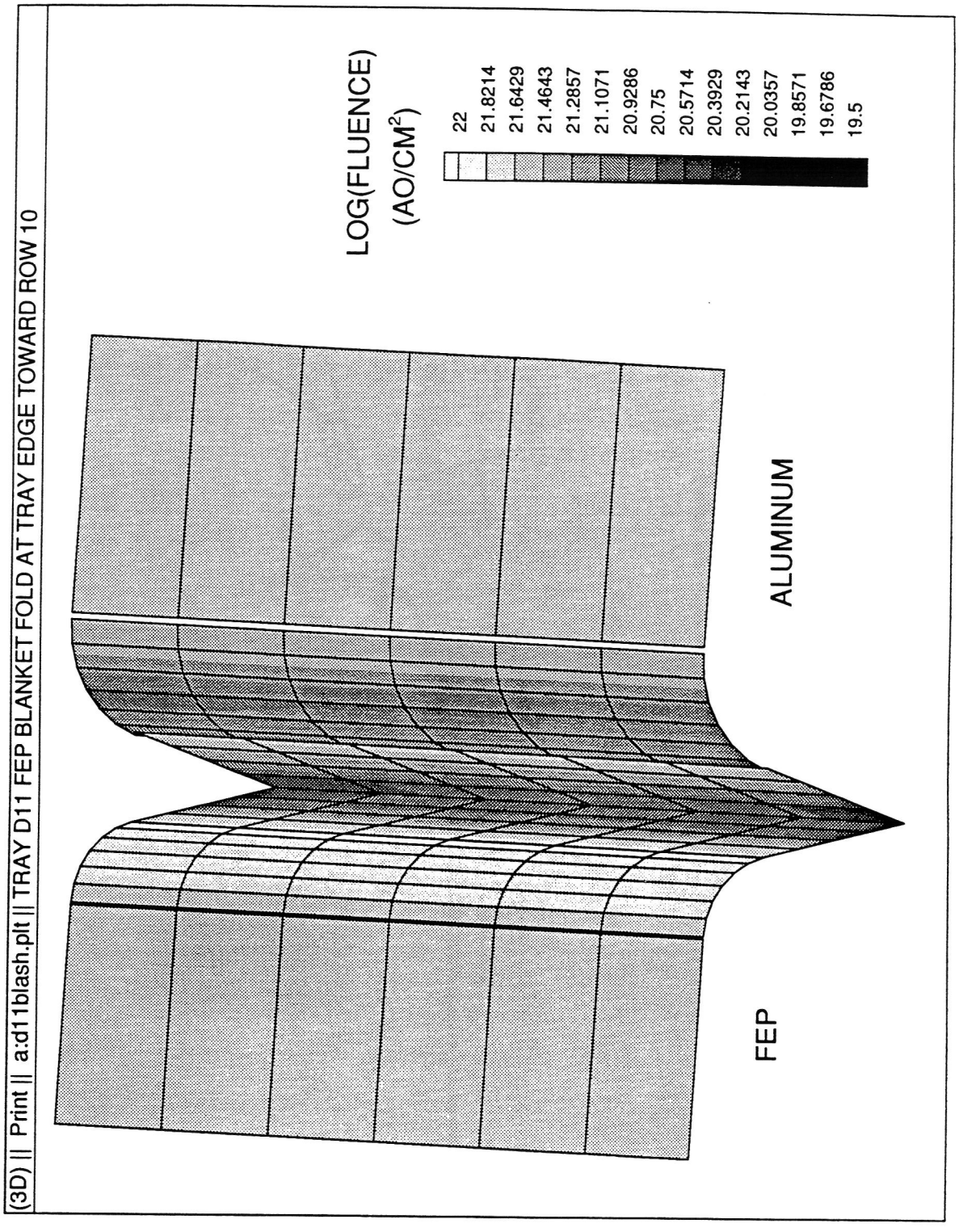

Figure 8.2-1. D-11 FEP Blanket Fold at Tray Edge Atomic Oxygen Exposure Given as Log_{10} AO Fluence (Atoms/cm^2).

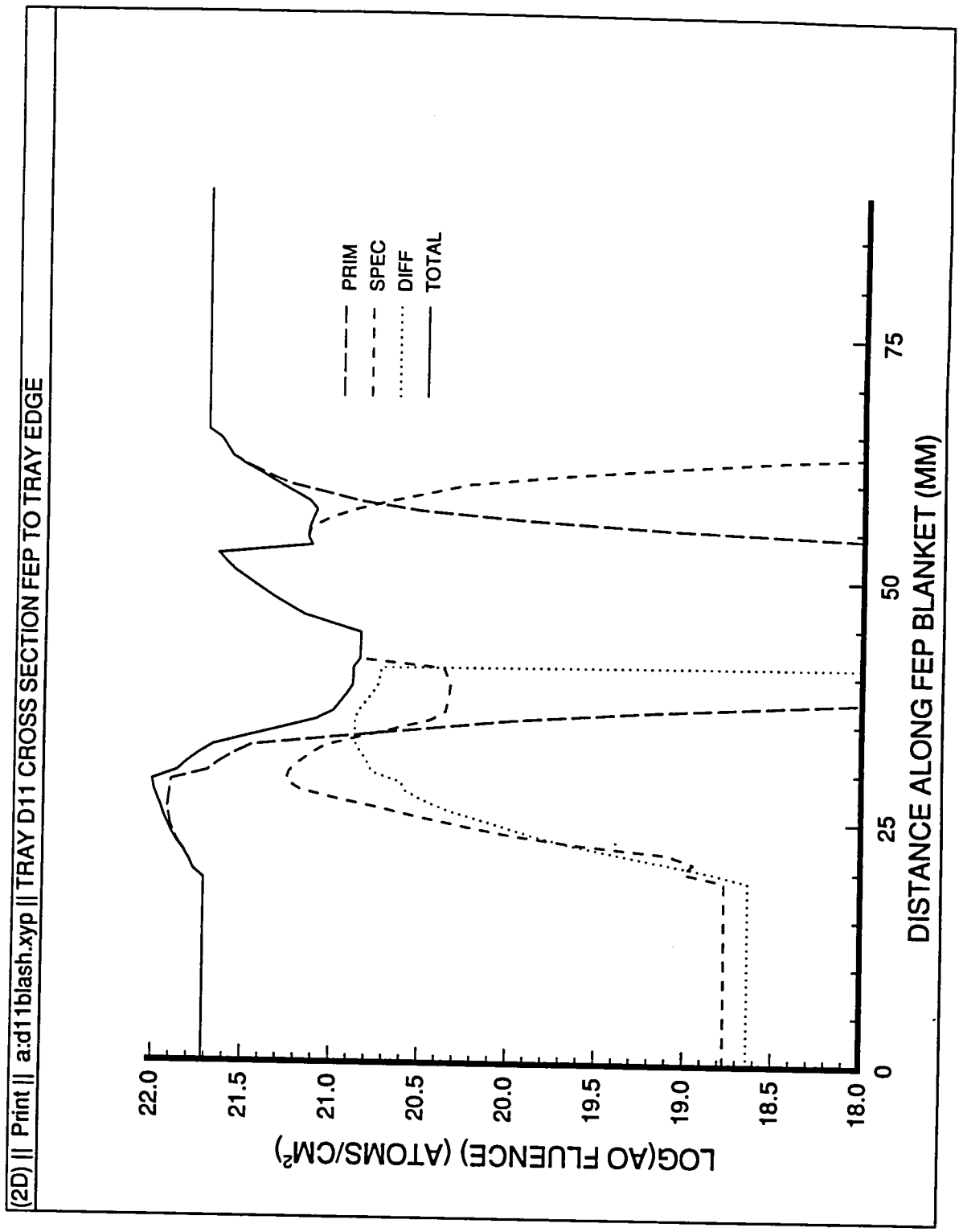

Figure 8.2-2. Atomic Oxygen Exposure Cross Section of Figure 8.2-1.

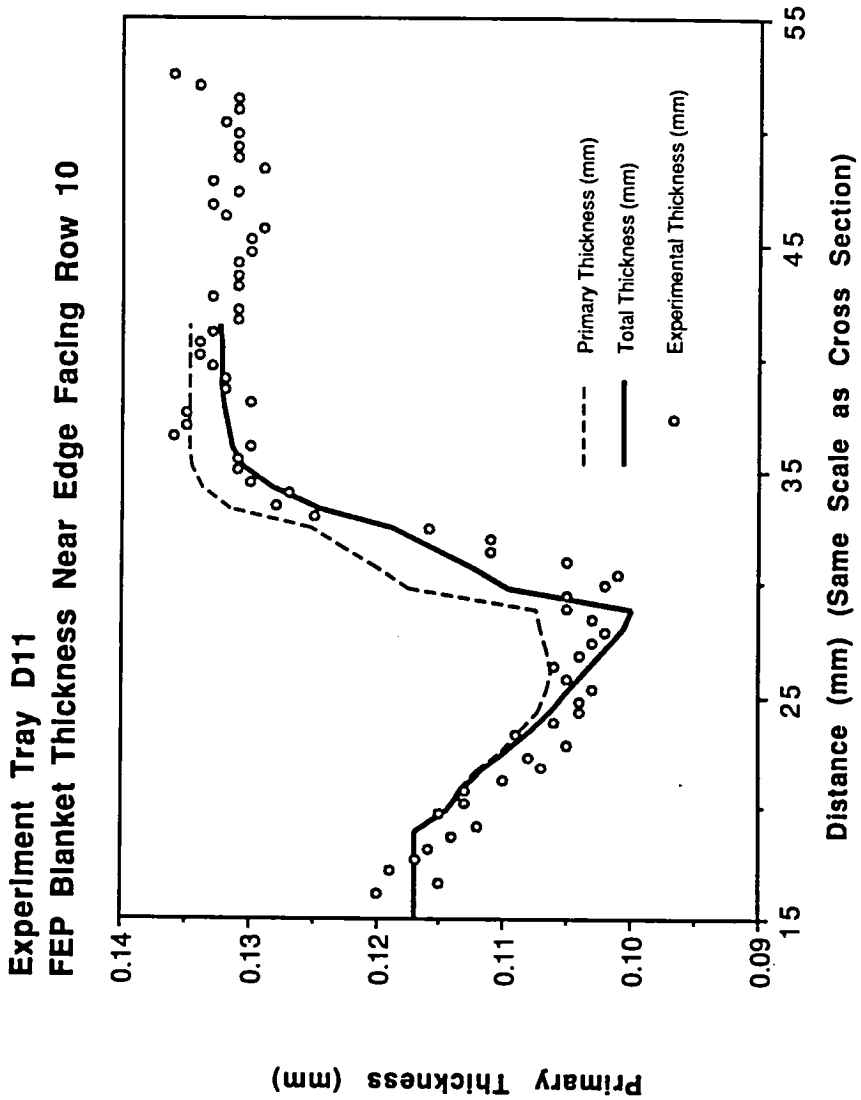

Figure 8.2-3. D-11 FEP Blanket Fold at Tray Edge Calculated vs Experimental FEP Thickness.

9.0 TRAY B-7 FEP BLANKET FOLD AT LONGERON TOWARD ROW 8

9.1 Experiment Location and Description

The tray B-7 blanket fold is located on LDEF on the row 8 side of tray 7 as shown in figure 9.1-1 (and color photo A9.1-1, p. A8). Figure 7.1-2 shows the orientation of the B-7 blanket fold on LDEF. The row 7 surface normal is oriented 68.1 degrees from ram direction. The top of figure 9.1-1 is oriented toward the space end of LDEF. The thermal control blanket is FEP and the longeron is aluminum.

9.2 Atomic Oxygen Exposure

Figure 9.2-1 shows LDEF mission atomic oxygen exposure to the B-7 blanket fold. In the figure, ram fluence strikes the parallel flat surfaces of the FEP blanket and aluminum longeron edge at an angle of 68.1 degrees from the vertical to these surfaces. In figure 9.2-1 the ram fluence comes from the right of the figure toward the left of the figure. Figure 9.2-2 is a cross section of the fluence to the angle bracket from left to right across the middle of the bracket. The figure shows primary, specular, and total AO fluence. Examination of the figures shows that primary fluence is uniform on the parallel surfaces of the FEP and aluminum and is most intense on the curved surface of the FEP because this surface is most nearly normal to the ram fluence. The curved surface of the aluminum longeron edge is shielded from primary AO fluence. The curved surface of the FEP reflects some fluence on to the top of the aluminum surface of the "V" formed by the FEP blanket and aluminum longeron edge. Almost all of the fluence in the "V" is due to reflected fluence. The lower part of the "V" receives about 4% as much fluence as the parallel flat surfaces of the FEP blanket and longeron edge.

The FEP thickness along a cross section of the FEP blanket was measured. The measured cross section started to the left of the curved FEP surface in figure 9.2-1 (or at about 5 mm in figure 9.2-2) and extends beyond the bottom of the "V" (the FEP blanket is in contact with the aluminum longeron side below the bottom of the "V" and is shielded from AO fluence; this the region from 41 to 45 mm in figure 9.2-2). Figure 9.2-3 shows these experimentally measured FEP thicknesses superimposed on a plot of calculated FEP thickness due to erosion from primary and total AO exposure. The calculated FEP thickness is based on

$$\text{Thickness (mm)} = 0.135 \text{ mm} - [3.4 \times 10^{-26} \text{ mm}/(\text{AO}/\text{cm}^2)] * [\text{AO fluence } (\text{AO}/\text{cm}^2)] .$$

In this equation 0.135 mm is the initial FEP thickness before exposure to atomic oxygen fluence. This value was determined by measuring the FEP thickness in the area shielded from AO fluence. The recession rate of 3.4×10^{-26} mm/(AO/cm^2) is based on the value given by Stein and Pippin (ref. 9).

Figure 9.2-3 shows that because relatively little AO fluence is reflected on to the FEP blanket, there is little difference in calculated FEP erosion whether or not reflected AO is considered. Agreement between calculated and measured FEP thickness is good to the right of about 20 mm in the figure. The FEP in the region to the left of 20 mm was wrinkled, so the measured FEP thicknesses there are not representative of the modeled flat blanket surface. Hence, this region should not be considered when comparing the calculated and measured FEP blanket thicknesses.

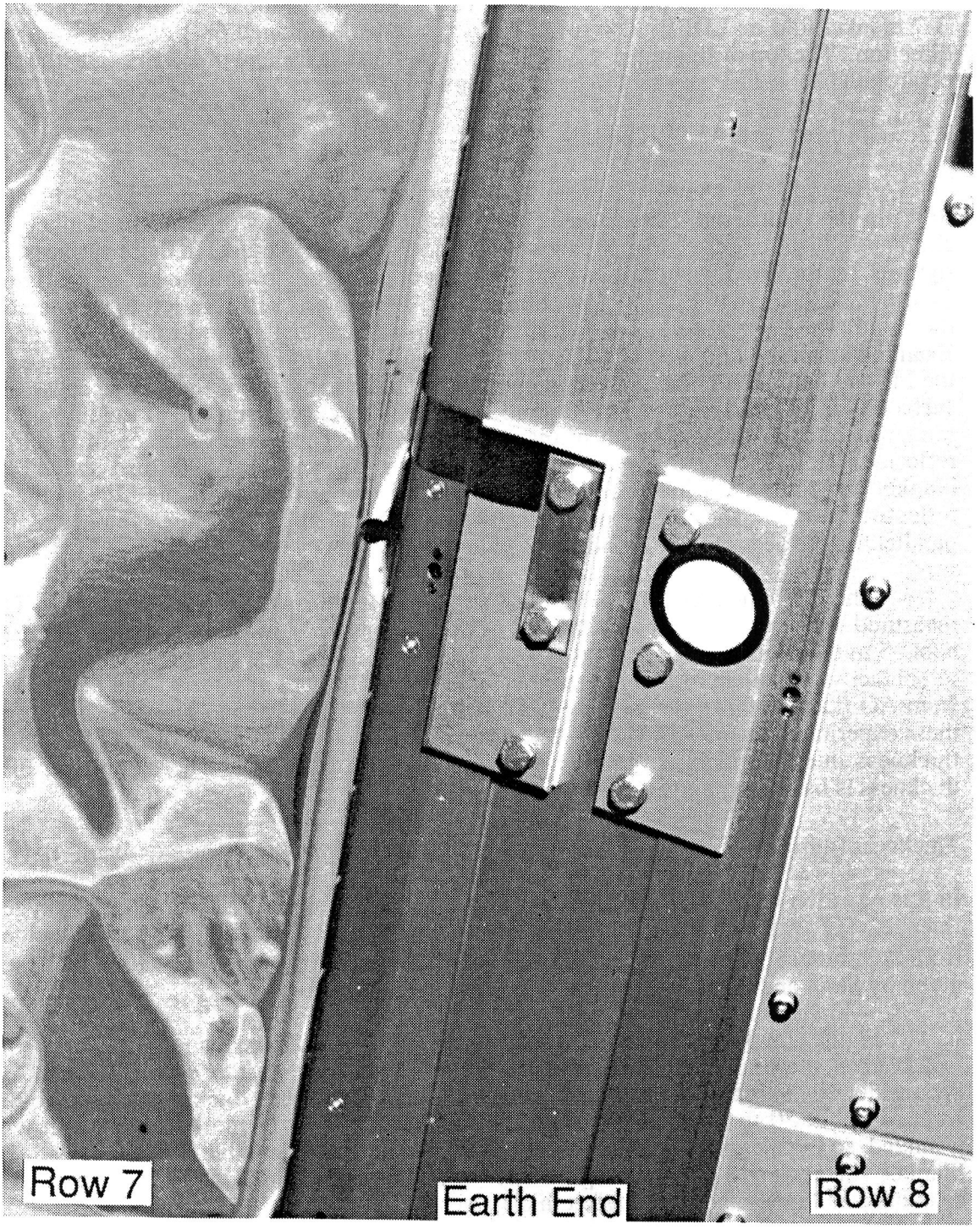

Figure 9.1-1. B-7 FEP Blanket Fold at Longeron Photo.

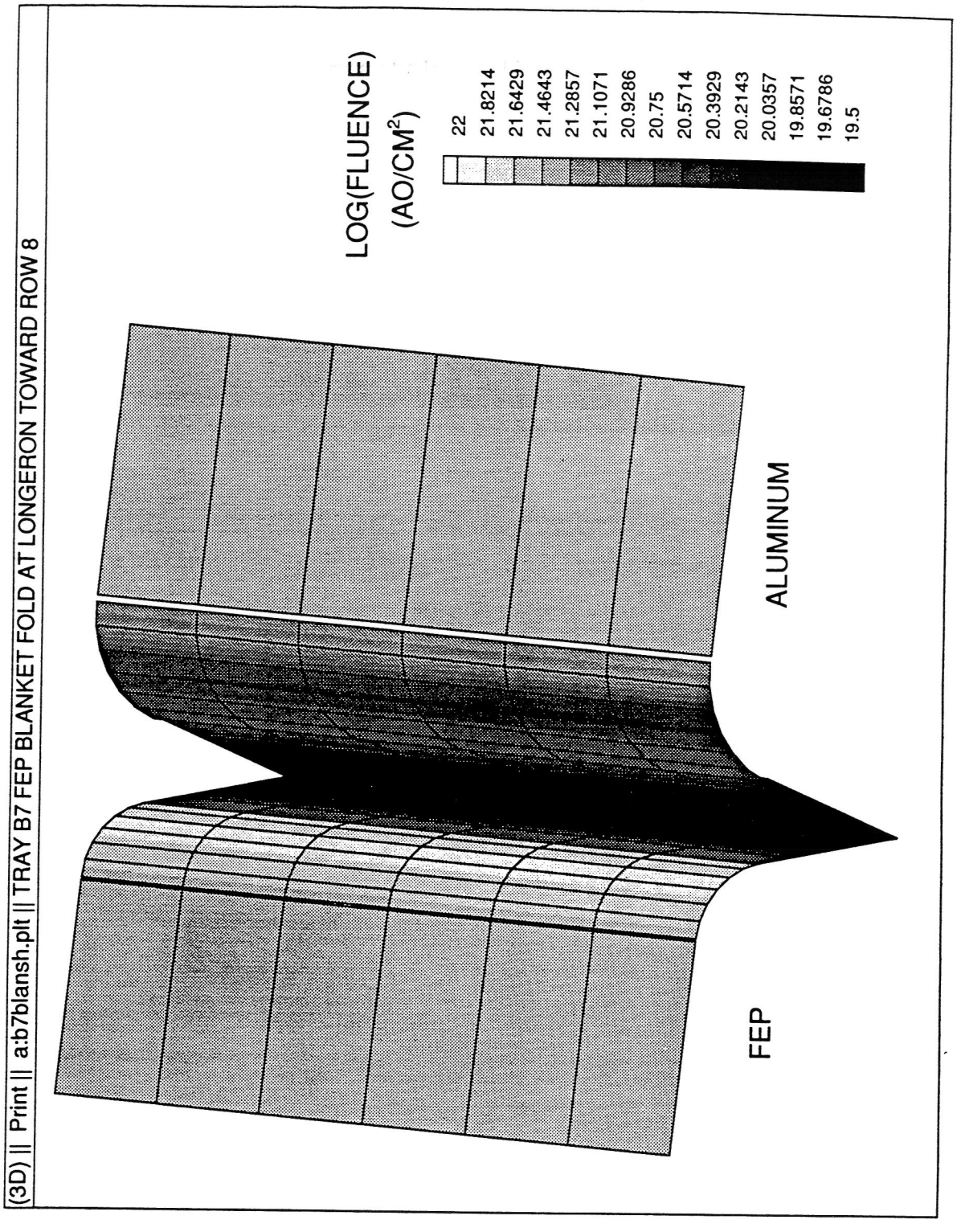

Figure 9.2-1. B-7 FEP Blanket Fold at Longeron Atomic Oxygen Exposure Given as Log_{10} AO Fluence (Atoms/cm^2).

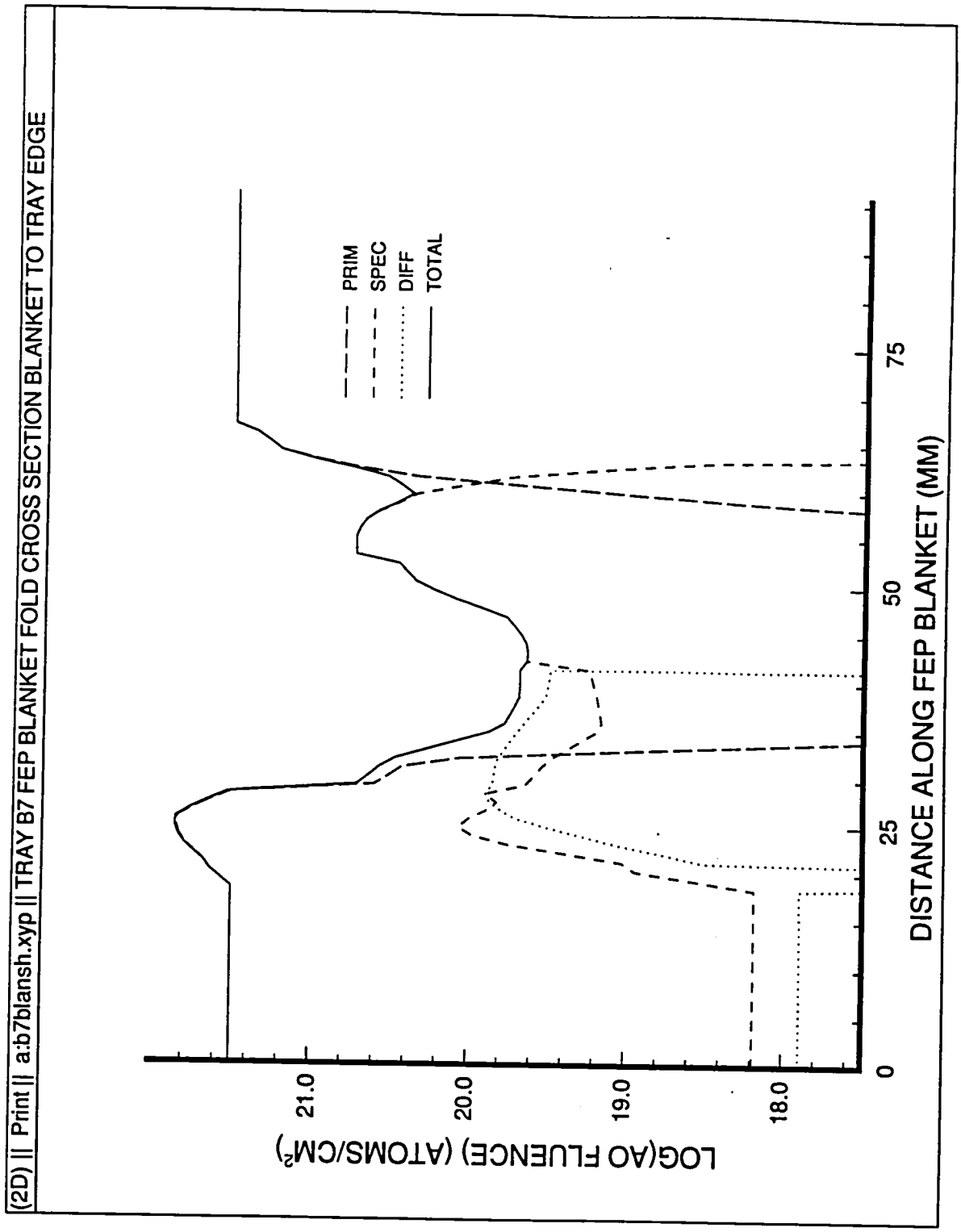

Figure 9.2-2. Atomic Oxygen Exposure Cross Section of Figure 9.2-1.

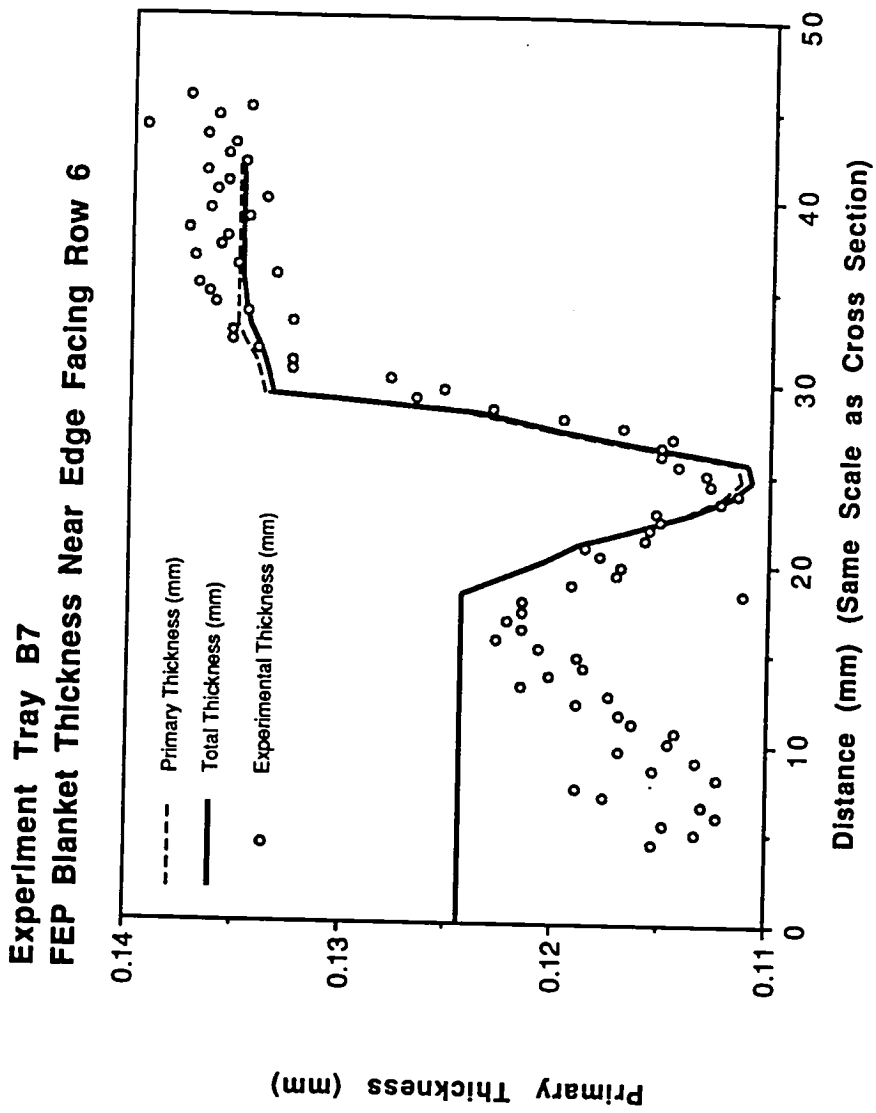

Figure 9.2-3. B-7 FEP Blanket Fold at Longeron Calculated vs Experimental FEP Thickness.

10.0 TRAY C-5 FEP BLANKET FOLD NEAR TRAY EDGE

10.1 Experiment Location and Description

The tray C-5 blanket fold is located on LDEF on the row 6 side of tray 5. The row 5 surface normal is oriented 128.1 degrees from ram direction. The thermal control blanket is FEP and the tray is aluminum.

This region was modeled so that predicted solar exposure to it could be compared to the measured variations in FEP surface structure with location (ref. 10).

10.2 Solar Exposure

Figure 10.2-1 shows the LDEF mission solar exposure to the FEP blanket and the aluminum tray edge in the region of the C-5 FEP blanket fold at the tray edge parallel to row 6. In the figure, the FEP blanket is on the left and the aluminum tray edge is on the right. Figure 10.2-2 shows a cross section of the solar exposure. Solar exposure is given for total direct and Earth-reflected solar exposure (GRTOT), direct primary solar exposure (PRIM), direct specular reflected solar exposure (SPEC), direct diffuse reflected solar exposure (DIFF), and total direct solar exposure (TOTAL). The cross section is taken along a line on the surfaces about midway from top to bottom in figure 10.2-1. Distance (the horizontal axis) in the cross section is measured from the left side of the FEP blanket in Figure 10.2-1 along the surface of the blanket and the aluminum tray side to the right side of the aluminum tray .

Examination of figure 10.2-2 shows that approximately one seventh of the total solar exposure is due to Earth-reflected solar radiation (the difference between the total direct and Earth reflected solar exposure and total direct solar exposure). The solar exposure to the flat FEP and aluminum surfaces parallel to row 5 is constant. The average Sun position is most nearly perpendicular to the curved part of the aluminum tray and results in the highest exposure to this surface because of the combined effects of direct and reflected solar radiation. Nearly all of the exposure in the "V" is due to reflections. That on the FEP is due mainly to diffuse reflection from the aluminum side of the "V"; that on the aluminum is due mainly to specular reflection from the FEP side of the "V."

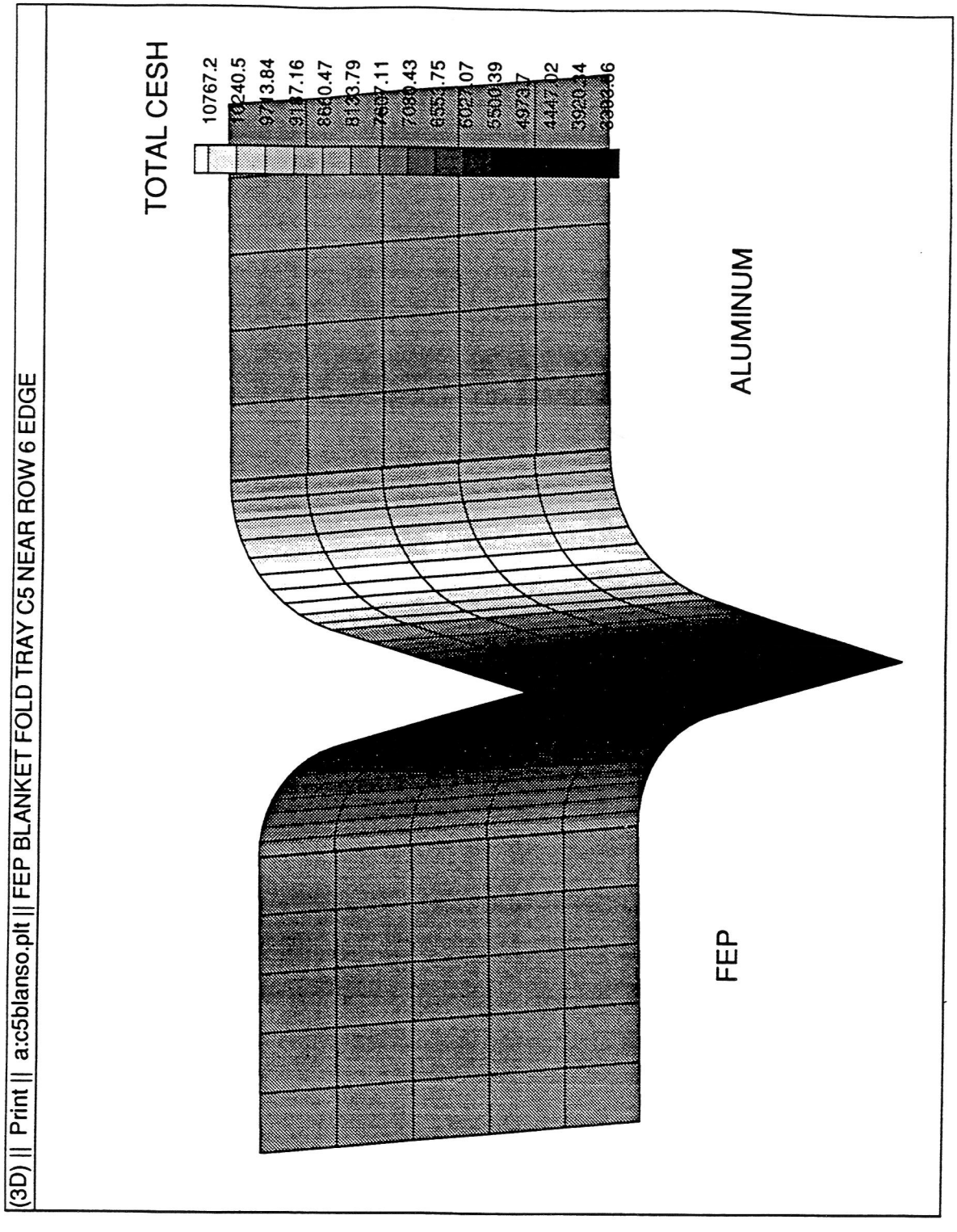

Figure 10.2-1. C-5 FEP Blanket Fold Near Tray Edge Solar Exposure in CESH.

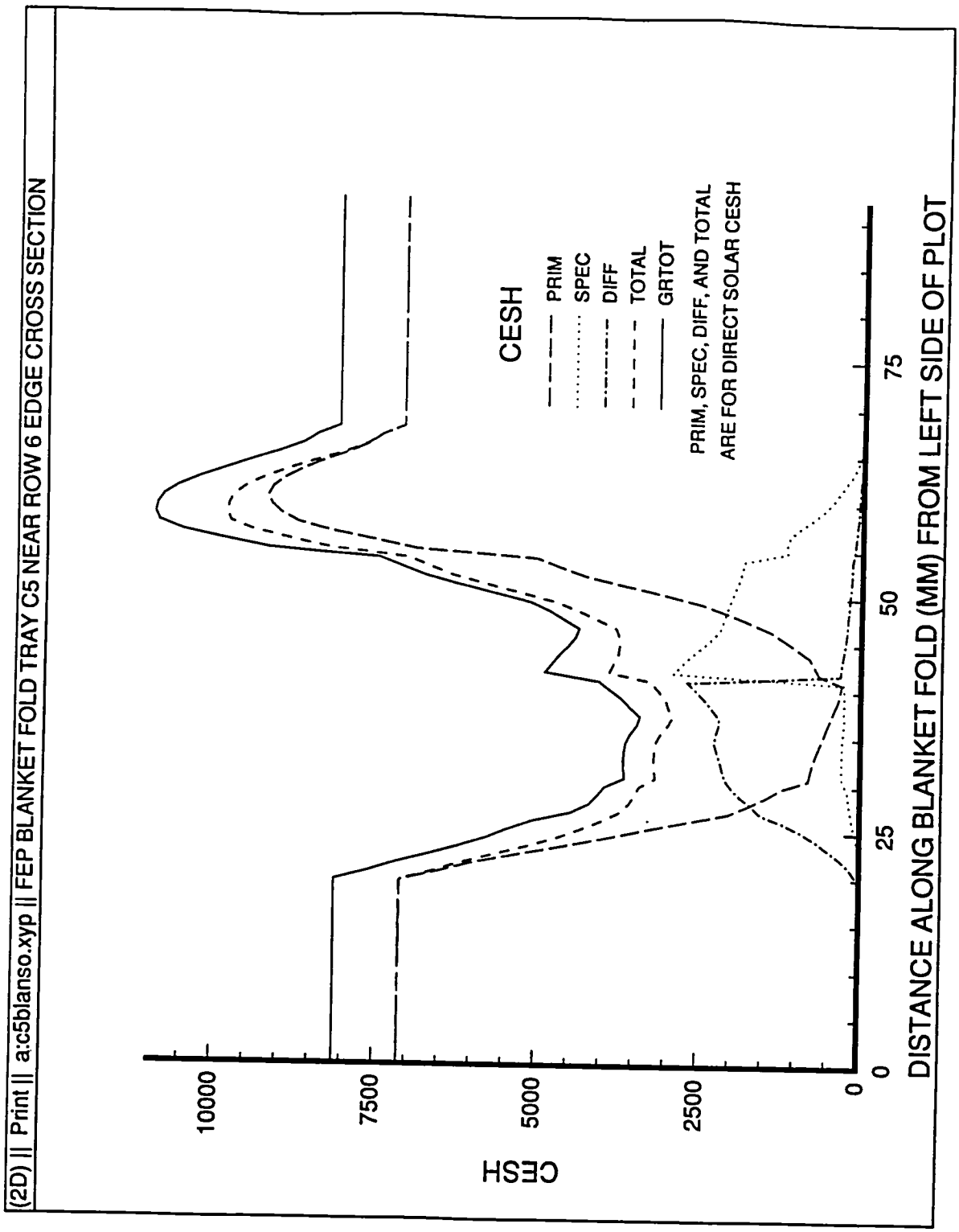

Figure 10.2-2. Solar Exposure Cross Section of Figure 10.2-1.

11.0 TRAY D-1 FEP BLANKET FOLD NEAR ROW 2 EDGE

11.1 Experiment Location and Description

The tray D-1 blanket fold is located on LDEF on the row 1 side of tray D-1 as shown in figure 11.1-1 (and color photo A11.1-1, p. A9). The row 1 surface normal is oriented 111.9 degrees from ram direction. The top of figure 11.1-1 is oriented toward the space end of LDEF. The thermal control blanket is FEP and the tray is aluminum.

This region was modeled so that predicted solar exposure to it could be compared to the measured variations in FEP surface structure with location (ref. 10).

11.2 Solar Exposure

Figure 11.2-1 shows the LDEF mission solar exposure to the FEP blanket and the aluminum tray edge in the region of the D-1 FEP blanket fold at the tray edge parallel to row 2. In the figure, the FEP blanket is on the left and the aluminum tray edge is on the right. Figure 11.2-2 shows a cross section of the solar exposure. Solar exposure is given for total direct and Earth-reflected solar exposure (GRTOT), direct primary solar exposure (PRIM), direct specular reflected solar exposure (SPEC), direct diffuse reflected solar exposure (DIFF), and total direct solar exposure (TOTAL). The cross section is taken along a line on the surfaces about midway from top to bottom in figure 11.2-1. Distance (the horizontal axis) in the cross section is measured from the left side of the FEP blanket in figure 11.2-1 along the surface of the blanket and the aluminum tray side to the right side of the aluminum tray.

Examination of figure 11.2-2 shows that approximately one sixth of the total solar exposure is due to Earth-reflected solar radiation (the difference between the total direct and Earth reflected solar exposure and total direct solar exposure). The solar exposure to the flat FEP and aluminum surfaces parallel to row 1 is constant. The average Sun position is most nearly perpendicular to the curved part of the FEP blanket and results in the highest exposure to this surface because of the combined effects of direct and reflected solar radiation. Nearly all of the exposure in the "V" is due to reflections. That on the FEP is due mainly to diffuse reflection from the aluminum side of the "V"; that on the aluminum is due mainly to specular reflection from the FEP side of the "V."

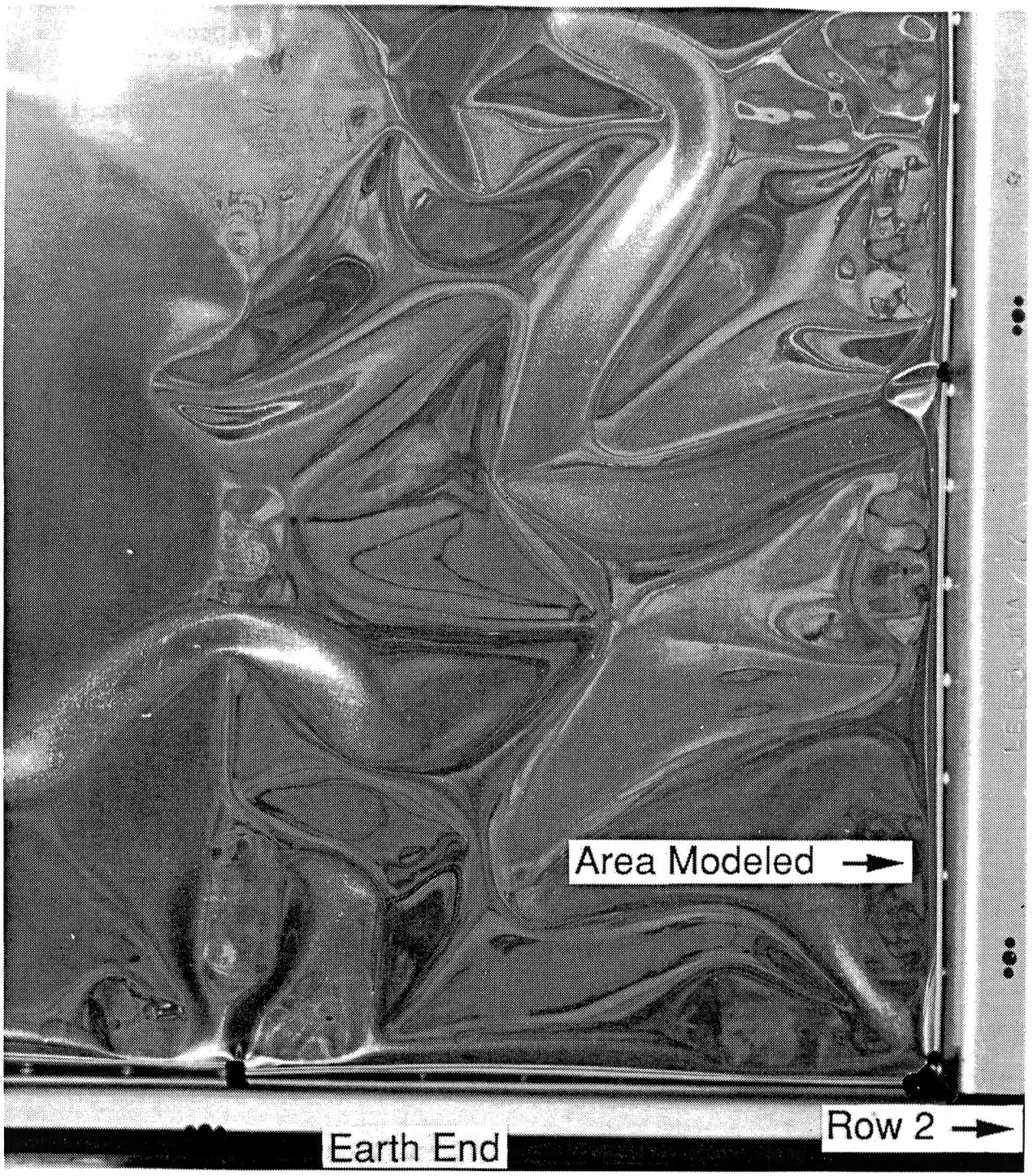

Figure 11.1-1. D-1 FEP Blanket Fold Near Row 2 Edge Photo.

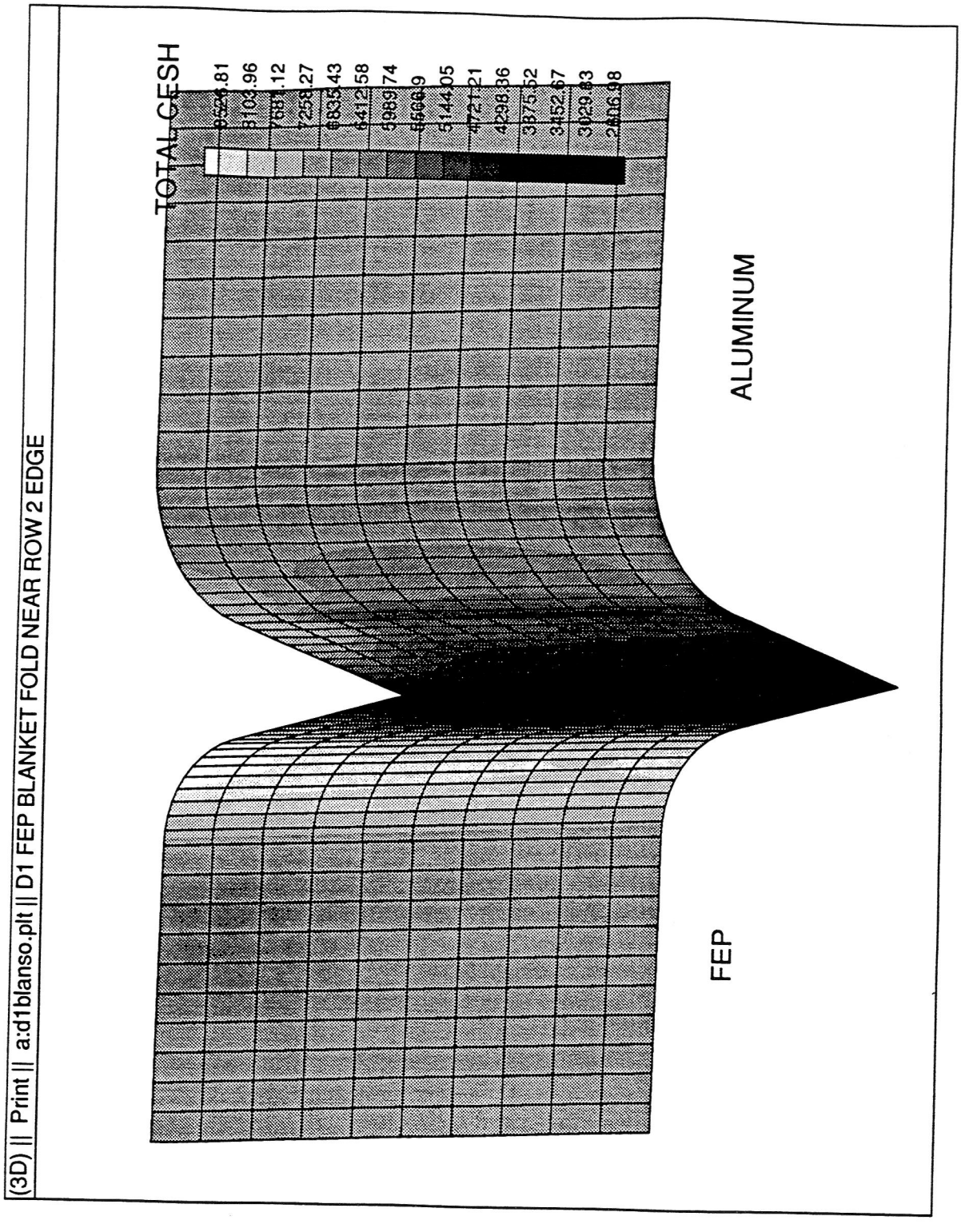

Figure 11.2-1. D-1 FEP Blanket Fold Near Row 2 Edge Solar Exposure in CESH.

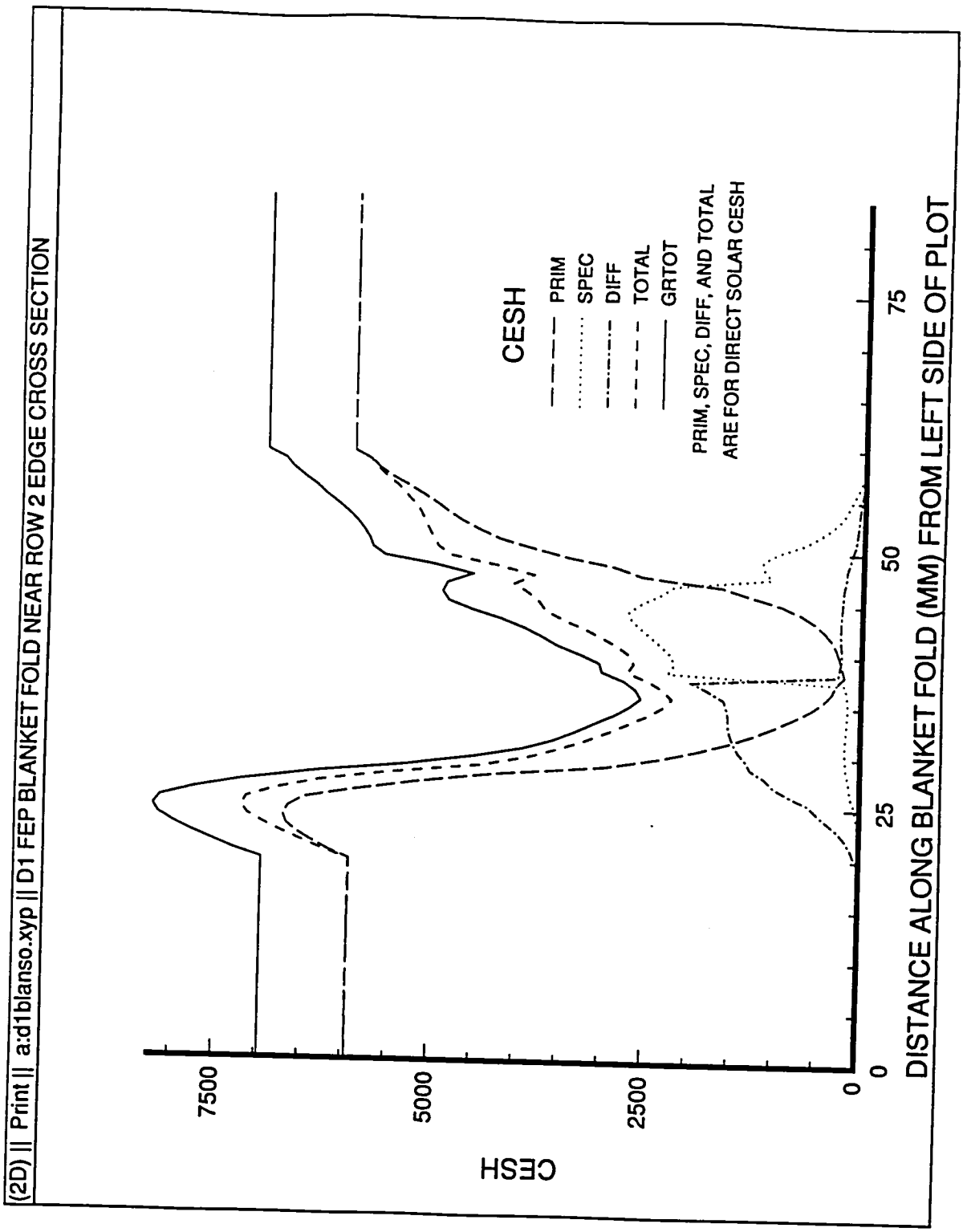

Figure 11.2-2. Solar Exposure Cross Section of Figure 11.2-1.

12.0 C-9 SCUFF PLATE

12.1 Experiment Location and Description

The C-9 scuff plate is located in LDEF experiment tray 9. Figure 12.1-1 (and color photo A12.1-1, p. A10) shows the location of this experiment. Row 9 is the LDEF row most nearly facing ram direction. All surfaces on the scuff plate are coated with yellow Chem Glaze-II paint. The tray surfaces are modeled as aluminum.

12.2 Atomic Oxygen Exposure

Figure 12.2-1 shows LDEF mission atomic oxygen exposure to the C-9 scuff plate. Both ram facing and row 9 facing surfaces of the scuff plate are represented. The large rectangular surface under the scuff plate represents tray C-9 and the large rectangular surface in the lower part of figure 12.2-1 represents row 10. The right side of the figure is oriented toward the space end of LDEF. Several AO fluences in log atoms/cm^2 are marked. The surfaces parallel to row 9 and facing ram receive a near constant AO fluence of 8.5×10^{21} atoms/cm^2 and row 10 receives a constant fluence of 7.4×10^{21} atoms/cm^2. The surfaces on the under side of the scuff plate show clearly the effects of shadowing and reflection. Some materials samples in tray C-9 under the scuff plate (under the left side of the scuff plate in figure 12.2-1) are partially shadowed from atomic oxygen. The maximum shadowing reduces the AO fluence to samples nearest the base of the scuff plate to about one third that on unshadowed surfaces of tray C-9.

12.3 Solar Exposure

Figure 12.3-1 shows LDEF mission solar exposure in CESH to the C-9 scuff plate. Solar exposure in CESH are indicated at several locations on the figure. As with AO exposure, the effects of shadowing and reflections are clearly shown on the figure. Tray C-9 material samples nearest the base of the scuff plate (to the left side of the scuff plate base in figure 12.3-1) receive about on third the CESH of samples which are not shielded.

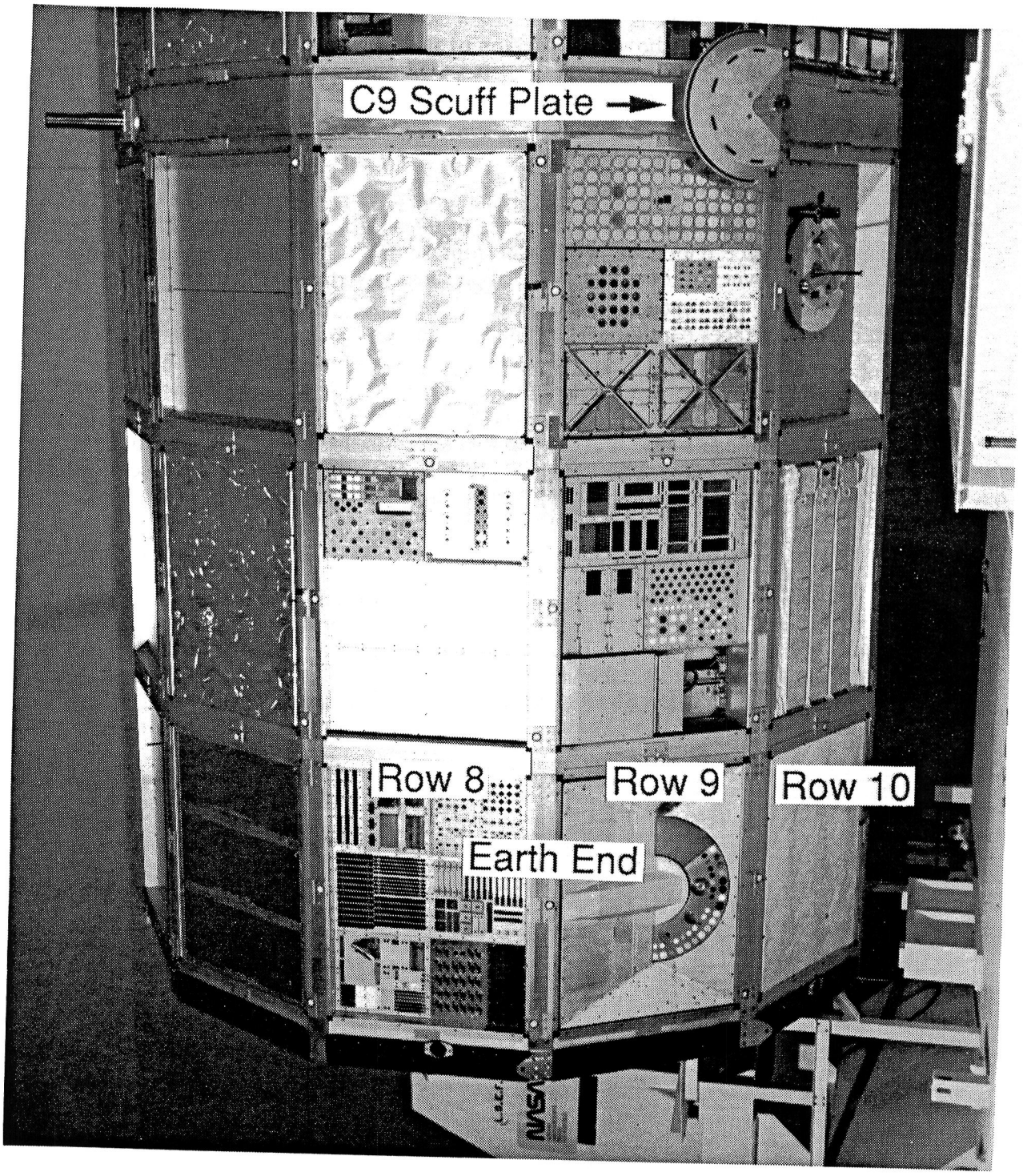

12.1-1. C-9 Scuff Plate Location Photo.

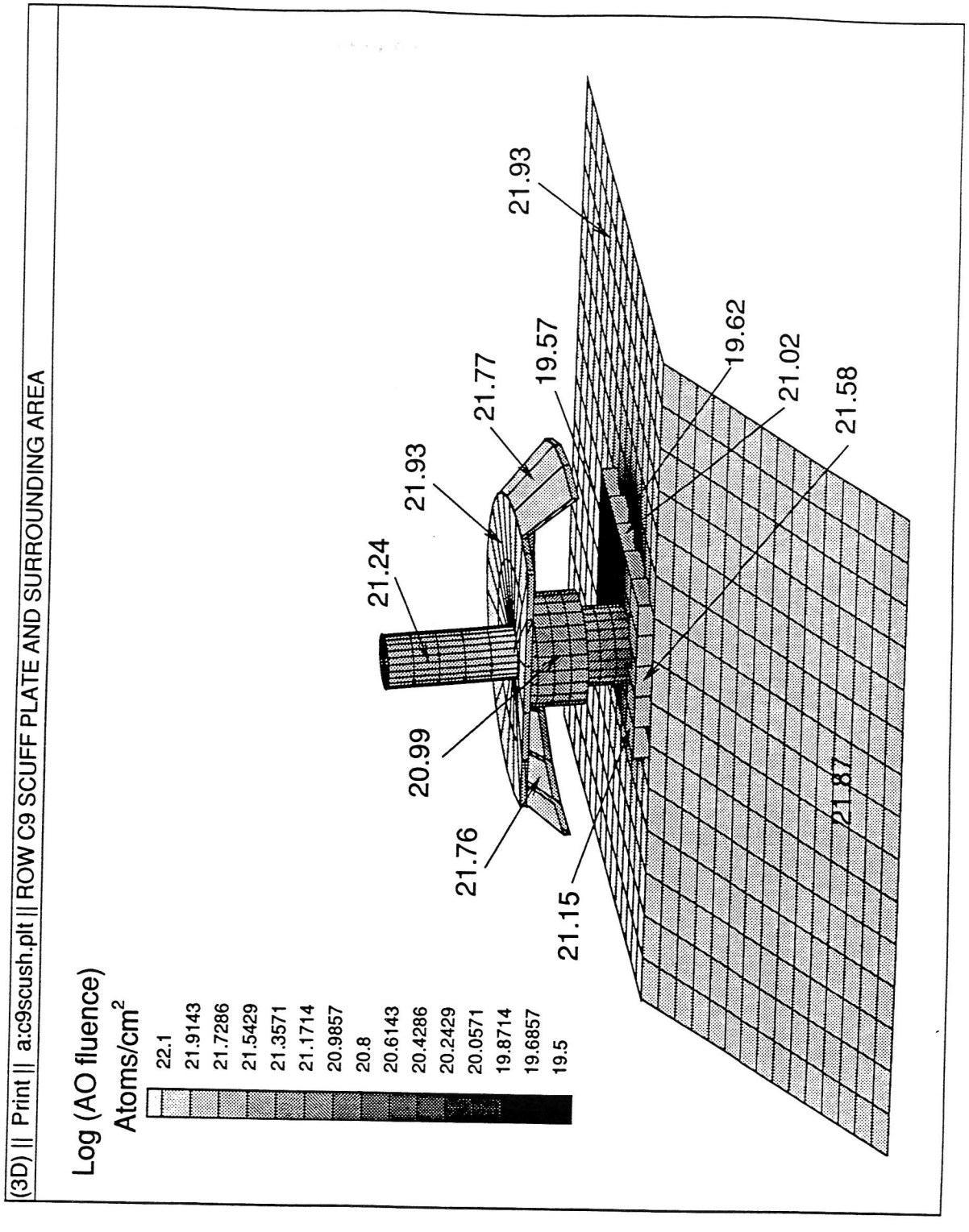

Figure 12.2-1. C-9 Scuff Plate Atomic Oxygen Exposure Given as Log_{10} AO Fluence (Atoms/cm^2).

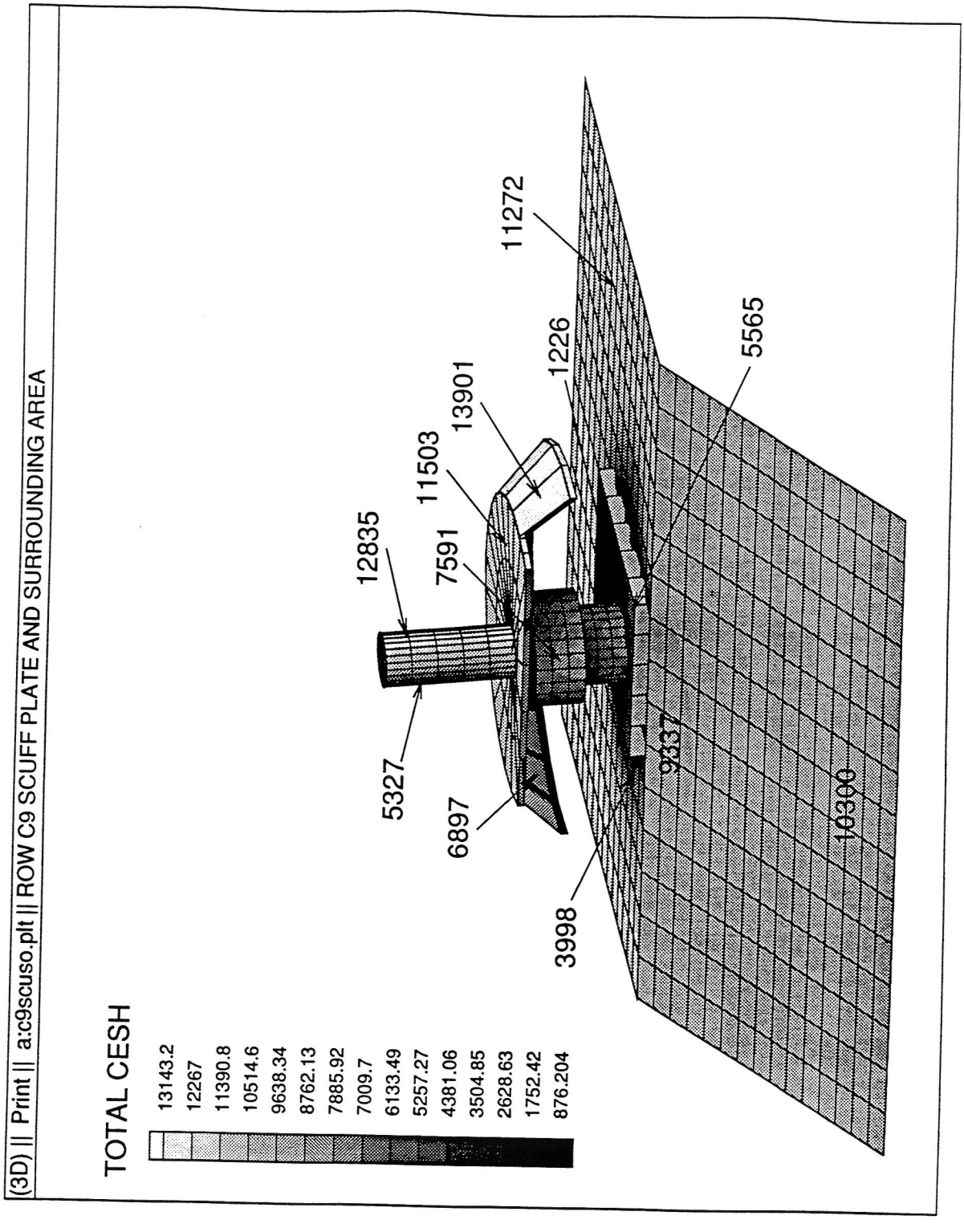

12.3-1. C-9 Scuff Plate Solar Exposure in CESH.

13.0 SPACE END TRAY CLAMP H-12 WITH THREE BOLTS

13.1 Experiment Location and Description

Tray clamp H-12 is located on the space end of LDEF. Figure 13.1-1 (and color photo A13.1-1, p. A11) shows the location of this tray clamp. All surfaces of the tray clamp are aluminum.

13.2 Atomic Oxygen Exposure

Figure 13.2-1 shows LDEF mission atomic oxygen exposure to the space end tray clamp H-12 and three bolt heads. The ram direction is from the right of the figure and nearly parallel to the plane of the clamp. The thin vertical plate above the clamp simulates the tray side which shields the top of the clamp from side AO fluences. Several AO fluences in log atoms/cm^2 are marked. Figure 13.2-1 clearly shows the effects of shadowing behind the bolt heads. The differences in the shadow patterns behind the bolt heads are primarily artifacts of the finite resolution of the grid on the clamp surface. Had the grid been made finer, the shadow patterns would be expected to be more nearly alike.

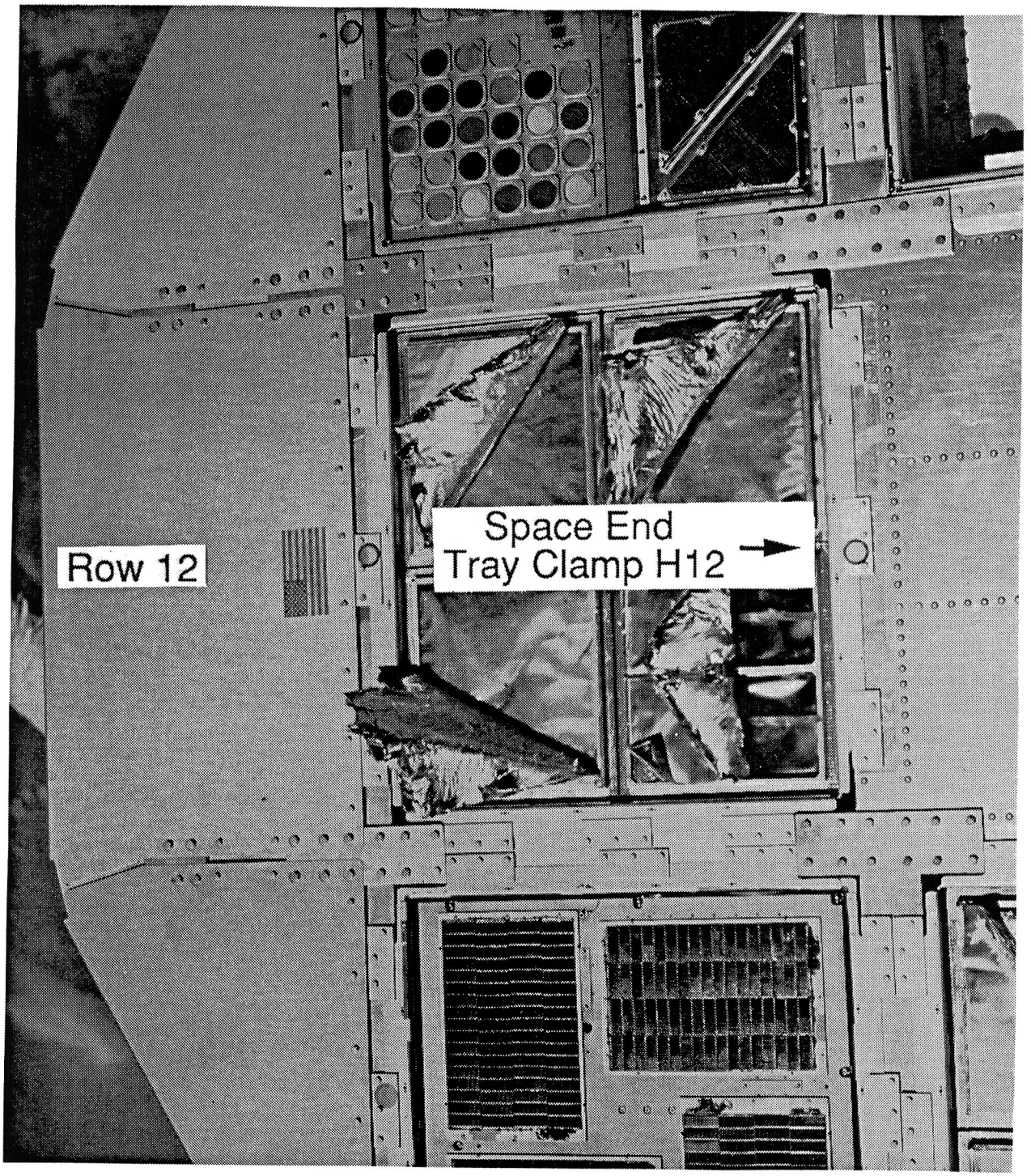

13.1-1. Space End Tray Clamp H-12 On-Orbit Photo.

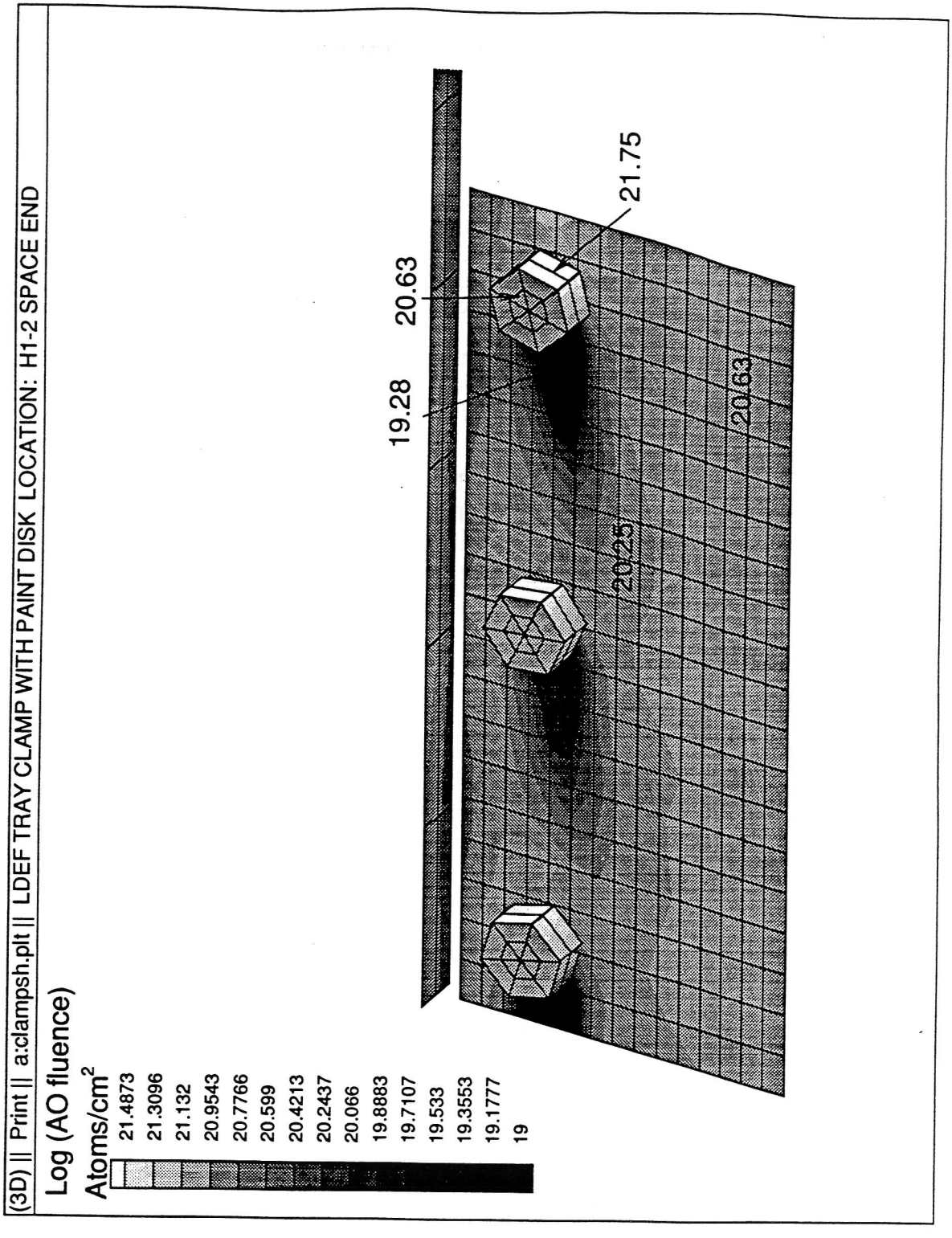

Figure 13.2-1. Space End Tray Clamp H-12 With Three Bolts Atomic Oxygen Exposure Given as Log_{10} AO Fluence (Atoms/cm^2).

14.0 ENVIRONMENT EXPOSURE CONTROL CANISTER (EECC) EXPERIMENT TRAYS

14.1 Experiment Location and Description

The B-9, C-2, D-4, D-8, and E-3 Environment Exposure Control Canisters (EECC) are located as shown in figure 14.1-1. This figure shows the orientation of the EECC experiment tray drawers when opened with respect to their enclosures. All surfaces of the EECC are modeled as aluminum. Only the experiment tray and front experiment tray lip and the lip of the EECC enclosure for each EECC are modeled.

EECC B-9, C-2, and E-3 experiment trays were either completely closed or completely exposed during the LDEF mission. EECC D-4 and D-8 experiment trays were exposed to the space environment in stages. Figure 14.1-2 lists the experiment tray exposure times for the EECCs.

EECC	Exposure	Exposure Start Date	Exposure End Date
B-9,C-2, and E-3	100% of tray exposed	April 17, 1984	January 29, 1985
D-4 and D-8	75% of tray exposed	April 21, 1984	September 15, 1984
	87.5% of tray exposed	September 15, 1984	November 26, 1984
	100% of tray exposed	November 26, 1984	January 26, 1985

Figure 14.1-2 EECC Exposure Sequence.

14.2 Atomic Oxygen Exposure

14.2.1 B-9, C-2, and E-3 EECC Experiment Trays. Figure 14.2.1-1 shows atomic oxygen fluence to the B-9 EECC experiment tray. The B-9 EECC experiment tray, which faces almost directly into the ram direction, receives a nearly uniform AO exposure except for slight shadowing and reflection near the lips of the tray and enclosure (left and right sides of fig. 14.2.1-1, respectively). The C-2 (141.9 degrees from ram) and E-3 EECC (171.9 degrees from ram) experiment trays are both on the trailing side of the LDEF and are well shielded from AO exposure. The exposure to these EECC experiment trays is 8 to 20 orders of magnitude less than on the B-9 EECC experiment tray. For engineering purposes the trailing edge EECC experiment trays may be considered to have had zero AO exposure.

14.2.2 D-4 and D-8 EECC Experiment Trays. Figure 14.2.2-1 shows atomic oxygen fluence to the D-8 EECC experiment tray. The D-4 EECC experiment tray (158.1 degrees from ram) is on the trailing edge of LDEF and received such a small AO fluence that the the fluence may be considered to be zero. The D-8 EECC experiment tray is 38.1 degrees from ram. Figure 14.2.2-1 clearly shows the effects of the sequenced exposure of the experiment tray, with decreasing AO fluence to the more recently exposed portions. Also evident is an increase in flux due to reflections from the lip of the experiment tray.

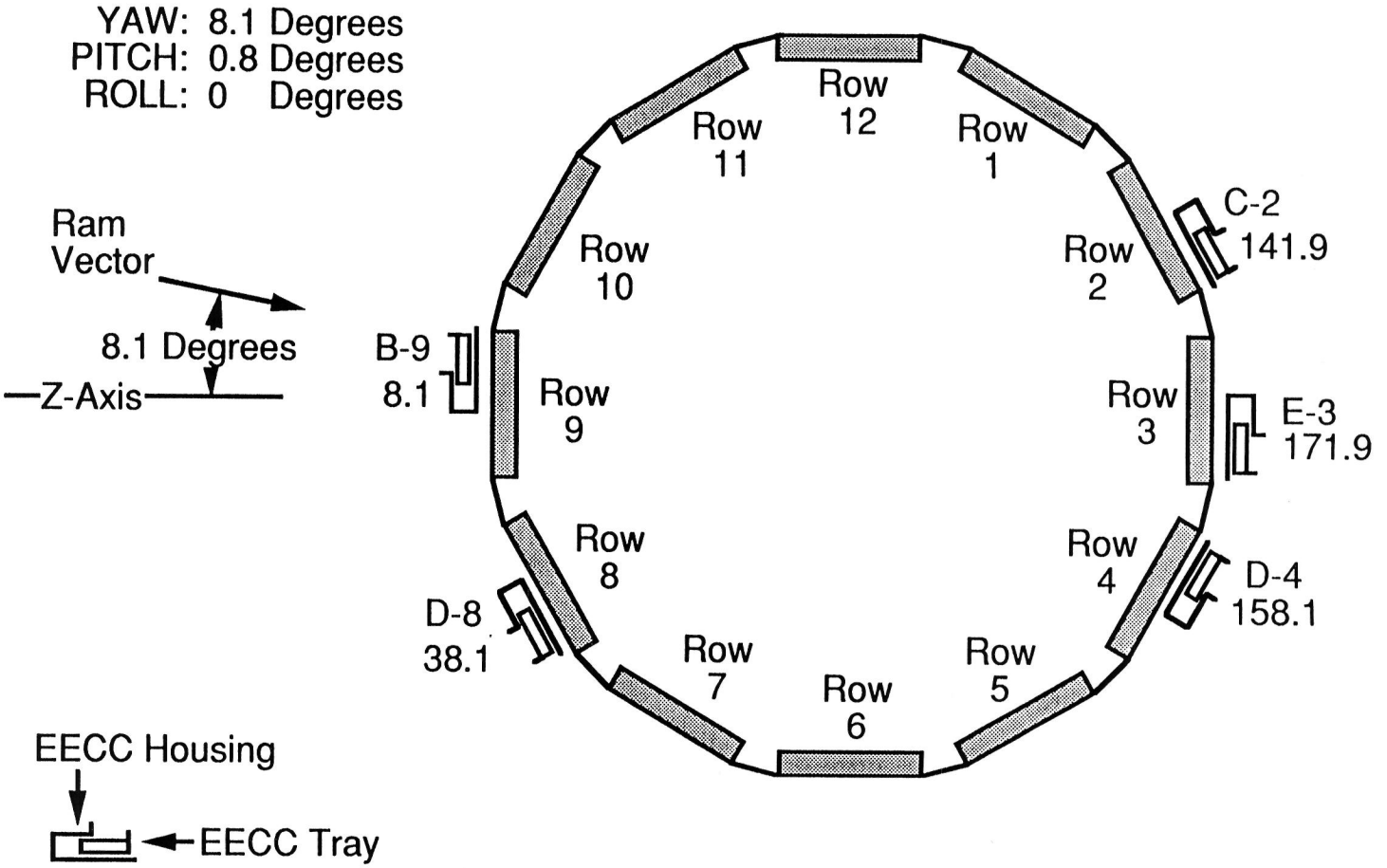

LDEF EECCS ORIENTATION AND
ANGLES FROM THE RAM DIRECTION IN DEGREES

14.1-1. EECC Orientations on LDEF.

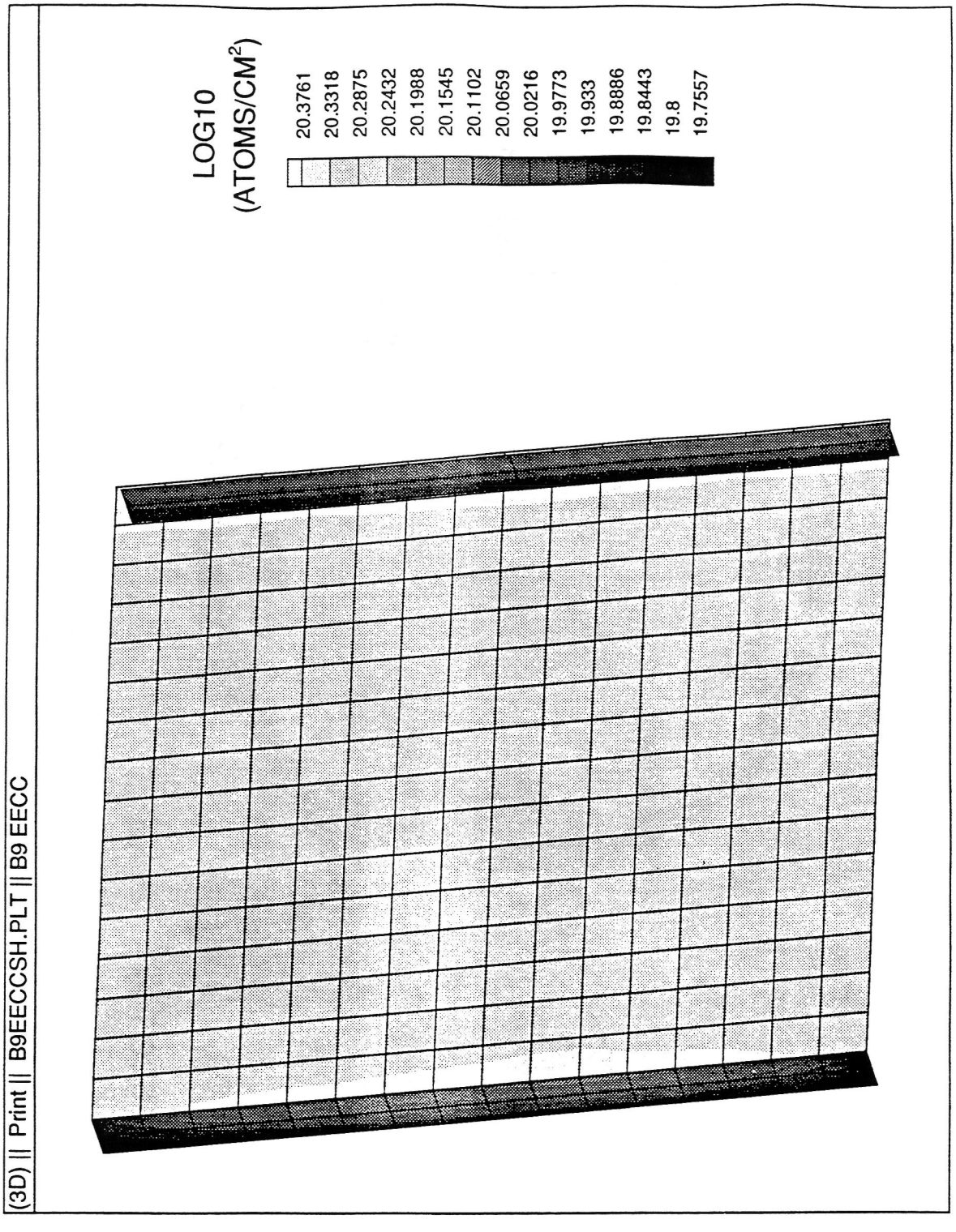

Figure 14.2.1-1. B-9 EECC Experiment Tray Atomic Oxygen Exposure Given as Log_{10} AO Fluence (Atoms/cm^2).

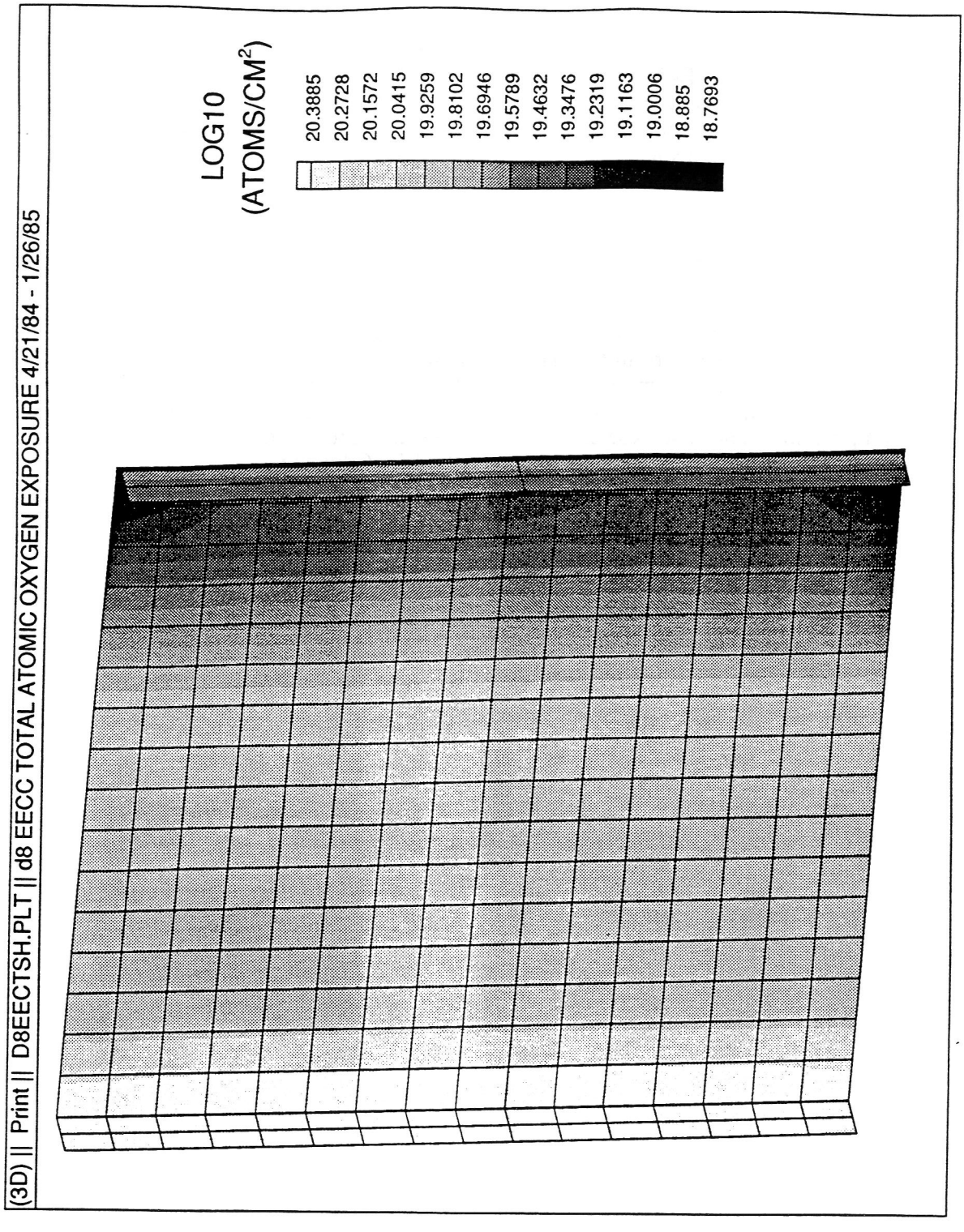

Figure 14.2.2-1. D-8 EECC Experiment Tray Atomic Oxygen Exposure Given as Log_{10} AO Fluence (Atoms/cm^2).

14.3 Solar Exposure

B-9, C-2, and E-3 EECC Experiment Trays. Figures 14.3.1-1 through 14.3.1-3 show solar exposure in CESH to the B-9, C-2, and E-3 EECC experiment trays. The B-9 EECC experiment tray, which faces almost directly into the ram direction, receives a nearly uniform solar exposure except for shadowing near the lip of the tray (left side of fig. 14.3.1-1). The C-2 (141.9 degrees from ram) is slightly shadowed from solar exposure by the experiment tray lip (right side of fig. 14.3.1-2) and receives some reflected exposure from the EECC cover lip (left side of fig. 14.3.1-2). The E-3 EECC (171.9 degrees from ram) experiment trays receives nearly uniform solar exposure, with the differences shown in figure 14.3.1-3 being of statistical nature rather than real.

14.3.2 D-4 and D-8 EECC Experiment Trays. Figures 14.3.2-1 and 14.3.2-2 show solar exposure in CESH to the D-4 and D-8 EECC experiment trays. The D-4 and D-8 EECC experiment trays both clearly show the effects of the sequenced exposure of the experiment trays, with decreasing solar exposure to the more recently exposed portions. The D-4 experiment tray shows an increase in solar exposure at about 75% exposure due to reflections from the lip of the EECC housing.

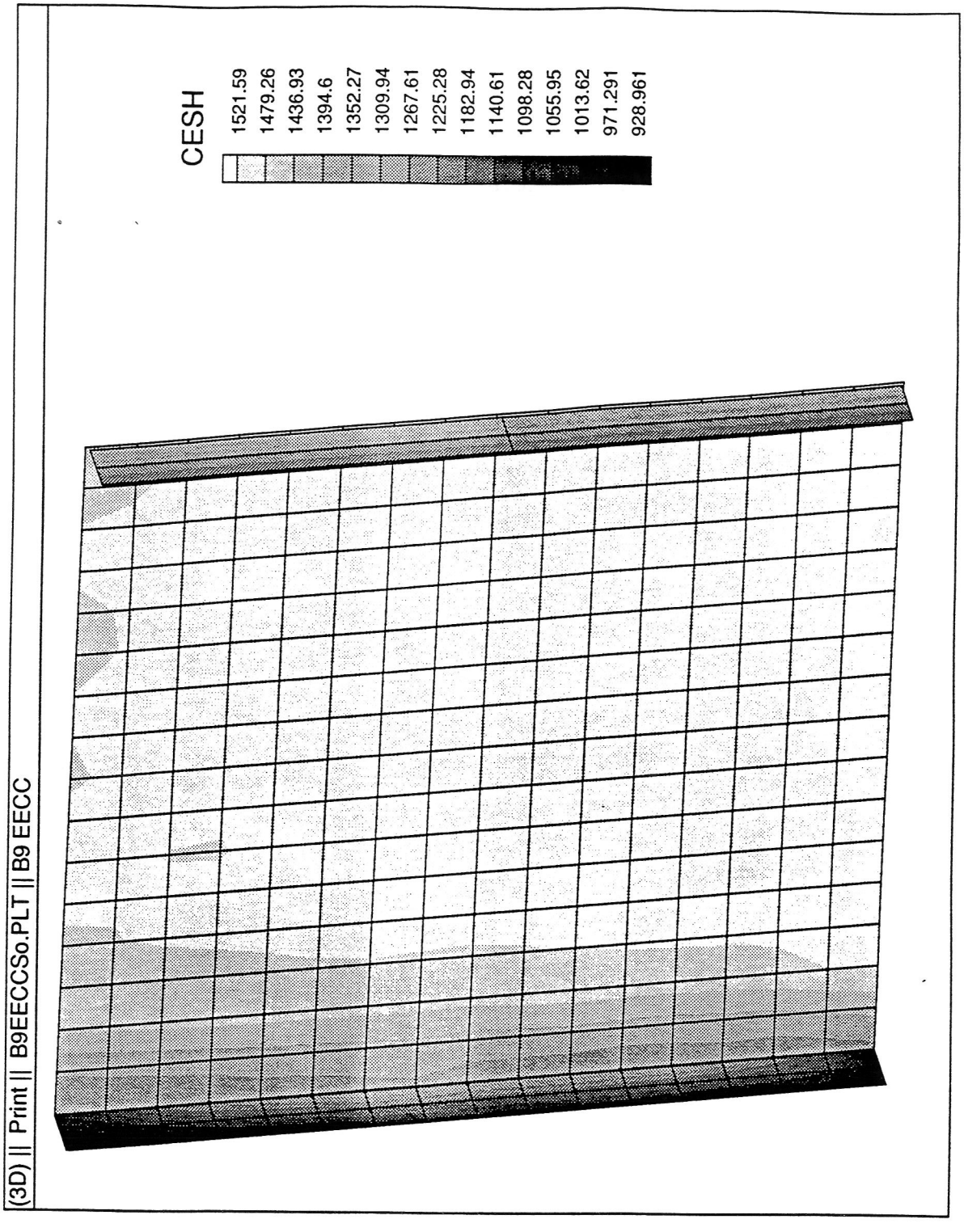

Figure 14.3.1-1. B-9 EECC Experiment Tray Solar Exposure in CESH.

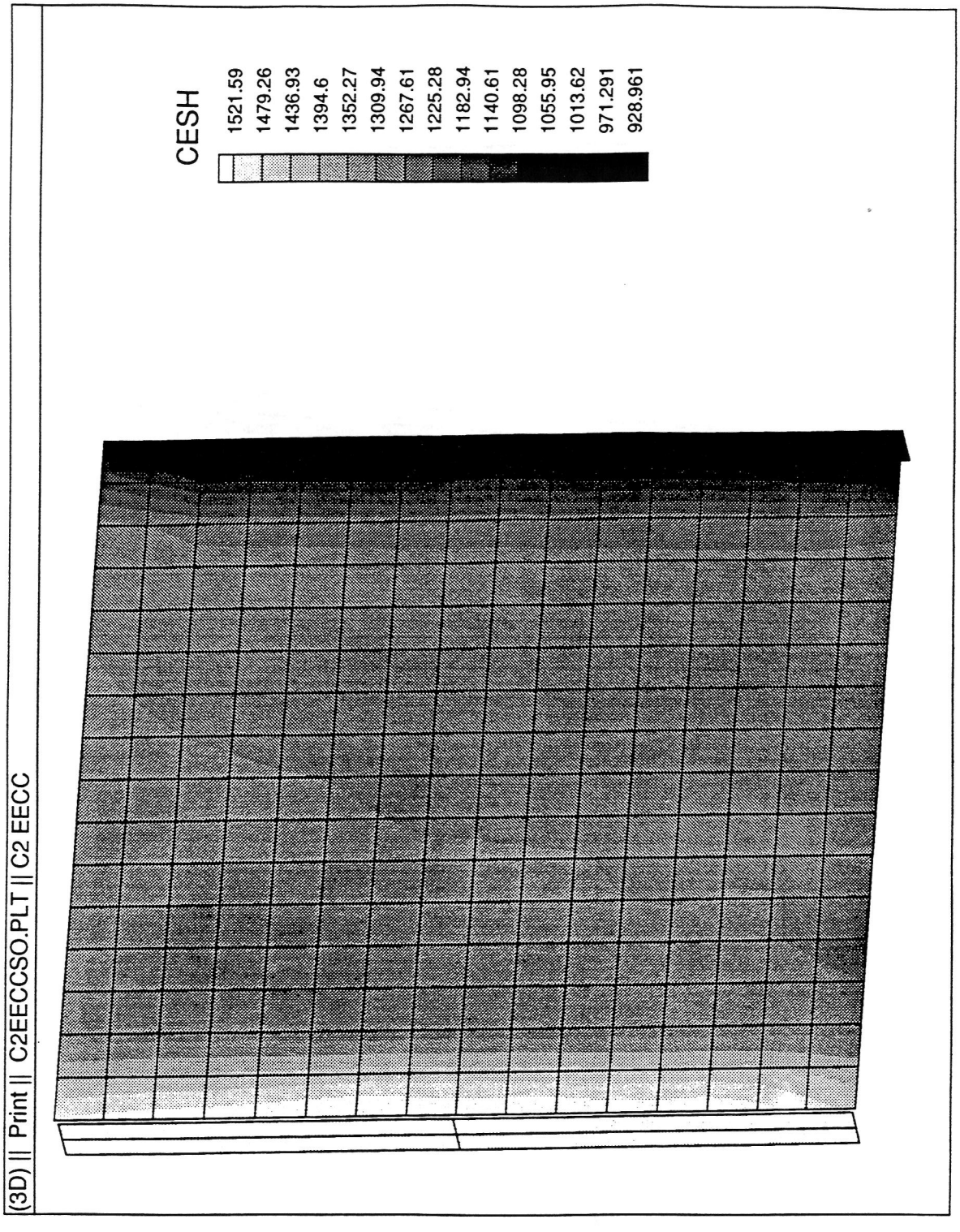

Figure 14.3.1-2. C-2 EECC Experiment Tray Solar Exposure in CESH.

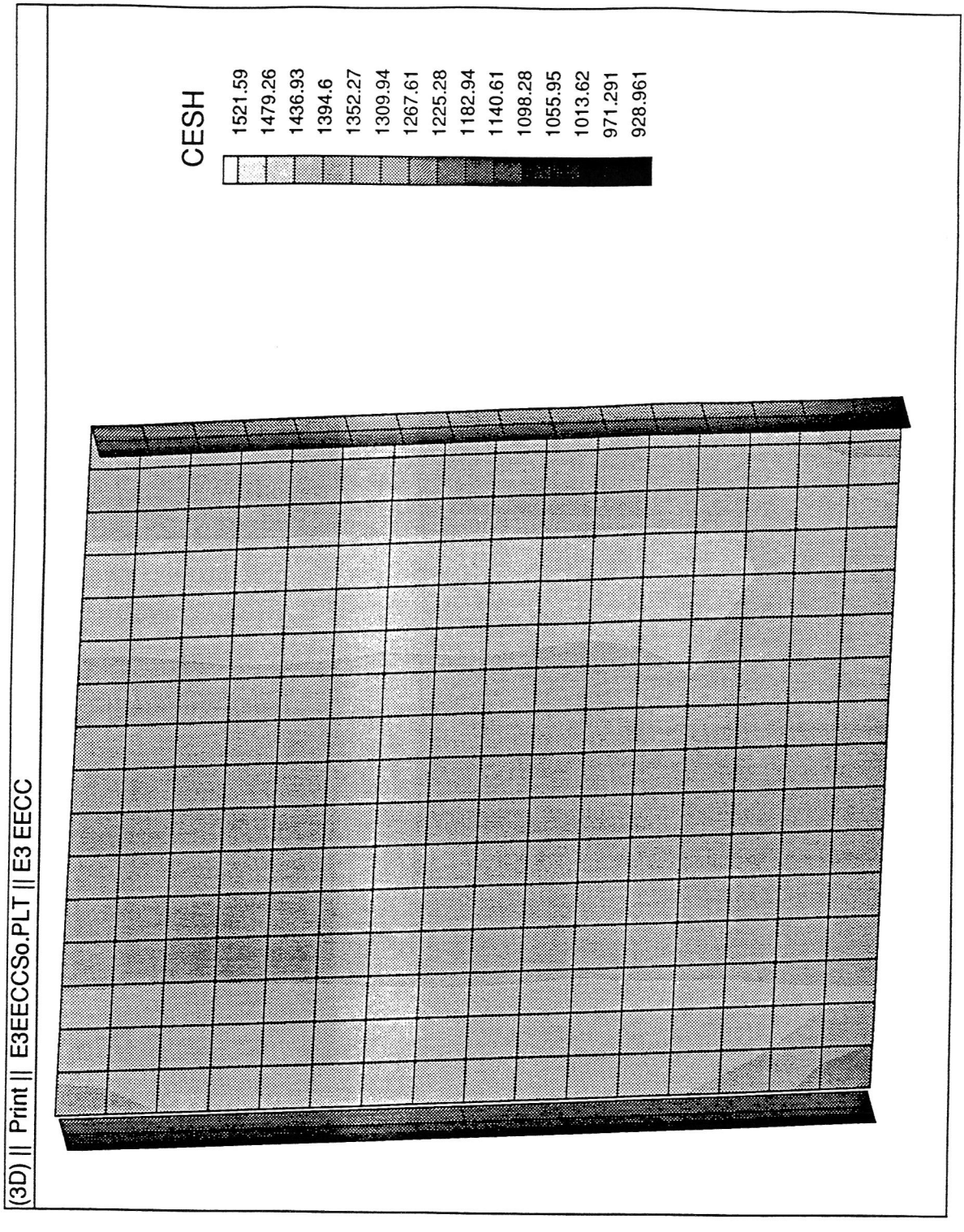

Figure 14.3.1-3. E-3 EECC Experiment Tray Solar Exposure in CESH.

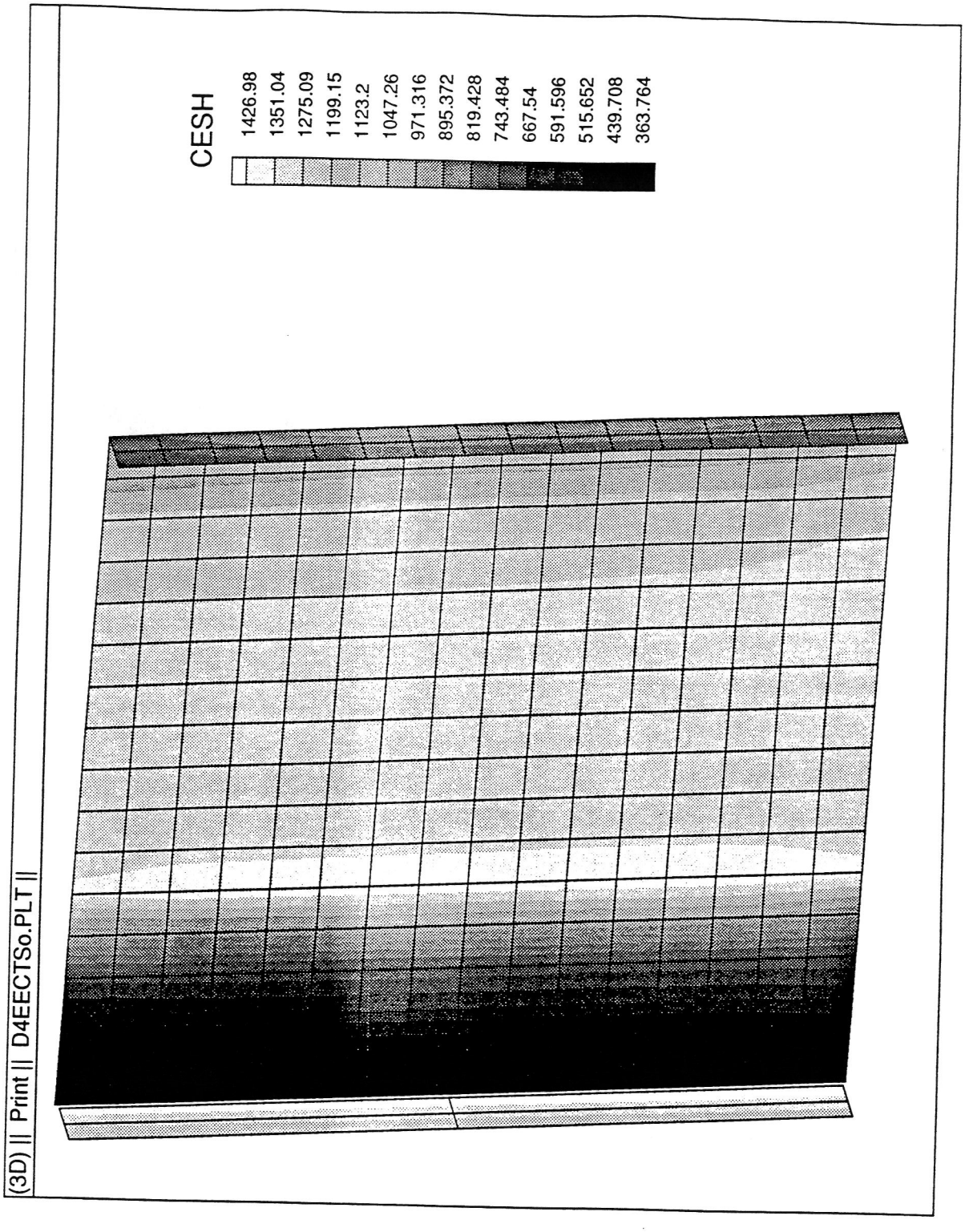

Figure 14.3.2-1. D-4 EECC Experiment Tray Solar Exposure in CESH.

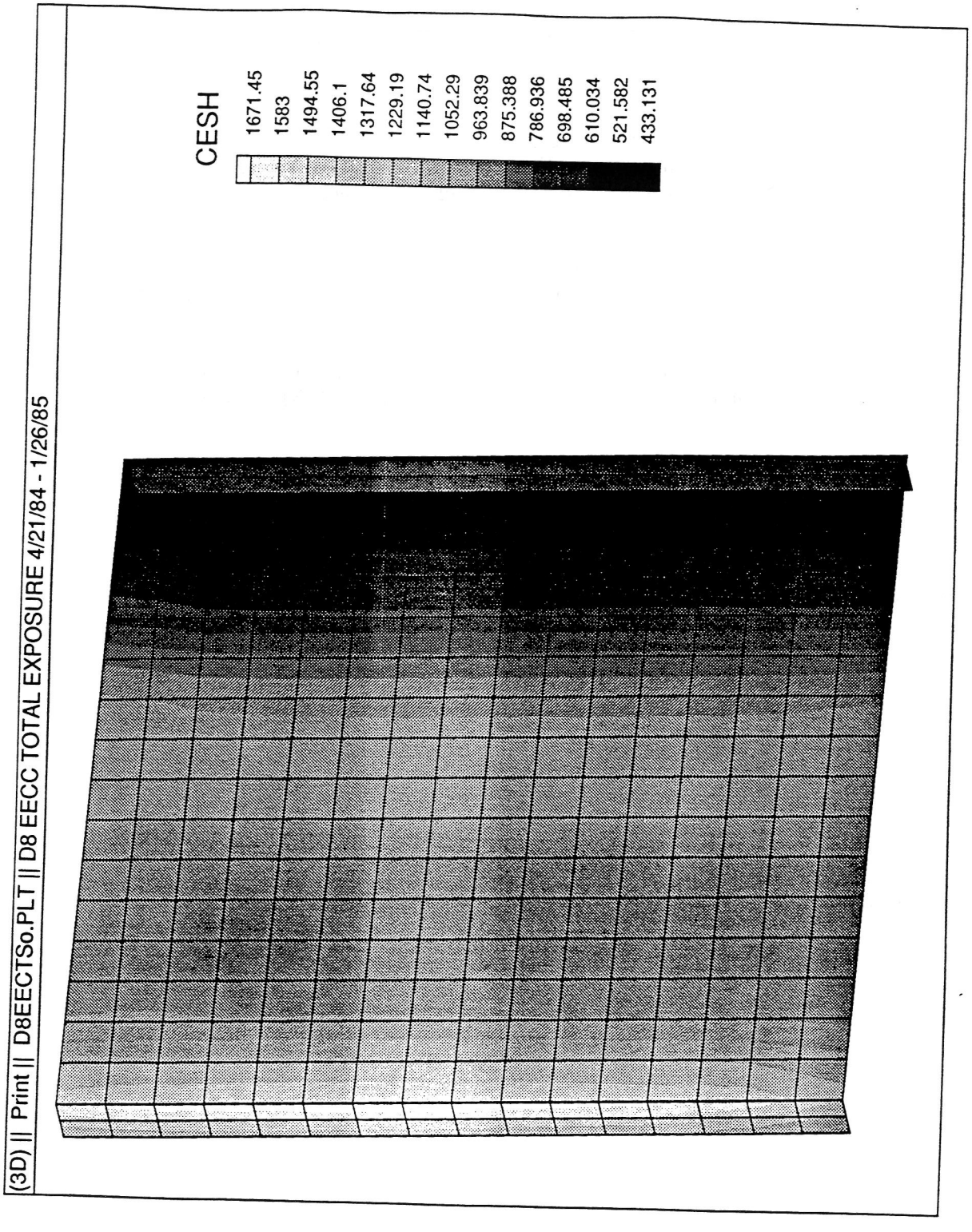

Figure 14.3.2-2. D-8 EECC Experiment Tray Solar Exposure in CESH.

REFERENCES

1. R. J. Bourassa, Gillis, J.R., Gruenbaum, P.E., "Operation of the Computer Model for Microenvironment Atomic Oxygen Exposure for SHADOWV2," Boeing Defense & Space Group, NASA CR-198190, August 1995.

2. Bourassa, R.J., Gillis, J.R., Gruenbaum, P.E., "Operation of the Computer Model for Microenvironment Atomic Oxygen Exposure for SHADOW Version 1.1," Memorandum 9-5571-SGH-94-003, Boeing Defense & Space Group, January 26, 1994.

3. Bourassa, R. J., Pippin, H.G., Gillis, J.R., "Model of Spacecraft Atomic Oxygen and Solar Exposure Microenvironments," presented at the LDEF Materials Results for Spacecraft Applications Conference, October 1992, Huntsville, Alabama, NASA CP-3257, p. 105.

4. Bourassa, R. J., Pippin, H.G., Gillis, J.R., "LDEF Microenvironments, Observed and Predicted," Second Post-Retrieval Symposium, NASA CP-3194, part 1, June 1992, p. 13.

5. Bourassa, R.J., Gruenbaum, P.E., Gillis, J.R., Hargraves, C. R., "Operation of the Computer Model for Direct Atomic Oxygen Exposure of Earth Satellites for FLUXAVG, Version 2.0," NASA CR-198188, August 1995.

6. Bourassa, R. J. and Gillis, J. R., "Atomic Oxygen Exposure of LDEF Experiment Trays," NASA Contractor Report 189627 (May 1992) and revised calculations September 1992.

7. Hedin, A. E., "MSIS-86 Thermospheric Model," *J. Geophys. Res.* **92**, 4649-4662 (1987).

8. Gillis, J.R., Bourassa, R.J., Gruenbaum, P.E., "Operation of the Computer Model for Microenvironment Solar Exposure for SOLSHAD Version 1.0," Boeing Defense & Space Group, NASA CR-198189, August 1995.

9. Stein, B. A. and Pippin, H. G., "Preliminary Findings of the LDEF Materials Special Investigation Group," *LDEF -- 69 Months in Space First Post-Retrieval Symposium*, NASA CP-3134, Part 2 (June 2-8, 1991) p. 617.

10. Pippin, H. G., "Analysis of Materials Flown on the Long Duration Exposure Facility: Summary of Results of the Materials Special Investigation Group," NASA CR-4664, July 1995.

APPENDIX A
COLOR PRINTS OF PHOTOGRAPHS SHOWN IN THE TEXT

Appendix A contains color prints of the black and white photographs shown in the main section of this document. Figure numbers in the Appendix A are identical to the figure numbers in the main section except that Appendix A figure numbers are preceded by an A.

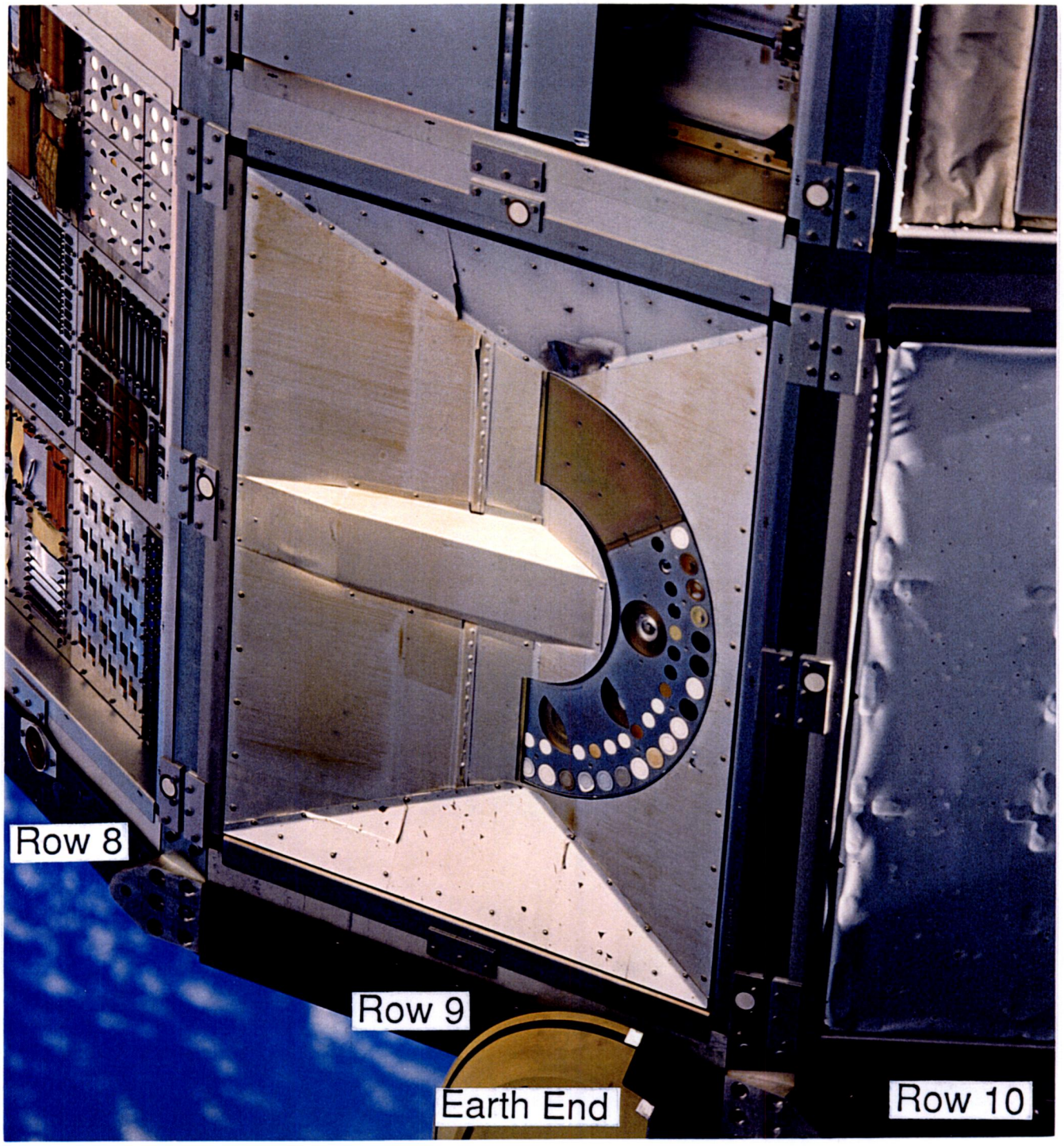

Figure A2.1-1. S0069 Thermal Control Surfaces Experiment On-Orbit Photo.

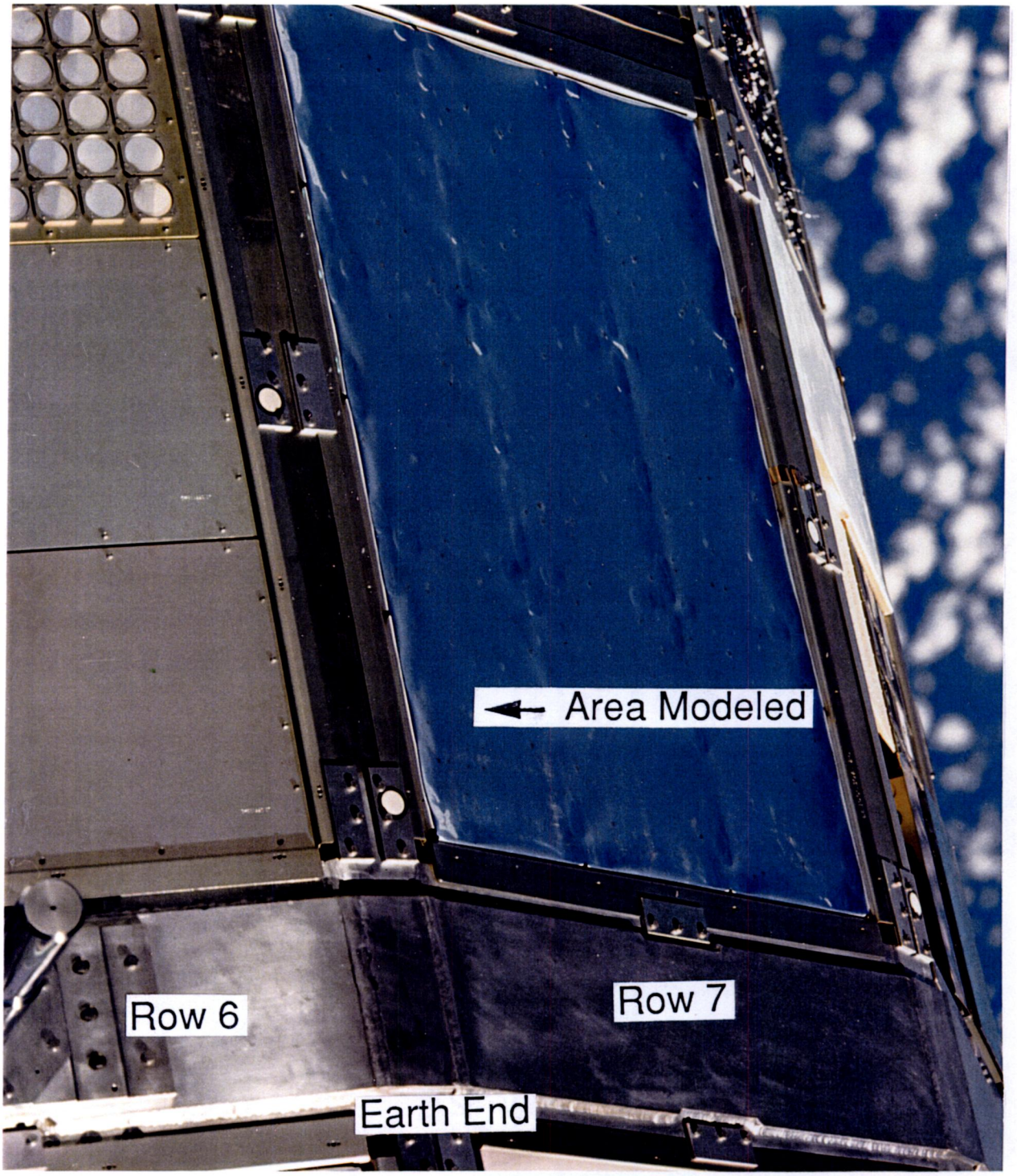

Figure A4.1-1. Row 7 Toward Row 6 FEP Blanket Fold On-Orbit Photo.

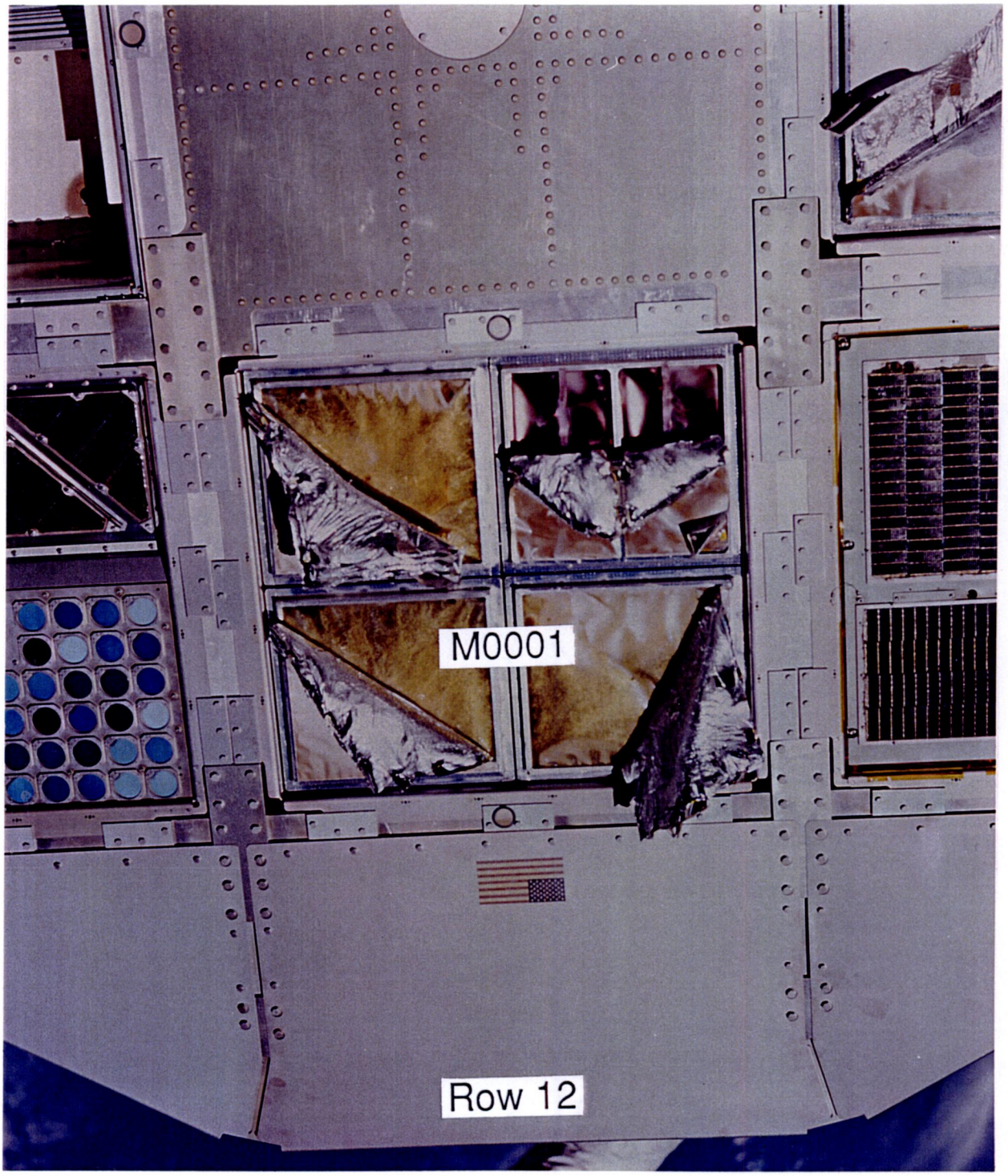

Figure A5.1-1. M0001 NRL Cosmic Ray Experiment On-Orbit Photo.

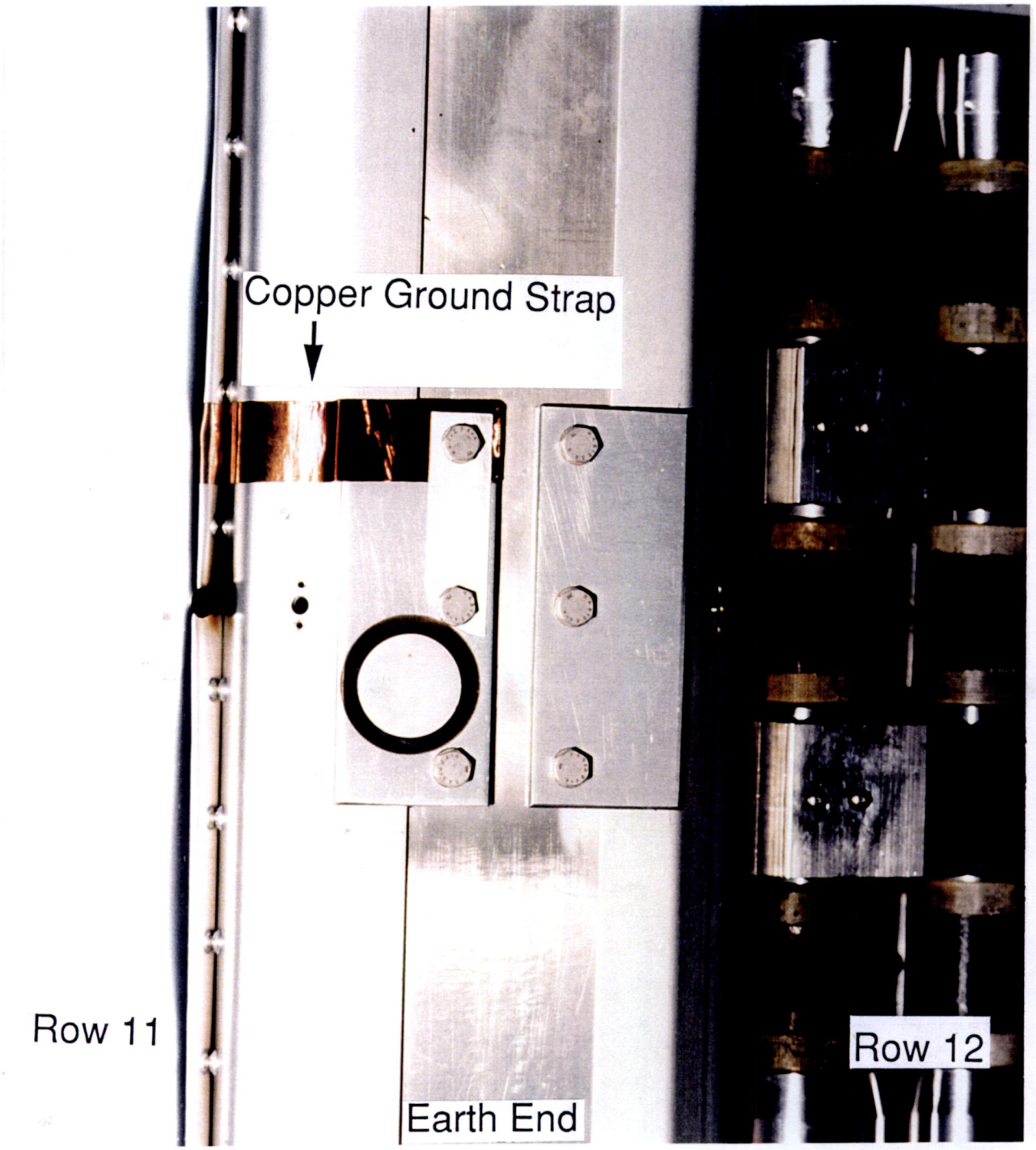

Figure A6.1-1. Tray D-11 Copper Ground Strap Photo.

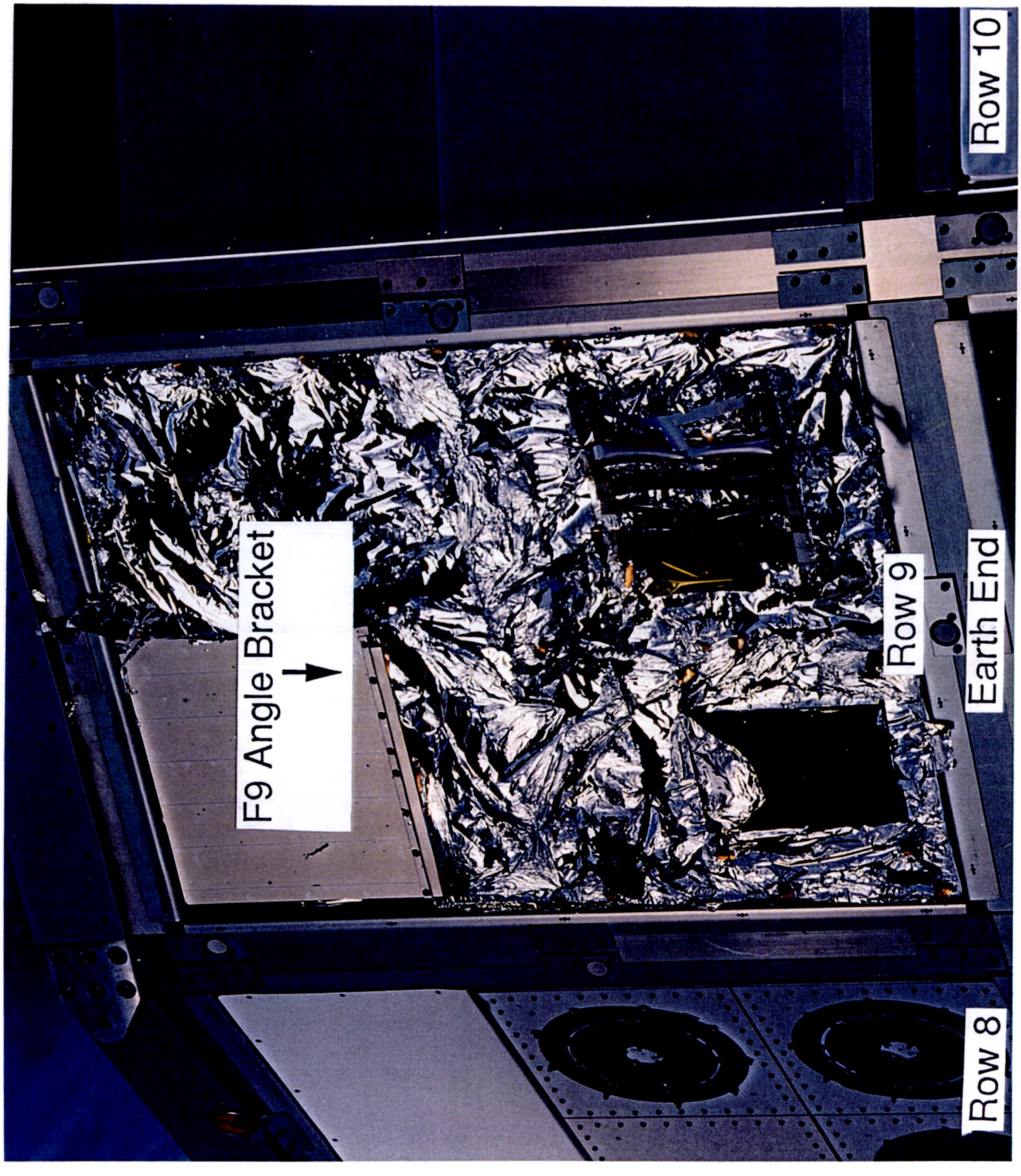

Figure A7.1-1. F-9 Angle Bracket On-Orbit Photo.

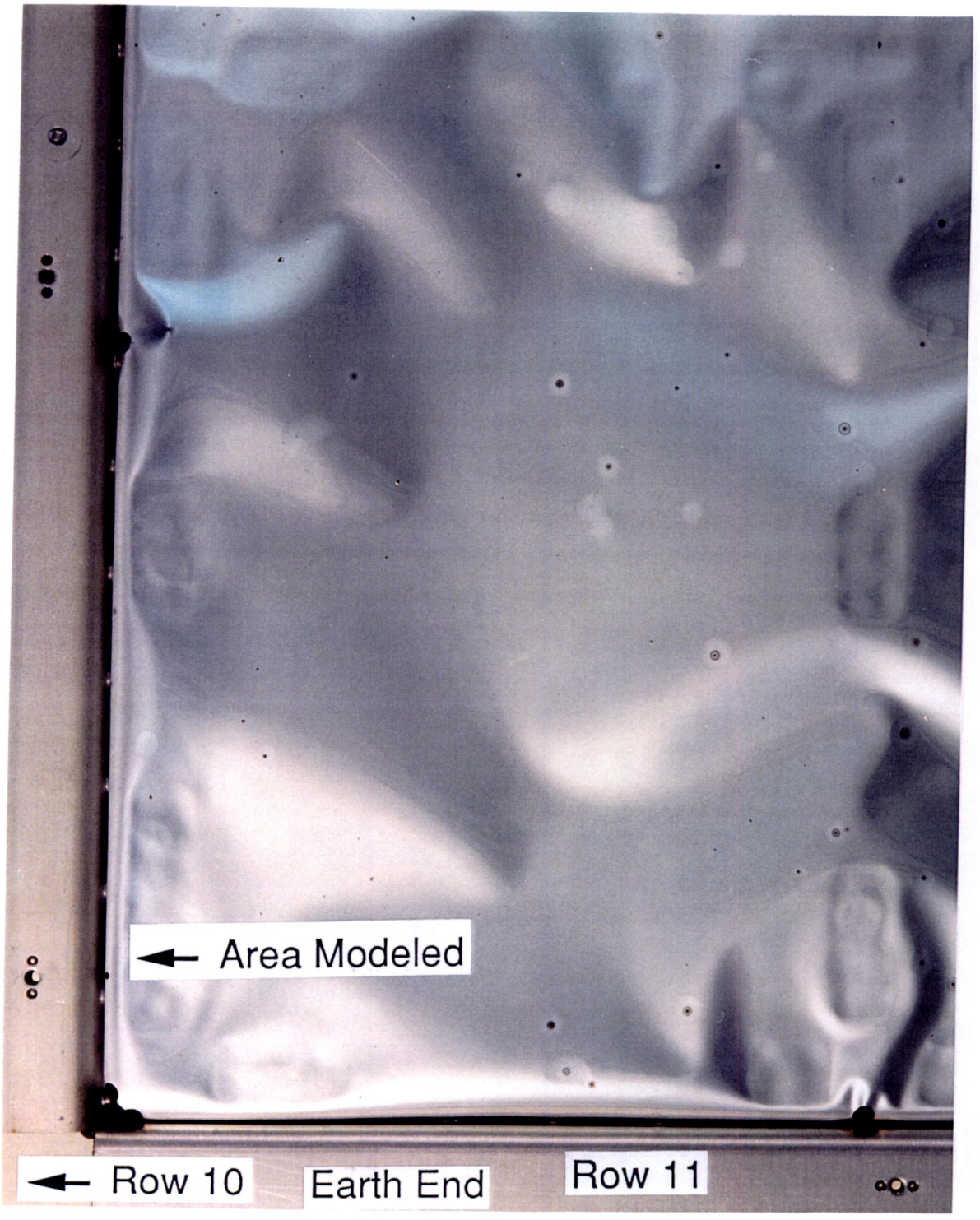

Figure A8.1-1. D-11 FEP Blanket Fold at Tray Edge Photo.

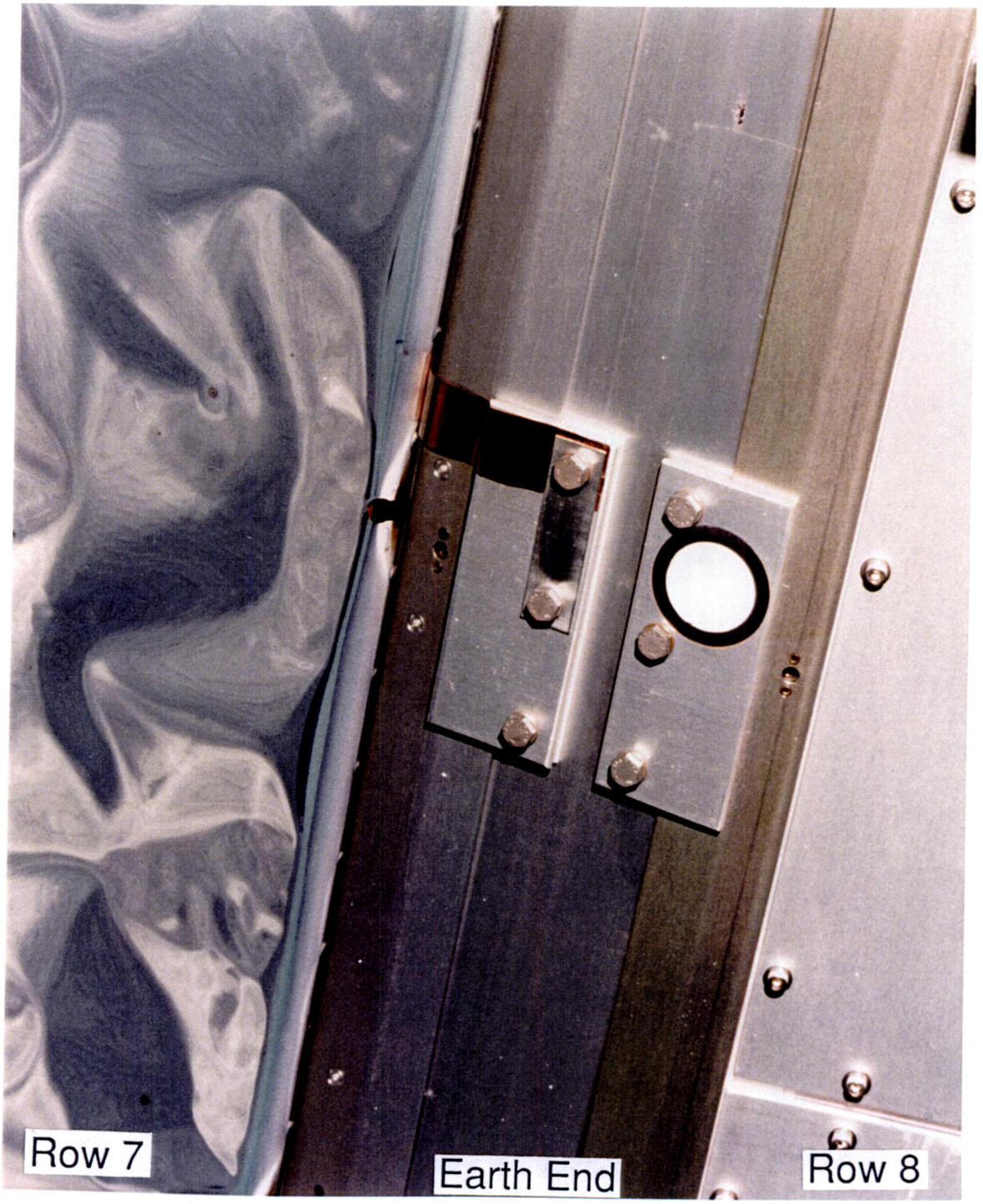

Figure A9.1-1. B-7 FEP Blanket Fold at Longeron Photo.

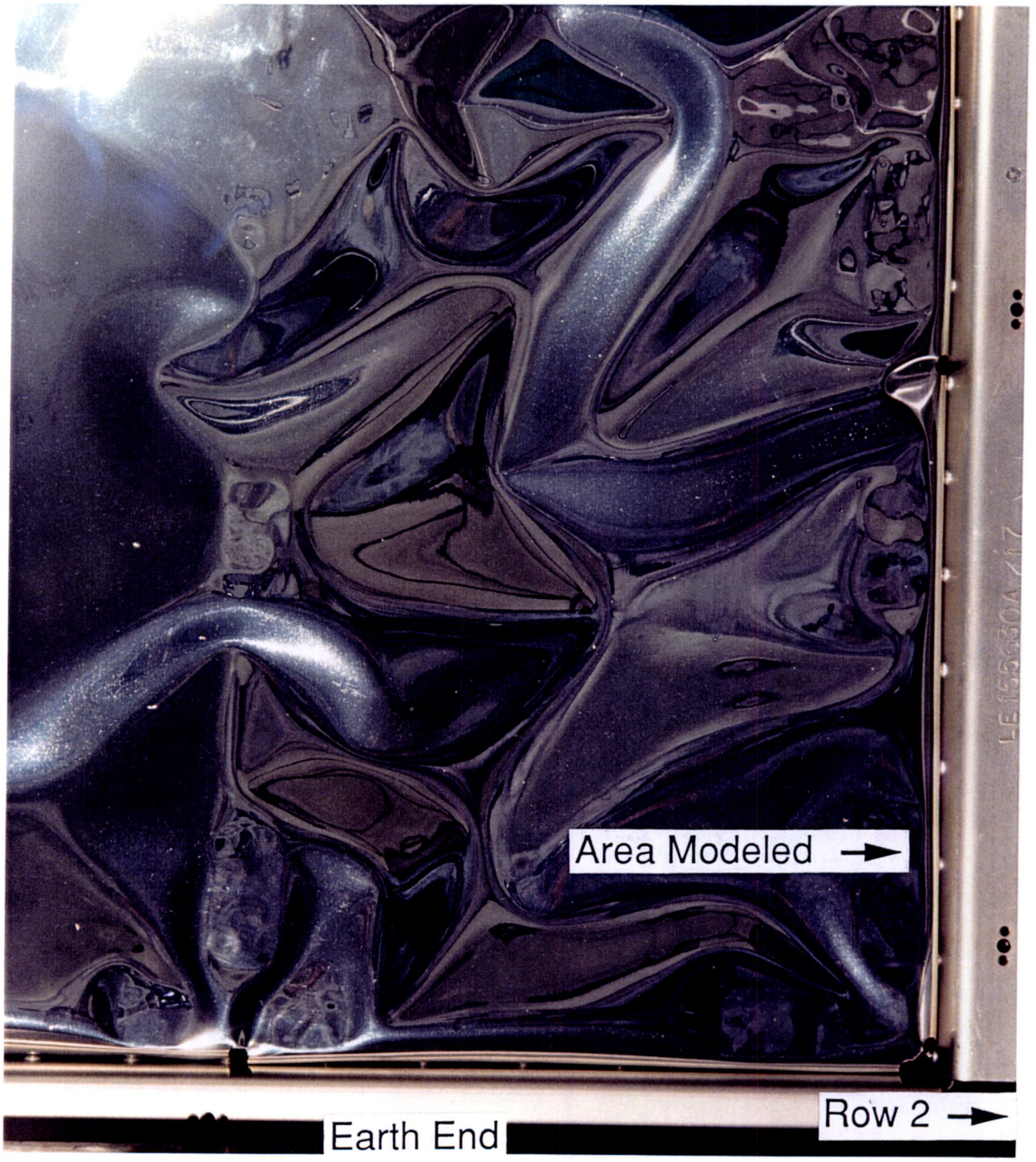

Figure A11.1-1. D-1 FEP Blanket Fold Near Row 2 Edge Photo.

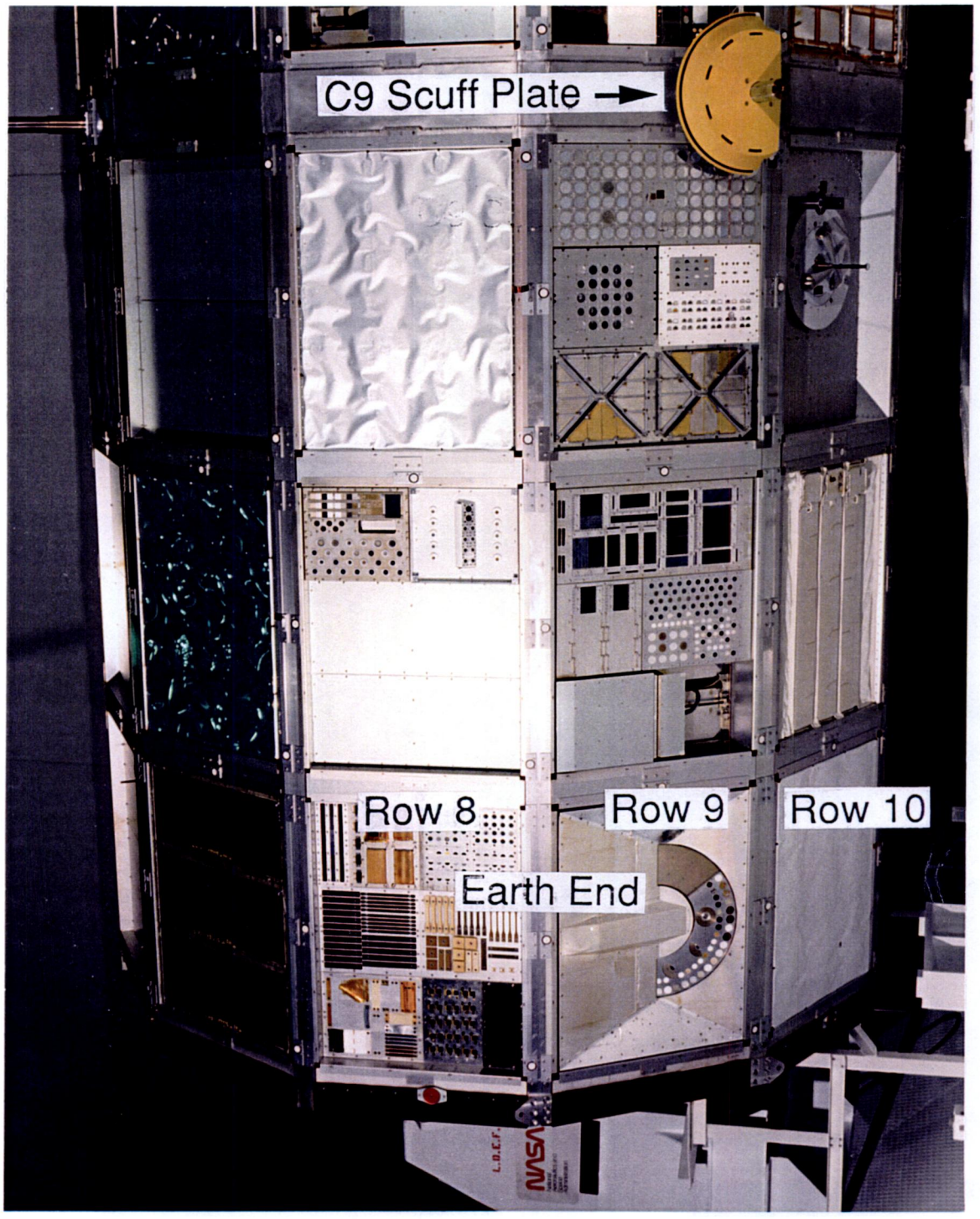

Figure A12.1-1. C-9 Scuff Plate Location Photo.

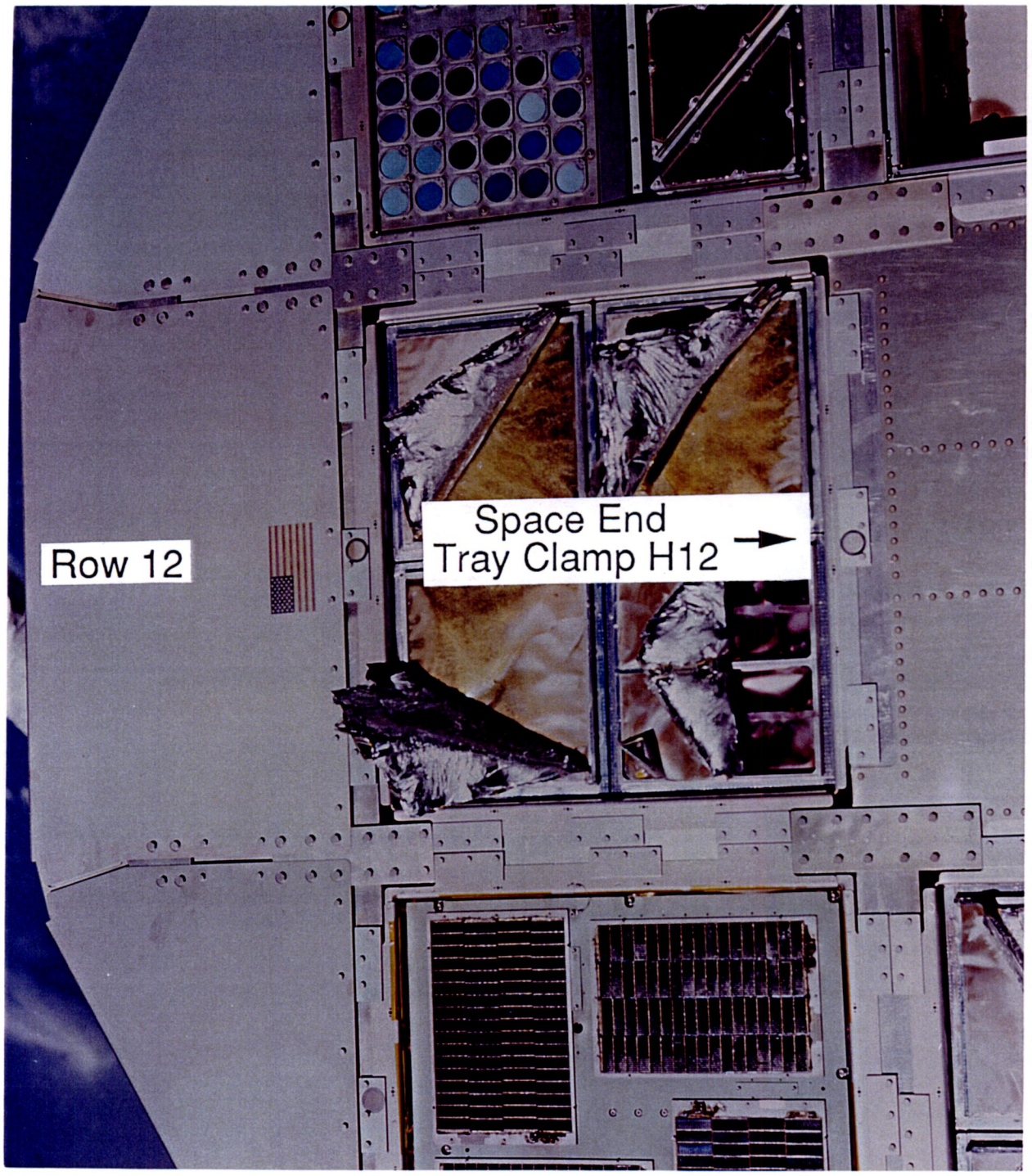

Figure A13.1-1. Space End Tray Clamp H-12 On-Orbit Photo.

REPORT DOCUMENTATION PAGE

Form Approved
OMB No. 0704-0188

1. AGENCY USE ONLY (*Leave blank*)	2. REPORT DATE	3. REPORT TYPE AND DATES COVERED
	August 1995	Contractor Report

4. TITLE AND SUBTITLE
Calculated Values of Atomic Oxygen Fluences and Solar Exposure on Selected Surfaces of LDEF

5. FUNDING NUMBERS
NAS1-18224 and NAS1-19247

233-03-02-02

6. AUTHOR(S)
J. R. Gillis, H. Gary Pippin, R. J. Bourassa, P. E. Gruenbaum

7. PERFORMING ORGANIZATION NAME(S) AND ADDRESS(ES)
Boeing Defense & Space Group
P. O. Box 3999
Seattle, WA 98124-2499

8. PERFORMING ORGANIZATION REPORT NUMBER

9. SPONSORING / MONITORING AGENCY NAME(S) AND ADDRESS(ES)
National Aeronautics and Space Administration
Langley Research Center
Hampton, VA 23681-0001

10. SPONSORING / MONITORING AGENCY REPORT NUMBER
NASA CR-198191

11. SUPPLEMENTARY NOTES
Langley Technical Monitor: Joan G. Funk

12a. DISTRIBUTION / AVAILABILITY STATEMENT
Unclassified - Unlimited
Subject Category 18

12b. DISTRIBUTION CODE

13. ABSTRACT (*Maximum 200 words*)

Atomic oxygen (AO) fluences and solar exposure have been modeled for selected hardware from the Long Duration Exposure Facility (LDEF). The atomic oxygen exposure was modeled using the microenvironment modeling code SHADOWV2. The solar exposure was modeled using the microenvironment modeling code SOLSHAD version 1.0.

14. SUBJECT TERMS	15. NUMBER OF PAGES
LDEF, atomic oxygen fluences, solar exposure, environmental exposure	98
	16. PRICE CODE: A05

17. SECURITY CLASSIFICATION OF REPORT	18. SECURITY CLASSIFICATION OF THIS PAGE	19. SECURITY CLASSIFICATION OF ABSTRACT	20. LIMITATION OF ABSTRACT
Unclassified	Unclassified	Unclassified	UL